Master's thesis

NTNU
Norwegian University of Science and Technology
Faculty of Economics and Management
Dept. of Industrial Economics and Technology Management

Trygve Magnus Aglen
Andreas Hofstad

L-shaped decomposition for the two-stage stochastic facility location problem with capacity adjustments

Master's thesis in Applied Economics and Operations Research
Supervisor: Peter Schütz
Co-supervisor: Šárka Štádlerová
June 2022

NTNU
Norwegian University of Science and Technology

Trygve Magnus Aglen
Andreas Hofstad

L-shaped decomposition for the two-stage stochastic facility location problem with capacity adjustments

Master's thesis in Applied Economics and Operations Research
Supervisor: Peter Schütz
Co-supervisor: Šárka Štádlerová
June 2022

Norwegian University of Science and Technology
Faculty of Economics and Management
Dept. of Industrial Economics and Technology Management

Kunnskap for en bedre verden

Norwegian University of Science and Technology

Department of Industrial Economics and Technology Management

TIØ4905 - Managerial Economics and Operations Research, Master's Thesis

L-shaped decomposition for the two-stage stochastic facility location problem with capacity adjustments

Authors:

Trygve Magnus Aglen

Andreas Hofstad

Supervisors:

Peter Schütz

Šárka Štádlerová

June, 2022

Preface

This thesis is written during the spring of 2022 and finishes our Master's of Science degree at the Norwegian University of Science and Technology, Department of Industrial Economics and Technology Management. This thesis builds on the work done in the specialisation project in TIØ4500 - Managerial Economics and Operations Research, during autumn 2021.

We want to thank our academic supervisor, Peter Schütz and co-supervisor Šárka Štádlerová for their excellent feedback and guidance during this thesis, at any hour of the day. Your feedback has been of the utmost importance throughout the months of working on this thesis. We would also like to thank Kristin Svardal from the Ocean Hyway Cluster for valuable data for the problem in this thesis. Lastly, we would like to thank our families for their encouragement and support throughout the work of this thesis. It could not have been done without you.

Trondheim, 2022-06-10

Trygve Magnus Aglen & Andreas Hofstad

Abstract

This thesis studies how to design an optimal hydrogen supply chain for maritime transportation in Norway. The transportation sector in Norway as a whole faces a transition to low- and zero-emission fuels. The maritime passenger transportation segment points out to be an important contributor to reducing emissions, having high emissions per passenger-kilometre. To realise the pathway to zero-emission maritime transportation, we need a comprehensive model for decision support. The decision must support the design of a future hydrogen supply chain that handles the uncertainty in customer demand.

We model the problem of solving a two-stage stochastic facility location problem with capacity adjustments. The model minimises the overall expected cost for investment in hydrogen-producing facilities, capacity adjustments, production and distribution for different production technologies over the planning horizon. We examine an alternative approach to solve the model with the aim of reducing the solution time, including developing an L-shaped algorithm and different additional acceleration methods. By reducing the solution time, we can solve larger instances of the problem, improving the capturing of the real world's uncertainty and ultimately providing better decision support.

The L-shaped decomposition technique always finds a feasible solution to our model within the defined termination criteria, but gets outperformed by standard commercial solvers for most of our problem instances. For the smallest instances, we are able to find optimal solutions with the use of our L-shaped algorithm. In addition, we manage to find better solutions for the largest instances with respect to objective value than the commercial solver within the termination criteria.

Our model suggests building a decentralised supply chain consisting of many facilities spread throughout Norway. Each facility is installed with electrolysis as production technology to cover hydrogen demand towards 2035 for our case study.

Sammendrag

Denne oppgaven har som mål å designe en optimal verdikjede for hydrogen til bruk i norsk maritim transport. Transportsektoren i Norge gjennomgår en overgang til bruk av lav- og nullutslippdrivstoff. Den maritime passasjertransporten utpeker seg som en viktig kandidat, da det er assosiert høye utslipp per passasjerkilometer i dette segmentet. For å kunne realisere overgangen til en maritim transportsektor med nullutslipp, er vi avhengig av et omfattende verktøy for beslutningsstøtte for å kunne designe en fremtidig verdikjede som håndterer usikkerheten i hydrogenetterspørselen.

Vi har utviklet en modell for å løse et two-stage stochastic facility location problem with capacity adjustments (to-stegs lokaliseringsproblem med kapasitetsjusteringer). Modellen minimerer den samlede forventede kostnaden for investering i hydrogenproduserende anlegg, kapasitetsjusteringer, produksjon og distribusjon for ulike produksjonsteknologier i løpet av planleggingshorisonten. Videre undersøker vi ulike tilnærminger for å redusere løsningstiden for modellen vår, inkludert utformingen av en L-shaped algoritme, sammen med ulike akselerasjonsteknikker. Ved å redusere løsningstiden kan vi løse større forekomster av problemet, fange usikkerheten knyttet til den virkelige verden i større grad, som til slutt resulterer i bedre beslutningsstøtte.

Ved bruk av våre foreslåtte dekomponeringsmetoder, er vi alltid i stand til å finne en lovlig løsning til modellen vår innenfor de definerte termineringskriteriene. Dekomponeringsteknikkene blir utkonkurrert av de vanlige kommersielle problemløserne for de fleste av probleminstansene våre. For de minste tilfellene er vi i stand til å finne optimale løsninger ved bruk av vår dekomponeringsteknikk. I de største instansene klarer dekomponeringsteknikken å finne fram til bedre løsninger enn standard kommersielle løsere, målt i målfunksjonsverdi.

Modellen vår foreslår å bygge en desentralisert verdikjede bestående av flere små fabrikker spredt omkring i Norge. Alle fabrikkene beyntter seg av elektrolyse som produksjonsteknologi for å kunne tilfredsstille hydrogenetterspørselen fram mot 2035 i vår case study.

Table of Contents

List of Figures **xiii**

List of Tables **xv**

1 Introduction **1**

2 Background **5**

2.1 Hydrogen production 5

2.1.1 Green hydrogen production 6

2.1.2 Grey and blue hydrogen production 8

2.2 Distribution of hydrogen 9

2.3 Future Demand 11

2.3.1 CO_2-tax 11

2.3.2 Potential customers in the Norwegian Maritime Sector 12

2.3.2.1 Maritime Passenger Transportation Sector 13

2.3.2.2 Offshore Fleet on the Norwegian Continental Shelf . 14

2.3.2.3 Domestic Fishing 15

2.4 Supply chain design 15

2.4.1 Facility location 15

2.4.2 General cost terms in hydrogen production 16

3 Literature Review **19**

3.1 Multi-Period Facility Location Problem 19

3.2 Multi-Period Facility Location with Capacity Adjustments 21

3.3 Stochastic Programming 22

3.3.1 Two-Stage Stochastic Multi-Period Facility Location Problems with Capacity Adjustments 23

3.3.2 Supply chain design under uncertainty 25

4 Problem Description **27**

5 Mathematical Model **29**

5.1 Modelling Approach 29

5.1.1 Decision variables 29

5.1.2 Modelling costs 30

5.2 Assumptions 31

5.3 Mathematical Formulation 31

6 Solution Method Approach **35**

6.1 Two-stage Stochastic Programming 35

6.1.1 Two-Stage Stochastic Linear Programs 35

6.1.2 L-shaped Method 36

6.1.3 Continuous L-shaped cuts vs. Integer L-shaped cuts 41

6.2 Benders Reformulation of the Mathematical Model 42

6.2.1 New Notation for the Benders Reformulation 42

6.2.2 Sub-problem 43

6.2.3 Master Problem 44

6.3 L-shaped Implementation 45

6.4 Acceleration Methods 46

6.4.1 Adding multiple cuts . . . 47
6.4.2 Alternative Master Problem solution strategy . . . 48
6.4.3 Combinations of methods . . . 49
6.4.4 Warm-start . . . 49

7 Case Study **51**

7.1 Infrastructure and Cost Data . . . 51
7.1.1 Customer Locations . . . 51
7.1.2 Facility location candidates . . . 52
7.1.3 Investment Costs . . . 53
7.1.4 Adjustment Costs . . . 54
7.1.5 Production Costs . . . 54
7.1.6 Distribution Costs . . . 55
7.2 Demand . . . 56
7.2.1 Maritime Passenger Transportation Sector . . . 56
7.2.1.1 Domestic Car Ferries . . . 57
7.2.1.2 High-speed Passenger Ferries . . . 57
7.2.1.3 Coastal Route . . . 58
7.2.2 Domestic Fishing . . . 59
7.2.2.1 Estimation of hydrogen fuel demand . . . 59
7.2.2.2 Timing of transition to hydrogen fuel . . . 59
7.2.2.3 Allocation of demand . . . 61
7.2.3 Offshore Fleet on the Norwegian Continental Shelf . . . 63
7.2.3.1 Ammonia demand projection for the NCS . . . 63
7.2.3.2 Estimating the hydrogen demand through fuel conversion . . . 64

7.2.3.3 Timing of hydrogen demand 64
7.2.3.4 Allocation of hydrogen demand 65
7.3 Generation of hydrogen demand scenarios 68
7.4 Problem instances 69

8 Computational Results **71**
8.1 Model performance analysis 71
8.1.1 Single-cut vs commercial solver 72
8.1.1.1 Results from instances F4C20T10Sx 72
8.1.1.2 Results from instances F7C20T10Sx 73
8.1.1.3 Results from instances F16C50T14Sx 74
8.1.1.4 Alternative approaches 78
8.1.2 Acceleration technique results 78
8.1.2.1 Comparing single-cut with acceleration techniques . . 79
8.1.2.2 Comparing results with or without warm-start 81
8.2 Economic analysis and decision support 83
8.2.1 Value of stochastic programming 83
8.2.2 Electrolysis vs. SMR+ 86
8.2.2.1 Supply chain configuration - EL & SMR+ 87
8.2.2.2 Economic analysis 89
8.2.2.2.1 Investment Costs 89
8.2.2.2.2 Adjustment Costs 90
8.2.2.2.3 Production Costs 90
8.2.2.2.4 Distribution Costs 91
8.2.2.3 Decision support 92

9 Future Research **93**

10 Concluding Remarks **95**

Bibliography **97**

List of Figures

2.1 Electrolysis flow chart (NCE 2020). 7

2.2 Estimated costs for hydrogen production with electrolysis in 2020 and 2030 (DNV 2019). 7

2.3 SMR+ flowchart (Broadleaf 2021). 9

2.4 SMR+ cost distribution. 9

2.5 Comparing volumetric density for different fuels based on lower heating values (U.S Department of Energy 2021). 10

2.6 Historic cost per CO_2-quota in Euros (Øvrebø 2022). 12

2.7 Number of vessels and CO_2-emissions in Norwegian Economic Zone (DNV 2019). 13

2.8 Long-term and short-term expansion paths (Pindyck & Rubinfeld 2018). 17

2.9 Facilities long-term and short-term cost functions. 18

5.1 Illustrations of how costs are modelled. 31

6.1 Block structure of the EF (Birge & Louveaux 2011). 37

7.1 Customer Locations for hydrogen in Norway. 52

7.2 Facility Location candidates in Norway. 53

7.3 Hydrogen demand scenario for high-speed passenger ferries in Norway (Aarskog & Danebergs 2020*a*). 58

7.4 Estimated hydrogen demand for the Norwegian fishing sector 2022-2030. 60

7.5 CO_2 Reduction Potential $[\frac{tonnes}{year}]$. 63

7.6 Estimated development in ammonia demand towards 2030 (Ocean Hyway Cluster 2020*a*). 64

7.7 Hydrogen Demand Forecast for the Offshore sector 2022-2035. 65

7.8 Estimated ammonia demand in different operational areas along the Norwegian coast in different 2030-scenarios (Ocean Hyway Cluster 2020*a*). 66

7.9 Historical and expected petroleum production 1970-2025 (NorskPetroleum 2021). 66

7.10 Historical petroleum production and forecast 2015-2030 (NorskPetroleum 2021). 67

7.11 Regional hydrogen demand 2023-2035 low-scenario 68

7.12 Aggregated Hydrogen Demand Forecast 2022-2035. 69

8.1 Upper and lower bound development for the single-cut algorithm and Gurobi on the instances F4C20T10Sx. 73

8.2 Upper and lower bound development for the single-cut algorithm and Gurobi on the instances F7C20T10Sx. 74

8.3 Upper and lower bound development for the single-cut algorithm and Gurobi on the instances F16C50T14Sx. 76

8.4 Development in objective value for single-cut vs. acceleration techniques for instances F4C20T10Sx. 80

8.5 Comparing single-cut with or without using warm-start for instances F4C20T10Sx. 82

8.6 First stage decisions 5-scenarios. 85

8.7 Max. installed initial capacity for *RP* and *EV*. 86

8.8 First stage decisions 5-scenarios. 87

8.9 Initial facility capacity vs. expected demand. 90

8.10 Average production cost per kg H_2 based on expected demand. 91

List of Tables

1.1 Emissions to air in [1000 tonnes CO_2-equivalents] for commercial fishing and domestic shipping (SSB 2021*b*), in addition to number of Norwegian registered vessels in the years 2013-2019 (SSB 2021*a*). . . . 2

2.1 The colour shades of hydrogen production (Broadleaf 2021). 6

7.1 Investment costs for electrolysis and SMR+ at the set of discrete capacity points (Aglen & Hofstad 2021). 54

7.2 Production costs for electrolysis and SMR+ at the discrete capacity points at maximum utilisation (Aglen & Hofstad 2021). 55

7.3 Hydrogen distribution costs in [€/km/kgH_2] (Aglen & Hofstad 2021). 55

7.4 Fuel conversion factors for MDO and H_2 (DNV 2015). 59

7.5 Conversion rate of diesel to fuel demand based on the relative change in projected CO_2-tax for 2021-2030 (Det Kongelege Klima- og Miljødepartement 2020). 60

7.6 Registered vessels and delivered round weight per region for 2017 (Fiskeridirektoratet 2021, 2022*b*). 62

7.7 Fuel conversion factors for ammonia and hydrogen. 64

7.8 Remaining reserves at producing fields on the NCS (NorskPetroleum 2021). 67

8.1 Hardware description. 72

8.2 The results from L-shaped and Gurobi for the F16C50T14Sx instances. 77

8.3 Value of stochastic programming for 2-, 5- and 10-scenario instances. 84

8.4 Initial capacity and time of investment for the RP and EV. 86

8.5 First stage decisions for EL & SMR+. 88

8.6 SMR+ compared to 5-scenario solution with EL at 12.2% gap. 89

Chapter 1

Introduction

Signing the Paris Agreement in 2015, 175 countries agreed to reduce greenhouse gas emissions by 40% by 2030 compared to the level in 1990. As the first Western country, Norway announced a more ambitious goal in 2020. Their goal from 2020 is to reduce emissions by 50 to 55%, an upgrade of 25 to 37.5% with the 2015 plan (NDC-Registry 2020). In Norway, the transportation sector accounts for approximately one-third of the total emissions. To meet the ambitious national environmental target set in 2020, the transportation sector must be a part of the process of reducing emissions. Following the Norwegian climate action plan for 2021-2030, the goal reported for the transportation sector is to cut emissions by 50% (Samferdselsdepartementet 2021).

The Norwegian climate action plan also targets domestic shipping and commercial fishing within the maritime transportation sector to halve emissions-to-air (Samferdselsdepartementet 2021). Based on annual fuel sales in Norway, SSB has estimated that emissions-to-air from domestic shipping and commercial fishing was 2.95 million tonnes CO_2-equivalents in 2017 (SSB 2021*b*). In comparison, a 1.85 million tonnes higher emissions to air estimation on 4.8 million tonnes CO_2-equivalents in 2017 is calculated by DNV (Regjeringen 2019). DNV uses vessel databases and AIS-data (Automatic Identification System) to create this emission estimate. Sales of fuel done overseas make up for the variation in the forecast of CO_2-emission. Both vessels operating between Norway and one international harbour and between Norwegian ports but not refuelling in Norway are included in ships bunkering overseas. Utilising the vessel databases and AIS-data for estimates of CO_2-emission is more accurate because they consider the uncertainty in fuel sales made overseas (Regjeringen 2019). CO_2-emissions from commercial fishing and domestic shipping are responsible for 22-36% of the CO_2-emissions from the transportation sector, independent of the estimation method. Based on fuel sales, the development in emissions to air is relatively stable, and the fleet maintains a regular size, as illustrated in Table 1.1.

Table 1.1: Emissions to air in [1000 tonnes CO_2-equivalents] for commercial fishing and domestic shipping (SSB 2021*b*), in addition to number of Norwegian registered vessels in the years 2013-2019 (SSB 2021*a*).

Years	**2013**	**2014**	**2015**	**2016**	**2017**	**2018**	**2019**
Emissions to air	3 704	3 820	3 626	3 486	3 627	3 578	3 725
Vessels	7 361	7 329	7 280	7 326	7 361	7 302	7 090

The Norwegian government's climate action plan presents some key instruments to help the transportation sector reach its goal of halving emissions by 2030. Examples of these instruments are subsidies for low- and zero-emission solutions making them more attractive, and CO_2-taxation where end-consumers of fossil fuel must pay tax to the government for their emissions (Samferdselsdepartementet 2021). The general idea for all the instruments is to encourage the development of alternatives to fossil fuels. For the transportation sector, hydrogen, electric batteries and ammonia are the most likely low- and zero CO_2-emission fuel type alternatives (Samferdselsdepartementet 2021). In addition to the key instruments in the climate action plan, the low- and zero-emission solutions are dependent on their technology to not have extra capital expenditure compared to fossil fuels. A cost-effective supply chain must be established to achieve this level of capital expenditure for low- and zero-emission technology.

The status for zero-emission fuel supply chains is that they are under constant development (Samferdselsdepartementet 2021). The message from the "National Transport Plan" is that the necessary infrastructure for these zero-emission fuels will be established with the technological development in shipping. Here, hydrogen is pointed out as one promising project (Samferdselsdepartementet 2021). There is no well-established hydrogen fuel supply chain in Norway for maritime transportation today (Mäkitie et al. 2021).

This thesis aims to provide decision support for designing a hydrogen supply chain, ultimately accelerating the transition to low- and zero-emission fuels for the maritime transportation sector in Norway. To provide such decision support, we develop a stochastic optimisation model. The model addresses critical challenges like locating hydrogen production facilities, production technology, distribution solutions and uncertainty in customer demand to design the optimal supply chain to minimise the overall expected costs. We perform a deep dive into alternative solution method approaches to reduce the solution time of our complex model and apply the L-shaped decomposition technique combined with different acceleration techniques to improve solution time further. Evaluating the results provides managerial insight into the hydrogen facility location problem for the maritime sector.

Our thesis is structured as follows: Chapter 2 covers technical insight into hydrogen production, costs and distribution. In addition, the chapter establishes relevant political aspects to consider when identifying future hydrogen customers in Norway. Chapter 3 reviews relevant literature on supply chain design under uncertainty. Next, Chapter 4 follows with a complete description of the problem. Chapter 5 presents a mathematical model to solve the problem described in Chapter 4. In Chapter 6, we discuss and implement a solution algorithm to decrease the solution time of the original model presented earlier in Chapter 5. We present our case data used for computational studies in Chapter 7, and Chapter 8 presents our computational results. Lastly, we present topics for future research and our concluding remarks in Chapter 9 and Chapter 10 respectively.

Chapter 2

Background

This chapter aims to present essential topics to the reader to understand the current hydrogen market and production better. Section 2.1 presents an introduction to hydrogen production in terms of costs and production method. Furthermore, the distribution of produced hydrogen is discussed in Section 2.2. In Section 2.3, we present hydrogen demand projections. Lastly, we discuss potential facility locations for the design of the hydrogen supply chain along in Section 2.4.

2.1 Hydrogen production

As hydrogen only has water as an emission product when used as a fuel, it is a promising fuel type with low- or zero CO_2-emission. On the other side, the environmental footprint from hydrogen fuel may not be CO_2-emission free. The variation in environmental footprint comes from differences in sources and processes when producing the hydrogen fuel (IRENA 2020). Consequently, when considering CO_2-emissions, it is common to differentiate hydrogen by production processes by splitting it into a colour shading like “green”, “blue”, and “grey”, as presented in Table 2.1 and the following sections.

Table 2.1: The colour shades of hydrogen production (Broadleaf 2021).

Characteristic	**Green**	**Blue**	**Grey**
Energy Source	Renewables	Hydrocarbon: natural gas or coal	Hydrocarbon: natural gas or coal
Feedstock	Water	Hydrocarbon: natural gas, coal, oil, biomass	Hydrocarbon: natural gas
Technology	Electrolysis	Gasification or Steam Methane Reforming	Gasification or Steam Methane Reforming
By-products	Oxygen	CO_2 (assumed captured and stored)	CO_2
Notional environmental footprint	Minimal	Low	Medium or high

2.1.1 Green hydrogen production

As green hydrogen is defined with renewables as an energy source, it is the only hydrogen type with no CO_2-emissions related to production. The feedstock for the production is water, and the only by-product is oxygen. For large scale production of green hydrogen, it is common to use electrolysis technology (IRENA 2020).

Electrolysis technology uses electrical energy as input and converts it into chemical energy. An electrolyser consists of two electrodes, which are named cathode and anode. The electrodes are separated by an electrolyte that directs an electric current. The electric current is then used to split water, which is used as feedstock, into hydrogen and oxygen (Broadleaf 2021). The hydrogen production process with electrolysis is illustrated in a simple flow chart in Figure 2.1. The electrolysis process is green as long as the electrical energy source comes from renewable energy.

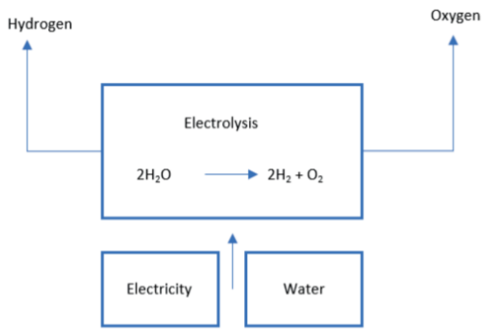

Figure 2.1: Electrolysis flow chart (NCE 2020).

Electrolyser technologies will typically have a unique dynamic capacity range that differs between 0% to 100% of production capacity. The technologies appropriate for Norwegian hydrogen production have a lower bound of 15% (NEL 2019). This bound implies that the lowest production quantity an electrolyser can run on is 15% of its capacity.

Currently, Proton Exchange Membrane Electrolysis (PEM), Solid Oxide Electrolyser (SOE) and Alkaline Electrolysis (AEL) are the leading electrolysis technologies (H2Bulletin 2021). The costs of using electrolysis as hydrogen production technology are greatly determined by the facility construction, the utilisation rate, and the price of electricity (GlobalCCSInstitute 2020). Estimating hydrogen production costs development between 2020 and 2030 is presented in Figure 2.2. Here, the proportion of the costs between the production process and the electrical power used is displayed. One remark is that the increase in the cost of electricity equalises the decline in costs of electrolysis. For this reason, there is a relatively low change in total expenditures between 2020 and 2030 for alkaline electrolysis (DNV 2019).

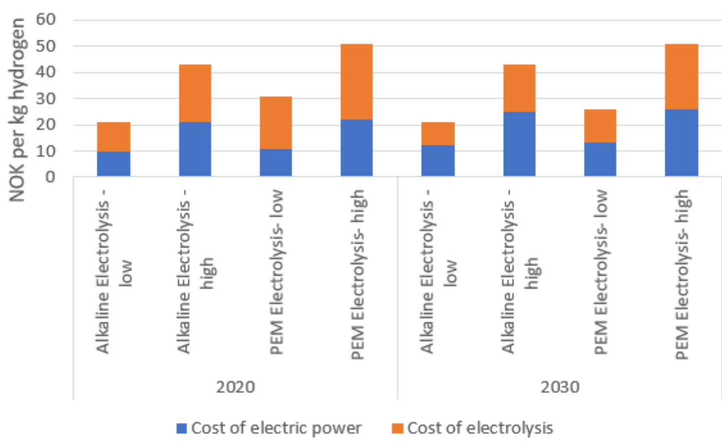

Figure 2.2: Estimated costs for hydrogen production with electrolysis in 2020 and 2030 (DNV 2019).

2.1.2 Grey and blue hydrogen production

Gasification or Steam Methane Reforming (SMR) are the production technologies utilised in producing grey hydrogen. Grey hydrogen is not suited as a zero-emission fuel type contender as its notional environmental footprint is medium to high from using natural gas or coal as feedstock. This production provides a high level of CO_2-emissions to air from by-products (IRENA 2020).

The environmental footprint for blue hydrogen is reported as low, making it suitable as a common CO_2-emission fuel type (Broadleaf 2021). Even though the production process is almost the same as for grey hydrogen, it is still a candidate despite the same energy source, feedstock, and production technology. The difference between blue and grey hydrogen is the introduction of Carbon Capture and Storage (CCS) in the production process resulting in Steam Methane Reforming with Carbon Capture and Storage (SMR+). The idea is to capture the CO_2 in production and store it, possibly underground. A barrier for the blue hydrogen is that just 85-95% of the CO_2 created in production can be captured through CCS, and therefore it is not emission-free. CCS can, in theory, capture up to 100% of the CO_2 produced in the process, but currently, the upper limit to the technical efficiency is approximately 95%. The barrier to reaching a 100% is that it requires a lot more funding for the last percentages of CO_2, as there is harder to capture the less concentrated gas. For this reason, companies will need a powerful financial incentive to invest in environmental friendly technology (Moseman 2021). Instead, blue hydrogen may serve as a stepping stone towards the realisation of a large scale zero CO_2-emission hydrogen fuel type such as green hydrogen (IRENA 2020).

The SMR+ process starts with natural gas and water as input. First, the natural gas is cleaned, leaving only pure methane gas, while the water is heated to steam. Afterwards, with a catalyst's assistance, the methane and steam are chemically transformed into a mix of carbon monoxide and hydrogen, called syngas, in the reformer. Furthermore, the syngas undergoes a water gas shift reaction to produce more hydrogen, again assisted by a catalyst. Here, we end up with CO_2 and hydrogen as output, which is eventually separated to the hydrogen, and CO_2 as a by-product which is then taken care of by the CCS technology (Broadleaf 2021). A simple illustration of the process is presented in Figure 2.3.

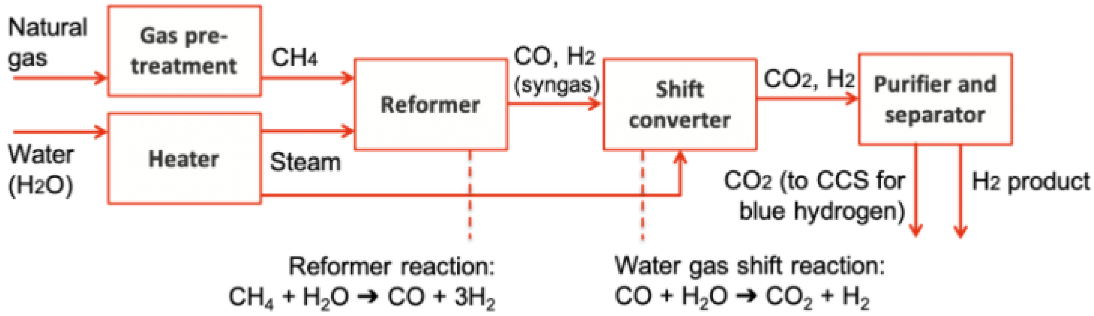

Figure 2.3: SMR+ flowchart (Broadleaf 2021).

Breaking down the cost structure for SMR+ shows that capital expenditures (CAPEX) contribute to a large share of the costs. High investment costs are associated with establishing the H_2 production plant and the CCS system, including a carbon capture facility and a transport and injection system. The cost of natural gas dominates the operational expenditures (OPEX) with over 60% of the total OPEX (Jakobsen & Åtland 2016). The CAPEX and OPEX cost structure breakdown is presented in Figure 2.4. Note that CAPEX is in a million Euros and OPEX is in a million Euros per year.

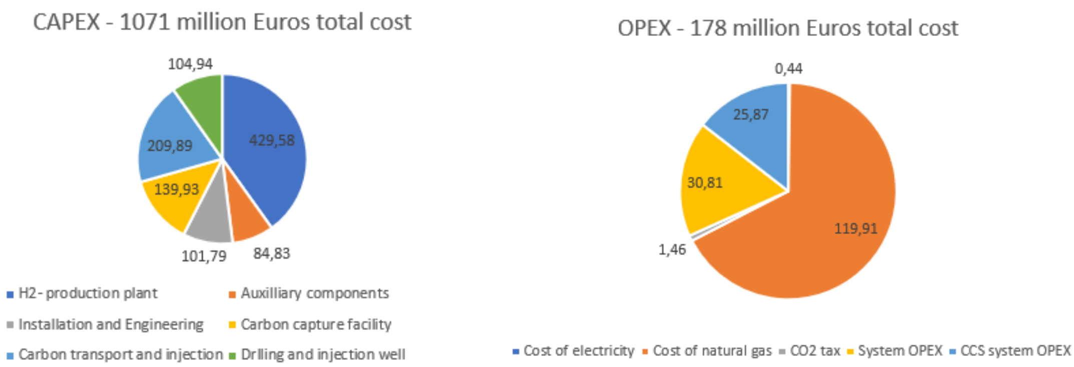

(a) CAPEX in million Euros.

(b) OPEX in million Euros per year.

Figure 2.4: SMR+ cost distribution.

2.2 Distribution of hydrogen

For the distribution of hydrogen, there are both economic and technological challenges. As illustrated in Figure 2.5, we see that variations of hydrogen will have a volumetric density ranging from about 0.8 to 2.1 $\frac{kWh}{L}$. That is four to five times lower volumetric density than for respective gasoline and diesel at best, illustrating that it requires more hydrogen in volume to deliver the same amount of energy as traditional fuels such as gasoline and diesel. Hydrogen's low volumetric density is a challenge for distribution as, generally, the volumetric density is considered the limiting factor when distributing by trucks (Aarskog & Danebergs 2020*b*). The volumetric density properties also show that hydrogen needs to be handled under high pressure (compressed), in very low temperatures (liquid) or combined with other chemical substances to achieve more energy per volume (U.S Department of Energy 2021).

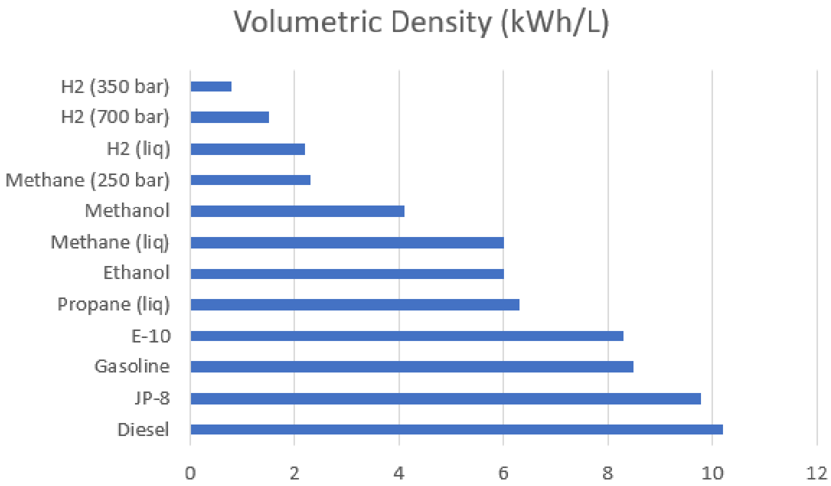

Figure 2.5: Comparing volumetric density for different fuels based on lower heating values (U.S Department of Energy 2021).

The preferred options for the distribution of hydrogen are in the forms of liquid, compressed, ammonia or liquid hydrogen organic carriers (LHOCs). Our focus will be on the distribution of liquid and compressed gaseous hydrogen, as the other two options carry more uncertainty due to the early stages of development for hydrogen distribution in Norway (SINTEF 2020). For liquid hydrogen, the hydrogen needs to be cooled down to -253°C, while compressed gaseous hydrogen is made by compressing the gas to 350 or 700 bars. Both processes must be done after the hydrogen is produced, resulting in additional costs and an energy loss (SINTEF 2020). For liquid and compressed gaseous trucks, there are special made cryogenic tanks and high-pressure trucks for distribution that are well suited for distributing hydrogen in Norway (SINTEF 2020). As Norway has strict regulations on resting time of 45 minutes after 4.5 hours of driving, limiting how far a driver can distribute hydrogen will be suitable. An alternative option would be to have two drivers, which would then again create high additional costs as the wage level is high in Norway (arbeidslivet.no 2019).

2.3 Future Demand

The current global hydrogen producers and their customers represent a highly closed market. Only 4% of the global hydrogen production in 2017 was sold on the free market, and hydrogen vehicles accounted for only 0.002% of the global hydrogen consumption (DNV 2019). Most hydrogen consumption occurs in industrial facilities close to the hydrogen's production site and is integrated within their supply chain. Hydrogen is a vital chemical input factor for ammonia, methanol and oil refineries. Together, these industries consume the lion's share of global hydrogen production.

A supply chain to support the utilisation of hydrogen in other sectors, e.g. hydrogen vehicles, does not currently exist. In Norway, such a hydrogen supply chain must be designed and built from scratch. In combination with stricter emission regulations for CO_2 and increasing global energy and fuel consumption, it is likely that the free market and demand for hydrogen will have a much higher potential soon and in the future years to come. One potential area containing answers to when low- and zero-emission solutions such as hydrogen become economically viable is the current CO_2-taxation in European countries due to the current EU Emissions Trading System (EU ETS).

2.3.1 CO_2-tax

The taxation of CO_2 is an active measure used in Norway and the EU to make it more attractive to seek low- and zero-emission solutions. In the EU this system is formally known as the EU Emissions Trading System (EU ETS). Norway has committed to participating in the EU ETS through "Klimakvoteloven" in 2005 (Oljedirektoratet 2022). Some of the prerequisites for creating demand for hydrogen through the CO_2-tax will be its pricing and which sectors it covers.

Figure 2.6 suggests a significant increase in the CO_2-quota prices. The EU Emissions Trading System entered phase 4 in 2021, restricting the total number of quotas and creating market stability reserves to obtain a more stable quota price (European Comission 2022). At the same time, we observe that reimbursement schemes that formerly refunded expenses for CO_2-emissions in some sectors are discontinued in Norway (Det Kongelege Klima- og Miljødepartement 2020).

Figure 2.6: Historic cost per CO_2-quota in Euros (Øvrebø 2022).

Sectors will typically switch to low- and zero-emission solutions when the costs resulting from the CO_2-tax surpass the costs of operating the new zero- or low-emission technology. The CO_2-taxation can then act as a trigger for the switch to zero- and low-emission technology and help push the cost down for zero- and low-emission technology in the meantime.

2.3.2 Potential customers in the Norwegian Maritime Sector

The most relevant vessel segments for hydrogen consist of segments related to large CO_2-emissions. Technology matureness plays an essential role as well in which segments that are feasible to utilise hydrogen in the near future. At last, vessels spending most of their time in the Norwegian economic zone are more likely to benefit from a hydrogen supply chain established on the Norwegian mainland, as they are more likely to use bunker locations on the Norwegian mainland. From Figure 2.7, it becomes apparent that different vessel segments vary in both fractions of domestic emissions and the number of vessels. Cruise ship types such as Coastal Route, International Ferries and Cruise, stand out as one of the most emission-intensive ship types in terms of the total number of vessels. Using the Coastal Route as an example, we see large emissions that are primarily domestic, spread over very few vessels. These vessels have included time windows for 2-3 bunkering locations from Bergen to Kirkenes in today's schedules. With this in mind, the Coastal Route as a future hydrogen customer may result in a few bunkering locations with great hydrogen demand spread along the coast. On the contrary, the fishing industry consists of many vessels spread throughout the entire Norwegian coastline, with a more limited range than the vessel types used on the Coastal Route. With such a large geographical spread of many smaller vessels and average emissions per vessel, this sector can require small hydrogen demand spread throughout the coastline distributed on many bunkering locations. Considering all these properties, designing a supply chain that operates optimal under possible future demand realisation becomes more critical, and handling the uncertainty in future demand more important.

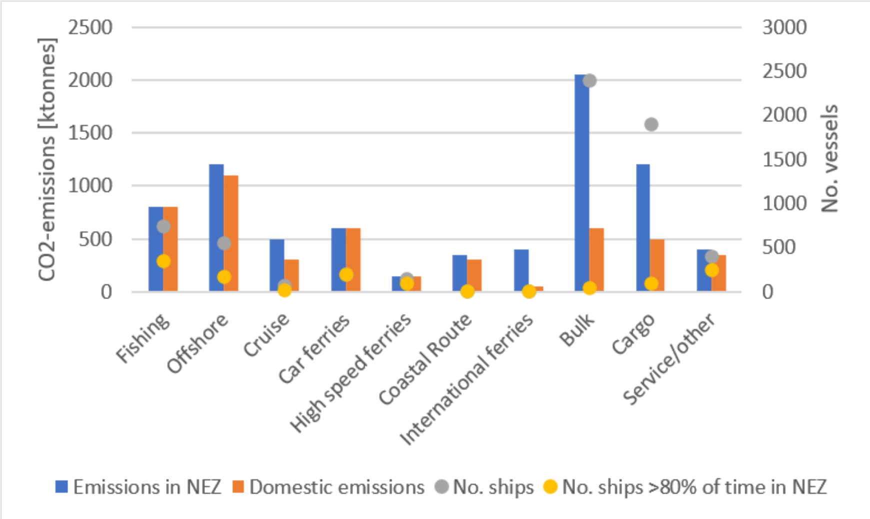

Figure 2.7: Number of vessels and CO_2-emissions in Norwegian Economic Zone (DNV 2019).

2.3.2.1 Maritime Passenger Transportation Sector

For the maritime passenger transportation sector in Norway, public tenders play an important role in setting the requirements for the operation of the different transportation contracts. Specific requirements such as zero- and low-emission technology can be set in these contracts. This is already the case for the ferry connection Bodø-Moskenes-Værøy-Røst from year 2025, where hydrogen as fuel is required (Samferdselsdepartementet 2021). The use of public tenders in the maritime transportation sector can result in large sudden increases in hydrogen demand. This type of demand is usually foreseeable, as new public tenders often are announced years before they take effect.

The maritime transportation sector in Norway also has a varied fleet-composition mix, ranging from small passenger vessels, high-speed ferries, domestic car ferries and cruise ships used in the Coastal route. Each segment has distinct characteristics setting different requirements for a hydrogen supply chain. These requirements can be related to different amount of energy demands, making some vessel segments more suitable for hydrogen than others. One possible result of different requirements within vessel segments is that only a fraction of vessels used in the maritime passenger transportation sector can convert to zero-emission technology or that some vessel segments undertake the technology switch to zero-emission technology later than others.

2.3.2.2 Offshore Fleet on the Norwegian Continental Shelf

Historically, Norwegian offshore shipping companies have had a proactive approach to seeking and applying new technology in collaboration with oil companies. Their incentive for implementing this new technology has been to produce more energy-efficient solutions (Konkraft 2020).

The EU ETS has engaged in phase 4 in 2021, resulting in more considerable restrictions in the total number of trading quotas. This restriction will cause a tax increase on CO_2, and the government predicts this to get the total cost of emission as 2000 $\frac{NOK}{tonneCO_2}$ measured in fixed 2020-prices towards 2030. In the government's climate action plan for 2021-2030, emphasis is placed on cooperation between the oil- and gas industry and the government in the work of developing low- and zero-emission solutions for the industry. As of now, there are competing low- and zero-emission fuels for the offshore industry. Ammonia is heavily discussed as one of the candidate zero-emission fuels, with supply ships already being converted to run on ammonia to test the new technology (SINTEF 2021). Hydrogen, either solely or in combination with batteries, is another competitor. Nevertheless, each technology can result in hydrogen demand if the hydrogen is used to produce ammonia. Similarly to the maritime passenger transportation sector, the offshore sector can experience that only a fraction of vessels convert to low- or zero-emission technology and create hydrogen demand or that different vessel segments switch to low- or zero-emission technology at different times.

The low- and zero-emission technology for the oil- and gas industry is subject to strict safety regulations as this industry is known to have value safety high. The oil- and gas industry on the Norwegian Continental Shelf practices the NORSOK-standard, which has a complete framework for safety regulations on all levels in the industry ranging from drilling to operation (Standards Norway 2021). It is not unlikely that the importance of safety in the sector leads to requirements of large technology matureness relative to other sectors for the low- and zero-emission solutions. These high safety standards for the industry could imply that if the offshore sector utilises zero-emission technology, it will bring the technology matureness for the zero-emission technology to a satisfactory level for every other sector identified in this section to start using it. The opposite outcome is that the hydrogen demand in the offshore sector comes later relative to the other sectors.

2.3.2.3 Domestic Fishing

The domestic fishing sector shares a principal target with the domestic shipping sector in Norway of halving emissions by 2030 compared to 2005 levels. Similar to the offshore sector, domestic fishing will experience increases in CO_2-taxes towards 2030 and will have to adapt to low- and zero-emission technology. Historically, the domesitc fishing sector has not been affected by CO_2-tax up until 2020 due to complete refunds of the fishermen's expenses regarding the CO_2-tax. Towards 2025, a compensation scheme that slowly aims to degrade to zero is in practice (Ocean Hyway Cluster 2021). This will in turn imply a much stronger incentive for the domestic fishing sector to seek zero- or low-emission solutions in the near future. Like the maritime transportation sector, the fishing sector has a mixed fleet composition. It will most likely require different technological solutions across the different vessel types, but not to the same degree as the vessel segments in the maritime transportation sector identified earlier.

2.4 Supply chain design

In this section, we identify the problem type of supplying the Norwegian maritime transportation sector with low- or zero-emission fuel, based on the inputs from the discussion held in this chapter so far. Furthermore, we elaborate on the general cost terms in production as these represent recurring elements when modelling problems of the identified type.

2.4.1 Facility location

DNV discuss the possible designs of a hydrogen supply chain regarding the maritime transport sector in their report one "Hydrogen Use and Production in Norway" (DNV 2019). They acknowledge that an entirely new supply chain must be designed to satisfy the requirements for hydrogen in the maritime transportation sector. When establishing a new supply chain, DNV highlight that it is often a question of whether the production should be centralised at a few locations, granting cost advantages from large-scale production in the form of lower production costs, or decentralised with a greater amount of smaller facilities granting the opposite cost structure. Centralised or decentralised production is a typical trade-off found in facility location problems or supply chain design. Either way of configuration, it is not given that the supply chain will be operating as optimal, depending on what possible future hydrogen scenarios are realised. Each scenario will have components from different vessel segments with distinctive characteristics.

2.4.2 General cost terms in hydrogen production

There is a relatively high level of costs associated with establishing and starting hydrogen production. We may split these costs into two groups: long-term and short-term costs. The costs connected with decisions spanning over a relatively long time horizon, possibly years, are the long-term costs. The long-term costs can be considered a minimisation problem between production input factors, often capital and labour. The sum of expenditures on capital and labour is minimised with respect to capital and labour usage and subject to the production function equality. The intersection between input factors isoquants and isocost curves, reveals the expansion path for the long-term costs with each optimal combination of capital and labour to produce its respective quantity in the long-term (Mathis & Koscianski 2002), as Figure 2.8 illustrates. Here, the optimal combination of capital, K_1, and labour, L_1, for the initial quantity level, q_1, is found as the intersection between the isocost curve, the line spanning between input cost points A and B, and the isoquant line for q_1. Figure 2.8 also shows the inflexibility of short-run production. Production costs cannot be minimised if the production quantities varies, due to the capital input level being fixed. Moving along the short-term expansion path from initial production quantity, q_1, to an increased production quantity q_2, the only option is that labour increases from L_1 to L_3. However, in the long-run the same quantity can be produced cheaper by increasing labour from L_1 to L_2 and capital from K_1 to K_2.

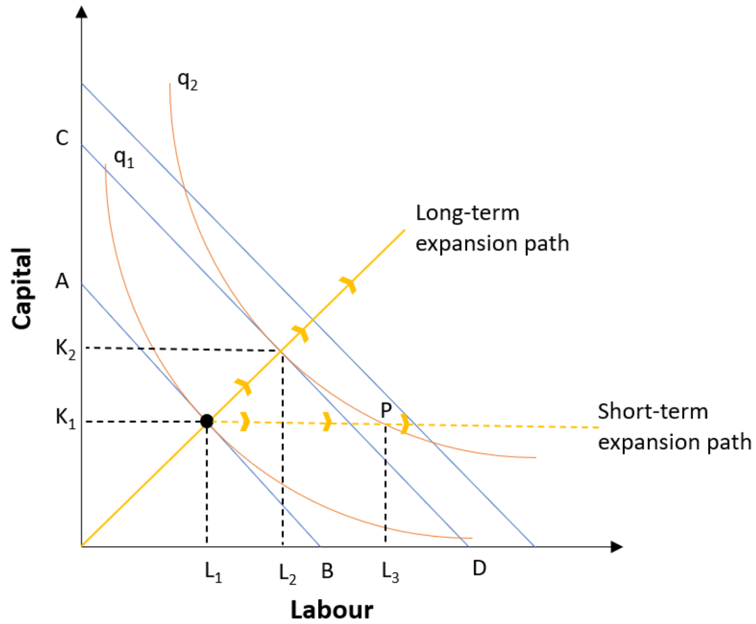

Figure 2.8: Long-term and short-term expansion paths (Pindyck & Rubinfeld 2018).

An investment in a production facility or adjusting the facility's capacity will have a long-term cost function associated with the decision. A short-term cost function will be connected to the long-term cost function at that capacity point. The short-term cost functions are tangent to the long-term cost function at a given facility capacity with its respective production quantity. Here there is only one input factor, as capital (investment in facility capacity) is held constant. The short-term function will then be convex on the assumption that the marginal return on the input factor is diminishing (Mathis & Koscianski 2002). This connection between the short-term cost functions and long-term cost functions is presented in Figure 2.9. The recognisable S-shape of the long-term cost function comes from the increasing and diminishing marginal cost functions. The long-term cost function shows economies of scale in the beginning with the average cost function decreasing. Later on, with sufficiently high output levels, dis-economies of scale appears as marginal cost increases (Pindyck & Rubinfeld 2018).

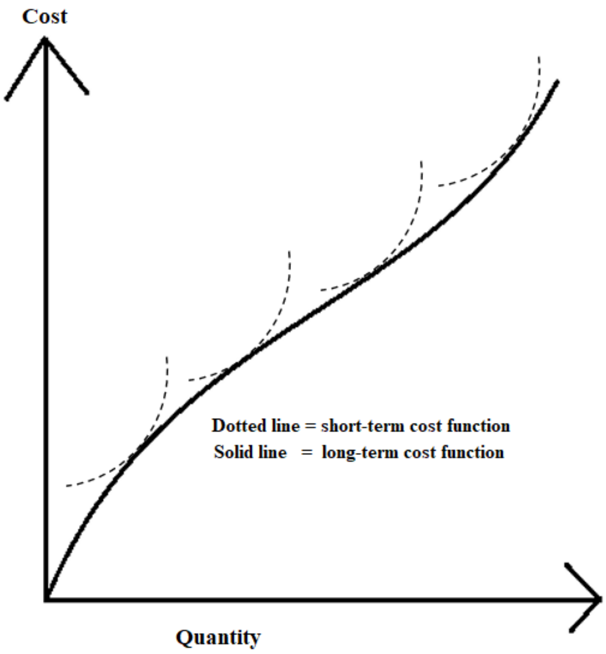

Figure 2.9: Facilities long-term and short-term cost functions.

The long term decisions in hydrogen production will be the options to establish facilities and later adjust their capacity. Decisions like production quantities and distribution, which may change daily, are associated with short-term costs. For the short term production process, there has to be at least one input factor that is held constant (Ioan & Ioan 2014). Typically for a hydrogen production process, the capital in factories is held constant, while labour is variable.

Corporations tend to exploit the phenomena of economies of scale to make improvements in their expenditure pattern by streamlining their production. By distributing costs over a more significant number of quantities when production increases and costs are reduced, are the corporations able to achieve economies of scale (Pindyck & Rubinfeld 2018). With lower marginal costs than average costs, simultaneously, the corporation gets economies of scale as the average costs decrease. Combining this with the fact that higher utilisation will have decreasing marginal costs, we get that a small facility with a high utilisation will achieve economies of scale compared to a large facility with low utilisation (Schütz 2009).

Chapter 3

Literature Review

This chapter discusses the literature that studies problems relevant to supply chain design. To begin with, we study a multi-period facility location problem and discuss some of its essential properties and limitations. Next, we extend the problem to involve capacity adjustments and study several models considering different approaches to modelling these capacity adjustments. Section 3.3 discusses using stochastic programming as a modelling framework in facility location and supply chain design.

3.1 Multi-Period Facility Location Problem

A multi-period facility location problem (MFLP) involves a set of time periods, a set of geographically spread customers and a set of facilities to satisfy customer demand. The MFLP is relevant when designing a facility configuration which faces changing costs over time or dynamic market conditions, such as varying customer demand. The problem involves decisions on where, when and how many facilities to open, along with the quantities to be distributed in each period to each customer. These decisions are taken for a given planning horizon to minimise the costs of locating facilities concerning expected changes in costs or market conditions over the planning horizon.

Wesolowsky & Truscott (1975) is one of the first to review a multi-period model for facility location to study the trade-offs between fixed distribution costs and expenditures for relocation of facilities. The problem involves locating a predetermined number of facilities at potential locations and allocating demand centres to these facilities. In addition, a limited number of facility location changes are allowed each period as facilities can be opened and closed in each period. This problem is also known as the discrete space location-allocation problem in the literature, where Wesolowsky & Truscott (1975) is the first to deal with multi-period or dynamic aspects of the problem. Let A_{jik} denote the present value of the cost of assigning node i to node j in period k. Moreover, let $c^{'}_{jk}$ and $c^{''}_{jk}$ denote the present value of cost of removing and establishing a facility at site j in period k respectively. Parameter m_k represents the maximum number of facility location changes allowed in period K. Variables x_{jik} denote if node i is assigned to node j in period k. Variables $y^{'}_{jk}$ and $y^{''}_{jk}$ indicate if facility is removed or established at site j in period k respectively. The model is formulated as:

$$\min \quad z = \sum_{k=1}^{K}\sum_{i=1}^{N}\sum_{j=1}^{M} A_{jik}x_{jik} + \sum_{k=2}^{K}\sum_{j=1}^{M}\left(c^{'}_{jk}y^{'}_{jk} + c^{''}_{jk}y^{''}_{jk}\right) \tag{3.1}$$

subject to:

$$\sum_{j=1}^{M} x_{jik} = 1, \qquad i = 1, ..., N; \quad k = 1, ..., K \tag{3.2}$$

$$\sum_{j=1}^{N} x_{jik} \leq Nx_{jik}, \quad j = 1, ..., M; \quad k = 1, ..., K \tag{3.3}$$

$$\sum_{j}^{M} x_{jik} = G, \qquad k = 1, ..., K \tag{3.4}$$

$$\sum_{j=1}^{M} y^{'}_{jk} \leq m_k, \qquad k = 2, ..., K \tag{3.5}$$

$$x_{jjk} - x_{jj,k-1} + y^{'}_{jk} - y^{''}_{jk} = 0, \qquad j = 1, ..., M; \quad k = 2, ..., K; \quad i \neq j \tag{3.6}$$

$$x_{jik} \in \{0, 1\}, \quad j = 1, ..., M; \quad i = 1, ..., N; \quad k = 1, ..., K \tag{3.7}$$

$$y^{'}_{jk}, y^{''}_{jk} \in \{0, 1\}, \quad j = 1, ..., M; \quad k = 1, ..., K \tag{3.8}$$

The objective function (3.1) minimises the cost of assigning nodes, removing and establishing facilities for the predetermined planning horizon. Constraint (3.2) ensures that each node i is assigned to exactly one node j in period k. Inequality (3.3) ensures that node i can only be assigned to node j if node j is self-assigned. Equation (3.4) makes sure that G self-assignments are made among the M nodes. Constraint (3.5) restricts the number of sites discontinued in each period from period 2 and throughout K. Constraint (3.6) links the appropriate relocation cost with its respective decision variable. Lastly are the binary requirements for variables x_{jik}, y'_{jk} and y''_{jk} in constraints (3.7) and (3.8) respectively.

This model shows how to handle shifts in e.g. demand or costs during a planning horizon through multi-period analysis. Here, the options for adjustments during the planning horizon are represented by removing or establishing a facility in a period, limited by an upper bound of location changes which may reflect organisational limitations. However, the decisions of removal or establishment are rather cost-intensive and comprehensive, seen through the perspective of supply chain design.

3.2 Multi-Period Facility Location with Capacity Adjustments

Multi-period facility location problems with capacity adjustments can be seen as extensions of the multi-period problem introduced earlier, where capacity adjustments add further flexibility to the multi-period analysis. Capacity adjustments at facility locations can involve both expansion and reduction, which overall allows the production to respond to demand shifts throughout the planning horizon. These capacity adjustments of a facility typically cost a lot less than the complete removal and establishment decisions discussed earlier. With the incorporation of these adjustments comes multiple modelling choices.

One choice of modelling when incorporating capacity adjustments, is if the adjustment is defined as a set of discrete points or as continuous space. The main emphasis of literature will be on the former, and it is often identified as a modular capacitated facility location problem as first presented by Shulman (1991), and later revised by Lee (1991), Mazzola & Neebe (1999) and Correia & Captivo (2003). Arya et al. (2004) demonstrates one of the simplest manners of discrete expansion in the k-capacitated facility location problem. Here, k copies of an initial facility can be added to an existing facility location, sharing the same cost and capacity. In this problem, capacity is simply defined as the maximum number of customers a facility can serve. Matos Dias et al. (2007), in similarity with Shulman (1991), Lee (1991), Mazzola & Neebe (1999) and Correia & Captivo (2003), work with capacities represented by modular structures each with a size and installation cost. Here, the total capacity at a facility is the sum of each module's capacity at the given location.

Jena et al. (2015) and Silva et al. (2021) also work with modular capacities but with a few more extensions to capacity adjustments. In addition to incorporate capacity adjustments, they model the adjustment decisions such that they allow for adjustment during each time period in contrast to only once during the planning horizon. They also extend the capacity adjustments decisions to involve the decisions of full opening and closure of a facility, temporary closure or relocation of capacity between facilities.

3.3 Stochastic Programming

The models considered so far in this chapter can be characterised as deterministic models where the outcome is known for certain. In the study of large-scale optimisation problems which try to capture and represent the real world, most of them will involve some sort of uncertainty. Stochastic programming is a modelling framework that aims to capture this uncertainty, where some model parameters are random variables with estimated or known distributions, and that are revealed after a few or every decision has been made. Birge & Louveaux (2011) present some relevant elements that can be subject to uncertainty in facility location problems. These elements are demand, production costs, distribution costs, prices charged to customers and distribution patterns, and can exist both simultaneously or by themselves.

For stochastic programming, the two-stage structure is the simplest form. This structure aims to make first-stage decisions that fit all possible realisations of the random variables. The first-stage decisions are taken under uncertainty. After the uncertainty is revealed, second-stage decisions can be taken as recourse decisions in order to improve the objective of the problem after the realisation of the random variables. Ravi & Sinha (2004) provide an example of a classical uncapacitated facility location problem with a two-stage stochastic structure. The problem aims to minimise the sum of variable costs and fixed setup costs by determining the location of an unknown number of facilities to serve market demand. The problem is formulated as:

$$\min z = \sum_{i \in F} f_i y_i^0 + \sum_{s=1}^{m} p^s \left(\sum_{i \in F} f_i^s y_i^s + \sum_{i \in F, j \in D} d_j^s c_{ij} x_{ij}^s \right) \tag{3.9}$$

subject to:

$$\sum_{i \in F} x_{ij}^s \geq d_j^s, \qquad j \in D, s \in S \tag{3.10}$$

$$x_{ij}^s \leq y_i^0 + y_i^s, \qquad i \in F, j \in D, s \in S \tag{3.11}$$

$$x_{ij}^s, y_i^s \in \{0,1\}, \qquad i \in F, j \in D, s \in S \tag{3.12}$$

The sets F, D and S denote the set of facilities, clients and scenarios, respectively. Let c_{ij} correspond to the distance between a facility and a client. Furthermore, let d_j^s denote the demand of each client, j, in a given scenario s. Facility opening decisions consist of both first-stage and second-stage decisions with corresponding costs of f_i^0 and f_i^s in scenario s. Let x_{ij}^s be a binary variable which corresponds to if client j is served by facility i in scenario s or not. If so, constraint (3.11) ensures that facility i must be opened in the first stage, the second stage, or both. The problem is single period with no specification of the second stage cost. When discussing facility location problems, this cost can correspond to the building of a new facility, expansion or the cost of unavailability of a facility in a scenario. Most of the applications of stochastic programming for problems involving tactical decisions use only continuous variables. In contrast, facility location or production planning applications involving strategic decisions typically require additional binary variables, making the problems much harder to solve.

3.3.1 Two-Stage Stochastic Multi-Period Facility Location Problems with Capacity Adjustments

In multi-period facility location problems, several parameters can be subject to uncertainty. The larger the time horizon for the problem is, the more difficult it will be to find the optimal location and configuration of facilities to satisfy customer requirements. The uncertain parameters in question can be costs related to investment, operation and distribution, or simply customer demand. Many studies use two-stage stochastic models as an approach to handle the uncertainty. Two-stage stochastic multi-period facility location problems with capacity expansions often tackle uncertain customer demand, and the action of adjusting the total installed capacity through capacity expansion or reduction at specific facilities (with/without closing and/or reopening) copes with the varying demand. Incorporating uncertainty in these types of problems often gives challenges such as large computational requirements. For that reason, studying the solution algorithms designed to solve each problem in this review is just as important as the mathematical formulation of them (Birge & Louveaux 2011).

Alonso-Ayuso et al. (2003) present a two-stage stochastic model for determining facility sizing, production topology, product allocation and selection, and vendor selection for raw materials under uncertainty. Here, facilities can have different capacities, allowing them to expand in defined time periods. The uncertainty in this problem relates to product net price and demand, the raw material supply cost and the production cost. The solution method applied to the problem is named the Branch and Fix Coordination, and is proven to work well on large scale stochastic mixed-integer problems. The technique takes advantage of scenario-wise decomposition schemes, and Alonso-Ayuso et al. (2003) present a specialisation of the Branch and Fix Coordination to be applied to a two-stage structure.

Correia & Melo (2021) introduce a two-stage stochastic multi-period facility location problem under uncertain demand as a consequence of two different customer segments each having distinct service requirements. To solve this problem, they present two different models which differ in whether modular adjustment decisions are treated as first-stage or second-stage decisions. In both models, initial facility location and capacities are defined as first-stage decisions and the operational decisions, such as distribution, are defined as second-stage decisions. Moreover, both models allow capacity expansion and reduction, and these are the only corrective actions for adjusting capacity as facilities must remain open throughout the planning horizon. The reason for this distinction is if the adjustment decisions are seen as strategic or tactical decisions. In an effort to decrease model run time, they develop sets of additional inequalities to improve the polyhedral description of the set of feasible solutions for both models. Through the additional inequalities, they are able to establish lower bounds for least total number of facilities open at a specific design period and minimum quantity of demand satisfied in each period between two design periods respectively. In addition, the Chvátval-Gomory rounding method is applied in both cases.

Ahmed et al. (2003) show that the two-stage structure can be extended to multi-stage structure for facility location problems. They extend the model by allowing revised decision to the capacity in each time stage based upon the uncertainty realised so far. However, our focus will remain on problems with two-stage stochastic structure in the rest of this chapter.

3.3.2 Supply chain design under uncertainty

Lucas et al. (2001) extend the stochastic multi-period facility location problem to involve the design of an entire supply chain under uncertainty. Here, the supply chain is defined by four major stages: production, packing at sites, transportation through distribution centres and delivery to customer zones. For infrastructure investments in distribution networks, the two-stage problem structure is shown to be a reasonable modelling approach due to an underlying temporal disconnection between investment decisions and the operation of the supply chain (Shapiro & Philpott 2007). However, with the involvement of a complete supply chain rather than a set of facilities, the problems tend to grow to large scale mixed integer-programming problems (MILPs) which often are rather computational extensive. Lucas et al. (2001) utilise Lagrangian relaxation in their study, and they show that it is an efficient solution algorithm in their case. Their problem is characterised by having first-stage decisions related to the opening and closing of facilities and capacity, while the second-stage decisions regard operational decisions, such as production quantity, packaging quantity and transportation. Moreover, they incorporate a shortage penalty for not meeting demand.

Santoso et al. (2005) showcases a different approach to solution algorithms for supply chain network design under uncertainty. They investigate the use of an integrated solution methodology consisting of the sample average approximation (SAA) scheme combined with an accelerated Benders decomposition algorithm. The problem consists of first-stage decisions related to configuration decisions of processing centres to build and which processing and finishing machines to procure, while the second-stage decisions relate to processing and transporting products from suppliers to customers. The stochastic parameters which are revealed in the second-stage of the problem are processing and/or transportation costs, supplies, demands and capacities. The results show great improvement in solution time versus sample time for the problem. For a real-world sized instance of the problem, the solution time went from just under 80 000 seconds to approximately 10 000 seconds when comparing the solution of a monolithic deterministic equivalent problem with the solution of the stochastic problem with the accelerated decomposition technique.

Oliveira et al. (2014) look into optimisation under uncertainty of the petroleum product supply chain. Their focus lies in solving their two-stage stochastic model of the planning problem. For that reason, they study the use of the L-shaped method (stochastic Benders decomposition) and the development of acceleration techniques to reduce solution time further. The problem includes the consideration of an integrated distribution network design, facility location and discrete capacity expansion under a multi-product and multi-period setting. The uncertainties are related to the product demand levels. The objective is to minimise the investment and logistics costs in order to meet demand at bases in the network. The first-stage decisions consist of which investment decisions related to capacity expansion and commodity arcs to implement and when, while the second-stage decisions regard inventory levels, product flows, supply levels at sources and supply provided at demand sites. The results show that the solution time decreases by 4.5 times for a larger number of scenarios in a realistic petroleum supply chain instance when comparing the accelerated algorithm with the full space equivalent deterministic problem.

Nunes et al. (2015) study the design of a hydrogen supply chain under uncertainty. In this problem, they use a two-stage stochastic structure. The objective is to minimise the cost of production, storage and transportation while satisfying demand at consumption points throughout the planning horizon. The hydrogen demand is uncertain and treated as stochastic in each time period. Investments in plants and warehouses are treated as first-stage variables, and the transportation and operation of the supply chain are left as second-stage variables in the model. To correctly represent the stochastic demand, large numbers of scenarios are generated. To overcome the computational requirements these scenarios introduce, Nunes et al. (2015) use the sample average approximation technique.

The field of supply chain design under uncertainty in operation research is too extensive to be able to highlight all the relevant papers for our thesis. However, we would like to draw attention to the review paper done by Govindan et al. (2017). Govindan et al. (2017) identifies and structures the most relevant papers from the last two decades regarding supply chain design problems under different types of uncertainty.

Chapter 4

Problem Description

The two-stage stochastic facility location problem with capacity adjustments studies where to construct, expand, or reduce production facilities to satisfy customers' uncertain demand. The objective is to establish the optimal schedule for where and when to open hydrogen production facilities, which capacity and production technology to install, adjust their capacity, and distribute the produced hydrogen.

We have a set of customers with uncertain hydrogen demand in our problem. A set of different demand scenarios specifies the uncertain customer demand. For hydrogen production, we are given a set of possible locations where production facilities may open. Different production technologies give the choice of how hydrogen should be produced at the production facilities. The production levels that can be installed are given by a set of discrete capacities for production. The planning horizon is specified by a set of time periods.

A two-stage structure characterises the problem. The first stage is associated with deciding where to establish facilities and how their initial capacities and production technology should be. These first-stage decisions are investment decisions and are related to long-term costs. The long-term costs are given as S-shape functions. The second stage includes deciding where and when to adjust capacity, how much to produce, and how to distribute in response to realised demand level. Except for capacity adjustments associated with long-term costs, the second stage decisions are generally related to short-term costs. The costs from production and distribution make up the short-term costs. The production costs follow piece-wise linear convex functions, while distribution costs are linear.

Moreover, there may be one opened production facility at each possible location. When determining to invest in a facility, two significant decisions must be made:

which production technology and initial production capacity to install. It is not allowed to switch production technology at an opened facility during the planning horizon. Prior to an eventual capacity adjustment, the available production capacity will be the upper limit for the facilities' hydrogen production. These two decisions are significant as they will be decided before realising the uncertain demand level. Therefore, they will be equal for all possible demand levels and a basis for the production level.

To respond to the realised customer demand level, adjusting the originally installed capacity by either expansion or reduction is an option. The costs of capacity adjustments are more expensive in total than investing in that capacity initially. The possibility of adjusting capacity can only be made after the facility is opened. The decisions to either expand or reduce capacity will offer more flexibility for the production to cope with the development in future hydrogen demand. The option to reduce the capacity also implies that a facility can be shut down, but the re-opening of a facility is not allowed.

Furthermore, production quantities are limited to each facility's production capacities and utilisation rates. The installed production capacity will serve as an upper bound for production quantities at any time period of the planning horizon. In contrast, the installed production technology's required minimum utilisation rate will be the lower bound for production quantities. Production that surpasses these bounds must be penalised. Regardless of future developments in customer demand, the customer demand must be either met or shortfall penalised.

Several production facilities can meet customers' demands at any given time, which suppliers who distribute to a customer can change between different time periods. However, facilities cannot be distributed to customers that surpass a given maximum travelling distance because of limitations in current distribution costs.

Our problem aims to minimise the expected discounted cost of the sum of investment, expansion, reduction, production, and distribution costs.

Chapter 5

Mathematical Model

This chapter presents our mathematical model for the problem described earlier in Chapter 4. Section 5.1 briefly explains the modelling approach. Then Section 5.2 introduces the general modelling assumptions. The chapter ends with the mathematical formulation of the problem in Section 5.3.

5.1 Modelling Approach

Our modelling approach is a continuation of the work done in Aglen & Hofstad (2021). We extend our model by including the possibilities of reducing production capacity and closing down factories. The model can now be characterised as a two-stage stochastic facility location with capacity adjustments with these new extensions.

5.1.1 Decision variables

We model the investment and eventually capacity adjustment decisions as a selection amongst available capacities from a discrete set. The capacity adjustments between the available capacities of an established facility are pre-decided discrete jumps. This approach is similar to in Aglen & Hofstad (2021). Like the modelling approach by Correia & Melo (2019), our investment decisions are independent of the demand scenarios, while the capacity adjustment decisions are dependent. We are modelling the capacity adjustments as dependent is to better react to each individual scenario.

Additionally to the capacity adjustments to handle the uncertain demand, we have included penalties for demand shortfalls and overproduction. For the model, this penalty for shortage in demand will allow for additional feasible solutions and add more flexibility to the model. On the other side, since the option to not meet the level of demand is not preferred, we model it as a relatively high cost. The incorporation of penalty cost for demand shortfall is similar to the method used in Lucas et al. (2001).

5.1.2 Modelling costs

Each given capacity has a short-term production cost function connected to it in our model, and these short-term production costs are piece-wise linear convex functions. Additionally, we model the costs such that lower utilisation of higher installed capacity is less favourable than higher utilisation of smaller installed capacity. This approach is similar to the one used in Aglen & Hofstad (2021). Figure 5.1a illustrates the approach for modelling capacity adjustments of facilities in our model. Let $C_{k'p}$ be the investment costs for capacity point k' and production technology p, and $Q_{bk'p}$ the corresponding initial invested capacity at breakpoint b. The adjustment costs $E_{k'k''p}$ are the costs for expanding to capacity $Q_{bk''p}$ from capacity $Q_{bk'p}$. Since, $C_{k'p}$ $< C_{k''p} + E_{k'k''p}$, investing in a more extensive facility right away is cheaper than expanding from an investment in a smaller facility. The β illustrates this additional cost in the figure. Similarly, Figure 5.1a illustrates the reduction from initial capacity $Q_{bk'p}$ to capacity Q_{bkp} and shows that it is more favourable to invest in a smaller capacity right away than to reduce down, avoiding the extra expenses represented as α. Moreover, our model also allows to reduce a facility's initial capacity, $Q_{bk'p}$, to zero - representing a facility shutdown with a corresponding cost.

We use separate variables connected with the investment and capacity adjustment decisions, respectively, to model the switch from one short-term production cost function to another after capacity adjustment. Figure 5.1b illustrates an example of this modelling approach, where an initial capacity of $Q_{bk'p}$, the production cost function $f_{bk'p}(q)$ applies, while after reducing the facility to capacity Q_{bkp}, the function $f_{bkp}(q)$ becomes active. The squared boxes of the functions are the capacities at 100 % utilisation, while the circles are breakpoints b of lower utilisation.

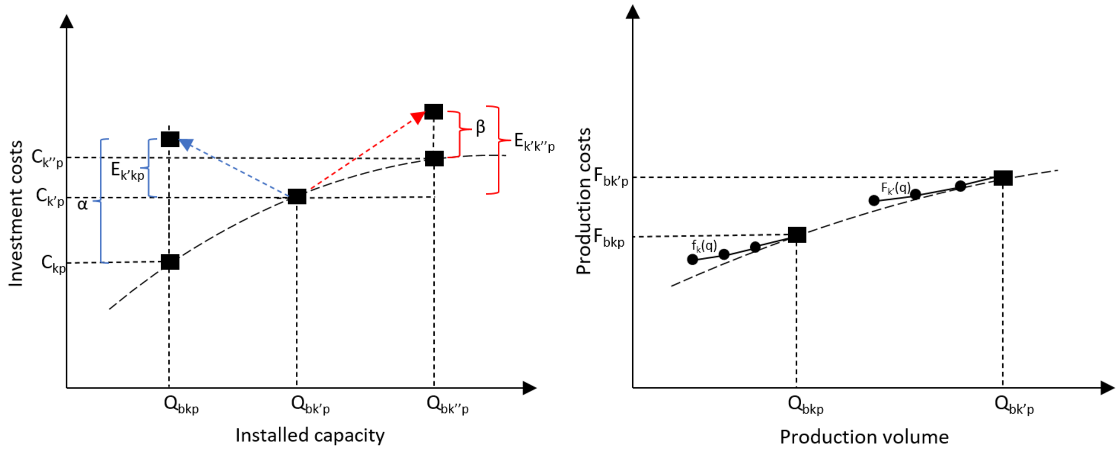

(a) Long-term costs.

(b) Short-term costs.

Figure 5.1: Illustrations of how costs are modelled.

5.2 Assumptions

- **The costs for investing and adjusting capacity are independent of time and location in the model.** The costs for opening or adjusting the capacity of a facility are not dependent on which time period the investment decision happens. In addition, the costs do not change with the selection of the location for the facility, implying that every possible facility location is equally valued.

- **The distribution costs depend only on distance and amount.** We assume that the preferred distribution technology is already decided and that the costs of the technology is a part of the cost function. Therefore, the distribution costs in our model only depend on the amount transported and the distance between the production facility and the customer.

5.3 Mathematical Formulation

First we present the notation we use in our model:

Sets

$\mathcal{B}$ - Set of breakpoints for the short-term cost function;
$\mathcal{I}$ - Set of facility locations;
$\mathcal{J}$ - Set of customer locations;

$\mathcal{K}$ - Set of possible discrete capacities;

$\mathcal{P}$ - Set of production technologies;

$\mathcal{S}$ - Set of scenarios;

$\mathcal{T}$ - Set of time periods.

Subsets

$\mathcal{L}_k \subseteq \mathcal{K}$ - Subset of discrete capacities not containing element k;

$\mathcal{T}' \subseteq \mathcal{T}$ - Subset of time periods excluding the first time period.

Parameters

C_{lp} -	investment costs for point l of capacity function, and technology p, $l \in \mathcal{L}_0, p \in \mathcal{P}$;
D^s_{jt} -	demand at customer j in period t, in scenario s, $j \in \mathcal{J}, t \in \mathcal{T}, s \in \mathcal{S}$;
E_{lkp} -	costs of capacity adjustment from point l to capacity in point k for technology p, $l \in \mathcal{L}_0, \{k \in \mathcal{K} \mid k \neq l\}, p \in \mathcal{P}$;
F_{bkp} -	costs at breakpoint b of the short-term cost function given for capacity k and for technology p, $b \in \mathcal{B}, k \in \mathcal{K}, p \in \mathcal{P}$;
L_{ij} -	1 if demand at customer location j can be served from facility i, 0 otherwise, $i \in \mathcal{I}, j \in \mathcal{J}$;
M -	penalty cost per unit hydrogen not supplied;
p^s -	probability of scenario s, $s \in \mathcal{S}$;
Q_{bkp} -	production volume at breakpoint b of the short-term cost function, for capacity point k and technology p, $b \in \mathcal{B}, k \in \mathcal{K}, p \in \mathcal{P}$;
R_t -	discount rate in period t, $t \in \mathcal{T}$;
T_{ij} -	distribution costs from facility i to customer j, $i \in \mathcal{I}, j \in \mathcal{J}$.

Decision variables

e^s_{it} -	amount of overproduced hydrogen at facility i in period t in scenario s, $i \in \mathcal{I}, t \in \mathcal{T}, s \in \mathcal{S}$;
w^s_{it} -	amount of penalised hydrogen at facility i in period t in scenario s, $i \in \mathcal{I}, t \in \mathcal{T}, s \in \mathcal{S}$;
u^s_{ijt} -	amount of customer demand at location j satisfied from facility i in period t in scenario s, $i \in \mathcal{I}, j \in \mathcal{J}, t \in \mathcal{T}, s \in \mathcal{S}$;
x_{ilpt} -	1 if facility is open at location i in period t, with originally installed capacity l, and technology p, 0 otherwise, $i \in \mathcal{I}, l \in \mathcal{L}_0, p \in \mathcal{P}, t \in \mathcal{T}$;
y^s_{ilkpt} -	1 if facility has been adjusted at location i in period t, from original capacity l, to capacity k, and technology p in scenario s, 0 otherwise, $i \in \mathcal{I}, l \in \mathcal{L}_0, \{k \in \mathcal{K} \mid k \neq l\}, p \in \mathcal{P}, t \in \mathcal{T}', s \in \mathcal{S}$;
μ^s_{ilbpt} -	weight of breakpoint b at location i for original capacity point l and technology p in period t in scenario s, $i \in \mathcal{I}, l \in \mathcal{L}_0, b \in \mathcal{B}, p \in \mathcal{P}, t \in \mathcal{T}, s \in \mathcal{S}$;
ν^s_{ikbpt} -	weight of breakpoint b at location i for adjusted capacity point k and technology p in period t in scenario s, $i \in \mathcal{I}, k \in \mathcal{K}, b \in \mathcal{B}, p \in \mathcal{P}, t \in \mathcal{T}', s \in \mathcal{S}$.

We now present the mathematical model. First, we introduce the first-stage problem with respective constraints. Next, we present the second-stage problem for a given scenario s with associated restrictions.

First-stage problem:

$$\min \quad \sum_{i\in\mathcal{I}}\sum_{l\in\mathcal{L}_0}\sum_{p\in\mathcal{P}} C_{lp}(\sum_{t\in\mathcal{T}'} R_t(x_{ilpt} - x_{ilp(t-1)}) + R_1 x_{ilp1}) + \sum_{s\in\mathcal{S}} p^s \Psi^s(x) \tag{5.1}$$

subject to:

$$\sum_{l\in\mathcal{L}_0}\sum_{p\in\mathcal{P}} x_{ilpt} \leq 1, \qquad i\in\mathcal{I}, t\in\mathcal{T}, \tag{5.2}$$

$$x_{ilpt} \geq x_{ilp(t-1)}, \qquad i\in\mathcal{I}, l\in\mathcal{L}_0, p\in\mathcal{P}, t\in\mathcal{T}', \tag{5.3}$$

$$x_{ilpt} \in \{0,1\}, \qquad i\in\mathcal{I}, l\in\mathcal{L}_0, p\in\mathcal{P}, t\in\mathcal{T}. \tag{5.4}$$

Equation (5.1) is the objective function, which aims to minimise the sum of the total discounted first-stage investment costs and the expected second-stage costs. Restrictions (5.2) ensure that only one facility can be opened at the given location i. Constraints (5.3) in combination with restrictions (5.2) guarantee that a facility cannot be re-opened if it has been closed. The first-stage variables binary requirements are stated in restrictions (5.4).

The second-stage problem $\Psi^s(x)$ for a given scenario $s\in\mathcal{S}$ is formulated as:

$$\begin{aligned}\Psi^s(x) = \min &\sum_{i\in\mathcal{I}}\sum_{k\in\mathcal{K}}\sum_{b\in B}\sum_{p\in\mathcal{P}}\sum_{t\in\mathcal{T}} R_t G_{bkp}(\mu^s_{ikbpt} + \nu^s_{ikbpt})\\ &+ \sum_{i\in\mathcal{I}}\sum_{l\in\mathcal{L}_0}\sum_{\{k\in\mathcal{K}|k\neq l\}}\sum_{p\in\mathcal{P}}\sum_{t\in\mathcal{T}'} R_t E_{lkp}(y^s_{ilkpt} - y^s_{ilkp(t-1)})\\ &+ \sum_{i\in\mathcal{I}}\sum_{j\in\mathcal{J}}\sum_{t\in\mathcal{T}} R_t T_{ij} u^s_{ijt} + \sum_{i\in\mathcal{I}}\sum_{t\in\mathcal{T}} R_t M(e^s_{it} + w^s_{it})\end{aligned} \tag{5.5}$$

subject to:

$$x_{ilp(t-1)} \geq \sum_{\{k\in\mathcal{K}|k\neq l\}} y^s_{ilkpt}, \qquad i\in\mathcal{I}, l\in\mathcal{L}_0, p\in\mathcal{P}, t\in\mathcal{T}', \tag{5.6}$$

$$y^s_{ilkpt} \geq y^s_{ilkp(t-1)}, \qquad i\in\mathcal{I}, l\in\mathcal{L}_0, \{k\in\mathcal{K}|k\neq l\}, p\in\mathcal{P}, t\in\mathcal{T}', \tag{5.7}$$

$$\sum_{b\in\mathcal{B}} \mu^s_{ilbpt} + \sum_{\{k\in\mathcal{K}|k\neq l\}} y^s_{ilkpt} = x_{ilpt}, \qquad i\in\mathcal{I}, l\in\mathcal{L}_0, p\in\mathcal{P}, t\in\mathcal{T}, \tag{5.8}$$

$$\sum_{b\in\mathcal{B}} \nu^s_{ikbpt} = \sum_{l\in\mathcal{L}_0} y^s_{ilkpt}, \qquad i\in\mathcal{I}, \{k\in\mathcal{K}|k\neq l\}, p\in\mathcal{P}, t\in\mathcal{T}', \tag{5.9}$$

$$\sum_{j\in\mathcal{J}} u^s_{ijt} + e^s_{it} - w^s_{it} - \sum_{k\in\mathcal{K}}\sum_{b\in\mathcal{B}}\sum_{p\in\mathcal{P}} Q_{bkp}(\mu^s_{ikbpt} + \nu^s_{ikbpt}) = 0, \quad i\in\mathcal{I}, t\in\mathcal{T}, \tag{5.10}$$

$$u^s_{ijt} \leq L_{ij} D^s_{jt}, \quad i\in\mathcal{I}, j\in\mathcal{J}, t\in\mathcal{T}, \tag{5.11}$$

$$\sum_{i\in\mathcal{I}} u^s_{ijt} = D^s_{jt}, \quad j\in\mathcal{J}, t\in\mathcal{T}, \tag{5.12}$$

$$e^s_{it} \geq 0, \quad i\in\mathcal{I}, t\in\mathcal{T}, \tag{5.13}$$

$$u^s_{ijt} \geq 0, \quad j\in\mathcal{I}, j\in\mathcal{J}, t\in\mathcal{T}, \tag{5.14}$$

$$w^s_{it} \geq 0, \quad i\in\mathcal{I}, t\in\mathcal{T}, \tag{5.15}$$

$$y^s_{ilkpt} \in \{0,1\}, \quad i\in\mathcal{I}, l\in\mathcal{L}_0, \{k\in\mathcal{K} | k\neq l\}, p\in\mathcal{P}, t\in\mathcal{T}', \tag{5.16}$$

$$\mu^s_{ilbpt} \geq 0, \quad i\in\mathcal{I}, l\in\mathcal{L}_0, b\in\mathcal{B}, p\in\mathcal{P}, t\in\mathcal{T}, \tag{5.17}$$

$$\nu^s_{ikbpt} \geq 0, \quad i\in\mathcal{I}, k\in\mathcal{K}, b\in\mathcal{B}, p\in\mathcal{P}, t\in\mathcal{T}'. \tag{5.18}$$

Equations (5.5) represent the second-stage objective function, which consists of the sum of discounted costs for production, capacity adjustment, distribution, and penalties for shortfall in demand and overproduction. Restrictions (5.6) link variables for investment and capacity adjustments, and guarantee that a facility can only expand or reduce capacity after it has been opened. Constraints (5.7) ensure that only one capacity adjustment can be made at an opened facility i. The combination of equations (5.8) and (5.9), guarantee that production is only allocated to facilities that have been opened, and link the installed capacity with its associated short-term cost function. The short-term production cost functions depend either on the original installed capacity l at facility i, or the capacity k after an adjustment of the capacity has been made. Restrictions (5.10) guarantee that all quantities produced are distributed to the customers to meet the demand level. Additionally it penalises overproduction and shortfall of demand. Equations (5.11) restrict which facility i can satisfy demand at customer j. Constraints (5.12) guarantee that demand will be satisfied. Restrictions (5.13) to (5.18) are the second-stage variables binary and non-negativity requirements.

Chapter 6

Solution Method Approach

In this chapter, we introduce the solution method used to solve the mathematical model presented in Chapter 5. First, Section 6.1 presents the relevant theory to exploit the structure of our two-stage stochastic facility location problem with capacity adjustments. Next, Section 6.2 shows the Benders reformulation of the model presented previously in Chapter 5. After that, Section 6.3 introduces our L-shaped decomposition algorithm based on the Benders reformulation of our problem. Lastly, in Section 6.4, we introduce some acceleration methods for our L-shaped decomposition algorithm.

6.1 Two-stage Stochastic Programming

This section aims to provide the reader with two-stage stochastic programs' theory and basic properties. In particular, we study the characteristic structure of two-stage stochastic programs and decomposition methods designed to exploit this structure.

6.1.1 Two-Stage Stochastic Linear Programs

Birge & Louveaux (2011) present the following formulation for a two-stage stochastic linear program:

$$\min z = c^T x + E_\xi[\min \ q_s^T y_s] \tag{6.1}$$

subject to:

$$Ax = b, \tag{6.2}$$

$$T_s x + W y_s = h_s, \tag{6.3}$$

$$x \geq 0, \quad y_s \geq 0, \tag{6.4}$$

Considering the formulation (6.1)-(6.4), we observe that this stochastic linear program consists of two stages. The division into two stages originates from the information available. We assume that there is a finite set of possible scenarios, $\mathcal{S}$, that may occur. Several decisions have to be taken before uncertainty is revealed. These decisions are named first-stage decisions, and the period for which these decisions are made is called the first stage. We denote the first-stage variables as x. These decisions are found in the first term in the objective function, (6.1), and the constraints, (6.2), which constitute the deterministic terms in the problem formulation. Additionally, we observe x in equations (6.3), where it is connected to decisions in the other stage. These decisions are named second-stage decisions, and the period for these decisions is called the second stage. Here, there are decisions to be made after the uncertainty is revealed. Furthermore, we notice that some of the parameters and variables have dependencies on a scenario, s. The x decisions are independent of s and are equal for all realisations of s. However, the dependency of y on s, which we call the second-stage variables, makes the problem more complex as the second-stage decisions are not necessarily the same under each scenario.

In some cases, the objective values and feasible regions have special properties useful for computation. One of these properties is if the problem has *relatively complete recourse*. In this case, every first-stage solution x, satisfying $Ax = b$, is also feasible in the second stage. *Complete recourse* is a special type of relatively complete recourse. This is the case when there exists $y \geq 0$ such that $Wy = t$ for all $t \in R$. This means there is always a recourse action no matter what first-stage solution x or the realisation of scenario s occurs.

6.1.2 L-shaped Method

Van Slyke & Wets (1969) were the first to present the L-shaped algorithm. They present the algorithm as a tool to solve stochastic programs. The basic principle of the L-shaped method, as presented by Birge & Louveaux (2011), is to approximate the recourse function in the objective function of problems with a structure to the formulation given by equations (6.1) - (6.4). The fundamental idea is to avoid several function evaluations for the recourse function, as the recourse function involves solving all second-stage recourse linear programs. Therefore, the recourse function is used to establish a master problem in x, where the recourse function is only evaluated exactly as a sub-problem. This is achieved by assuming finite support for the random vector ξ. Let $s = 1, ..., S$ index the possible realisations and p_s its respective probability, which is illustrated in equation (6.5) . We are now able to rewrite the problem (6.1) - (6.4) into a deterministic equivalent problem in the extensive form (EF), under the assumption that one set of second-stage decisions, y_s, is associated to each realisation of ξ, i.e. q_s, h_s and T_s. The extensive form (EF) is given below:

$$\min z = c^T x + \sum_{s=1}^{S} p_s q_s^T y_s \tag{6.5}$$

subject to: (6.2) - (6.4)

The characteristic block-diagonal structure for two-stage problems is evident in the extensive form, as illustrated in Figure 6.1. The block-diagonal matrix grows very large, even for a moderate number of scenarios. Algorithms such as Benders decomposition or the L-shaped method exploit this block structure. Benders decomposition is a reformulation and decomposition method to solve large linear programs. The L-shaped method is Benders decomposition applied to stochastic programs (Louveaux & Birge 2009).

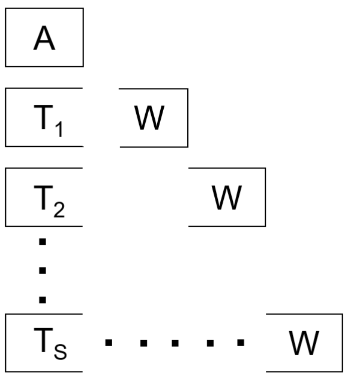

Figure 6.1: Block structure of the EF (Birge & Louveaux 2011).

Before applying the L-shaped algorithm to the EF problem with objective function (6.5) and the assumption of relatively complete recourse, it is common to reformulate it through the use of Benders reformulation. Benders reformulation splits the original problem formulation into two separate problems called the master problem and sub-problem, respectively.

$$\begin{aligned}
\min \quad & c^\top x + \theta && (6.6)\\
\text{s.t.} \quad & Ax \geq b, && (6.7)\\
& \theta \geq \sum_{s=1}^{S} p_s q_s^T y_s, && (6.8)\\
& x \in \mathbb{R} && (6.9)\\
& y_s \in \mathbb{R} && (6.10)
\end{aligned}$$

Benders reformulation applied to the problem formulation given by equations (6.2)-(6.5) results in a master problem in the form given by equations (6.6)-(6.10). Here, we find the deterministic term again in the objective function along with restriction (6.7). Constraints (6.8) represent cuts, later referred to as optimality cuts, which initially are an empty set and get generated iteratively when moving between the master and sub-problem. The last term in the objective function estimates the second-stage costs. Due to the assumption of relatively complete recourse, optimality cuts are the only cuts we are adding to our master problem. This reformulation represents an approach called the single-cut technique. The name single-cut comes from that contribution from all scenarios are summed in one cut as we see in constraints (6.8).

The sub-problem is given by (6.11)-(6.13):

$$\begin{aligned}
\min \quad & q_s^\top y && (6.11)\\
\text{s.t.} \quad & Wy = h_s - T_s x && (6.12)\\
& y \in \mathbb{R} && (6.13)
\end{aligned}$$

In the sub-problems, the optimality cuts can be generated by solving the (6.11)-(6.13) problem. If we exploit the fact that $y \in R$ and assume boundedness for our sub-problem, we can formulate the dual problem of the sub-problem with π denoting the dual variables. The dual feasible space does not depend on the y-variables. If the dual feasible space is non-empty, the primal problem is bounded and non-empty, meaning that the original problem is feasible, which is always the case with relatively complete recourse. This will, in turn, result that the recourse function is computable from solving the sub-problem formulated as (Luedtke 2016):

Assuming $\Pi_s := \left\{\pi : \pi^\top W \leq q_s\right\} \neq \emptyset$:

$$\begin{aligned} Q_s(x) &= \min_y \left\{q_s^\top y : Wy = h_s - T_s x, y \in \mathbb{R}_+\right\} \\ &= \max_\pi \left\{\pi^\top \left(h_s - T_s x\right) : \pi^\top W \leq q_s\right\} \\ &= \max \left\{\left(\pi^s\right)^\top \left(h_s - T_s x\right) : \pi^s \in \mathrm{XP}\left(\Pi_s\right)\right\} \end{aligned}$$

where $\mathrm{XP}\left(\Pi_s\right)$ is the finite set of extreme points of Π_s.

We observe that we can formulate optimality cuts from the optimal dual solution $(\hat{\pi}^s)$ to the sub-problem on the form:

$$\theta \geq \sum_{s=1}^{S} p_s \left(\hat{\pi}^s\right)^\top \left(h_s - T_s x\right) \tag{6.14}$$

The L-shaped algorithm iteratively moves between the master and sub-problem discussed above, starting with a relaxed master problem initially containing no cuts. The algorithm generates cuts of two types for a general problem, and optimality cuts are added by solving the sub-problems discussed above. In addition, feasibility cuts may be added if the problem does not have relatively complete recourse. Below is the outline for the L-shaped algorithm for a general two-stage problem.

L-Shaped Algorithm

Step 0. Set $r = i = v = 0$ (v is the iteration counter, while r and i are vectors containing the feasibility and optimality cuts).

Step 1. Set $v = v + 1$. Solve the linear program given by Equation 6.15 to Equation 6.19.

$$\min z = c^T x + \theta \tag{6.15}$$

subject to:

$$Ax = b, \tag{6.16}$$

$$D_\ell x \geq d_\ell, \qquad \ell = 1, \ldots, r, \tag{6.17}$$

$$E_\ell x + \theta \geq e_\ell, \qquad \ell = 1, \ldots, i, \tag{6.18}$$

$$x \geq 0, \qquad \theta \in R. \tag{6.19}$$

Let (x^v, θ^v) be an optimal solution to problem (6.15)-(6.19). If no (6.18) is present (optimality cut), θ^v is set equal to $-\infty$ and is not considered in the computation of x^v.

Step 2. Check if x^v is feasible in the second-stage. If not generate feasibility cut by solving the linear program for $s = 1, \ldots, S$

$$\min w' = e^T v^+ + e^T v^- \tag{6.20}$$

subject to:

$$Wy + Iv^+ - Iv^- = h_s - T_s x^v \tag{6.21}$$
$$y \geq 0, \quad v^+ \geq 0, \quad v^- \geq 0 \tag{6.22}$$

where $e^T = (1, \ldots, 1)$, until, for some s, the optimal value $w' > 0$. In this case, let σ^v be the associated dual multipliers and define

$$D_{r+1} = (\sigma^v)^T T_s \tag{6.23}$$

and

$$d_{r+1} = (\sigma^v)^T h_s \tag{6.24}$$

to generate a constraint (called a feasibility cut) of type (6.17). Set $r = r + 1$, add to the constraint set (6.17), and return to Step 1. Otherwise, go to Step 3.

Step 3. Generates optimality cuts for feasible x^v.
For $s = 1, \ldots, S$ solve the linear program:

$$\min w = q_s^T y \tag{6.25}$$

subject to:

$$Wy = h_s - T_s x^v, \tag{6.26}$$
$$y \geq 0. \tag{6.27}$$

Let π_s^V be the dual multipliers associated with the optimal solution of Problem s of type as (6.26). Define

$$E_{i+1} = \sum_{s=1}^{S} p_s \cdot \left(\pi_s^V\right)^T T_s \tag{6.28}$$

and

$$e_{i+1} = \sum_{s=1}^{S} p_s \cdot \left(\pi_s^V\right)^T h_s. \tag{6.29}$$

Let $w^v = e_{i+1} - E_{i+1}x^v$. If $\theta^v \geq w^v$, stop; x^v is an optimal solution. Otherwise, set $i = i + 1$, add to (6.18) (optimality cut), and return to Step 1.

6.1.3 Continuous L-shaped cuts vs. Integer L-shaped cuts

Laporte & Louveaux (1993) discuss the implications of applying the L-shaped method to problems with first stage binary decision variables and integer second stage variables. For a two-stage stochastic program where the second stage variables are relaxed to continuous, they present the following proposition:

Proposition 1. *Any continuous L-shaped optimality cut is a lower bound on the recourse function.*

Proposition 1 implies that if the vector containing the second stage variables is relaxed to be continuous, an optimality cut generated from solving the belonging sub-problem, will serve as an lower bound for the cut.

In recent times, more effort has been put into improving the lower bound of continuous L-shaped cuts identified by Laporte & Louveaux (1993) when the problem involves two-stage stochastic mixed-integer programs (SMIPs) in which mixed-integer decisions appear in both stages. Qi & Sen (2016) design time-staged decomposition algorithms for solving SMIPs, and present different algorithms inspired by earlier work from Chen et al. (2012). Both papers share the idea of a hierarchy of multi-term disjunctions to convexify a feasible set of a mixed-integer linear program. The approach is different from relying on dual information and continuous relaxation for the approximation of the second stage value function. Chen et al. (2012) use a convexification scheme for the second stage based on the cutting plane tree method. Qi & Sen (2016) display two closely related convexification schemes, one based on Branch and Bound convexification method, and the other on the cutting plane tree method. Angulo et al. (2016) present and combine two different strategies to improve the performance of the L-shaped algorithm for integer problems. The first method alternates between linear and mixed-integer sub-problems to avert time-consuming exact evaluations of the recourse function. In the second method, optimality cuts are generated from a linear program that considers information from all solutions found up to a certain stage of the program to improve the approximation of the recourse function's shape. We will not look into any of these techniques in this thesis, but present it as a suggestion for future research.

6.2 Benders Reformulation of the Mathematical Model

The Benders decomposition splits the complex problem, formulated in Chapter 5, into two more easily solvable problems, here represented by the master and sub-problem. The aim of this section is to present a formulation that is able to solve faster for large problem instances.

This section describes the Benders reformulation of our mathematical model. Almost all indices, sets, parameters and decision variables are equal, as in Chapter 5. Only new notation will be further explained.

6.2.1 New Notation for the Benders Reformulation

Parameters

$\hat{x}_{ilpt}$ -	First stage investment decisions from solved master problem in current L-shaped iteration, $i \in \mathcal{I}, l \in \mathcal{L}_0, p \in \mathcal{P}, t \in \mathcal{T}$;
α^s_{ilpt} -	Dual value of constraint (5.6) in current L-shaped iteration, $i \in \mathcal{I}, l \in \mathcal{L}_0, p \in \mathcal{P}, t \in \mathcal{T}, s \in \mathcal{S}$;
β^s_{ilpt} -	Dual value of constraint (5.8) in current L-shaped iteration, $i \in \mathcal{I}, l \in \mathcal{L}_0, p \in \mathcal{P}, t \in \mathcal{T}, s \in \mathcal{S}$;
γ^s_{ijt} -	Dual value of constraint (5.11) in current L-shaped iteration, $i \in \mathcal{I}, j \in \mathcal{J}, t \in \mathcal{T}, s \in \mathcal{S}$;
τ^s_{jt} -	Dual value of constraint (5.12) in current L-shaped iteration, $j \in \mathcal{J}, t \in \mathcal{T}, s \in \mathcal{S}$.

Decision Variables

θ - Estimator of total second-stage costs given single-cut algorithm in current iteration,

θ^s - Estimator of total second-stage costs in scenario s given multi-cut algorithm in current iteration, $s \in \mathcal{S}$.

6.2.2 Sub-problem

The sub-problem is given by objective function (6.30) and constraints (6.31) - (6.43). The sub-problem corresponds to the LP-relaxation of the second-stage problem, $\Psi^s(x)$, defined by equations (5.5)-(5.18). Solution $\hat{x}$ from the master problem is the optimal investment decision in the current iteration, and used as input in the sub-problem to generate the right-hand sides of constraints of (6.31) and (6.33).

$$\begin{aligned}\Psi^s(\hat{x}) = \min \sum_{i\in\mathcal{I}}\sum_{k\in\mathcal{K}}\sum_{b\in B}\sum_{p\in\mathcal{P}}\sum_{t\in\mathcal{T}} R_t G_{bkp}(\mu^s_{ikbpt} + \nu^s_{ikbpt}) \\ + \sum_{i\in\mathcal{I}}\sum_{l\in\mathcal{L}_0}\sum_{\{k\in\mathcal{K}|k\neq l\}}\sum_{p\in\mathcal{P}}\sum_{t\in\mathcal{T}'} R_t E_{lkp}(y^s_{ilkpt} - y^s_{ilkp(t-1)}) \\ + \sum_{i\in\mathcal{I}}\sum_{j\in\mathcal{J}}\sum_{t\in\mathcal{T}} R_t T_{ij} u^s_{ijt} + \sum_{i\in\mathcal{I}}\sum_{t\in\mathcal{T}} R_t M(e^s_{it} + w^s_{it})\end{aligned} \tag{6.30}$$

subject to:

$$\sum_{\{k\in\mathcal{K}|k\neq l\}} y^s_{ilkpt} \leq \hat{x}_{ilp(t-1)}, \qquad i\in\mathcal{I}, l\in\mathcal{L}_0, p\in\mathcal{P}, t\in\mathcal{T}'(\alpha^s_{ilpt}), \tag{6.31}$$

$$y^s_{ilkp(t-1)} - y^s_{ilkpt} \leq 0, \qquad i\in\mathcal{I}, l\in\mathcal{L}_0, \{k\in\mathcal{K}|k\neq l\}, p\in\mathcal{P}, t\in\mathcal{T}', \tag{6.32}$$

$$\sum_{b\in\mathcal{B}} \mu^s_{ilbpt} + \sum_{\{k\in\mathcal{K}|k\neq l\}} y^s_{ilkpt} = \hat{x}_{ilpt}, \qquad i\in\mathcal{I}, l\in\mathcal{L}_0, p\in\mathcal{P}, t\in\mathcal{T}(\beta^s_{ilpt}), \tag{6.33}$$

$$\sum_{b\in\mathcal{B}} \nu^s_{ikbpt} - \sum_{l\in\mathcal{L}_0} y^s_{ilkpt} = 0, \qquad i\in\mathcal{I}, \{k\in\mathcal{K}|k\neq l\}, p\in\mathcal{P}, t\in\mathcal{T}', \tag{6.34}$$

$$\sum_{j\in\mathcal{J}} u^s_{ijt} + e^s_{it} - w^s_{it} - \sum_{k\in\mathcal{K}}\sum_{b\in\mathcal{B}}\sum_{p\in\mathcal{P}} Q_{bkp}(\mu^s_{ikbpt} + \nu^s_{ikbpt}) = 0, \quad i\in\mathcal{I}, t\in\mathcal{T}, \tag{6.35}$$

$$u^s_{ijt} \leq L_{ij} D^s_{jt}, \qquad i\in\mathcal{I}, j\in\mathcal{J}, t\in\mathcal{T}(\gamma^s_{ijt}), \tag{6.36}$$

$$\sum_{i\in\mathcal{I}} u^s_{ijt} = D^s_{jt}, \qquad j\in\mathcal{J}, t\in\mathcal{T}(\tau^s_{jt}), \tag{6.37}$$

$$e^s_{it} \geq 0, \qquad i\in\mathcal{I}, t\in\mathcal{T}, \tag{6.38}$$

$$u^s_{ijt} \geq 0, \qquad j\in\mathcal{I}, j\in\mathcal{J}, t\in\mathcal{T}, \tag{6.39}$$

$$w^s_{it} \geq 0, \qquad i\in\mathcal{I}, t\in\mathcal{T}, \tag{6.40}$$

$$y^s_{ilkpt} \geq 0, \qquad i\in\mathcal{I}, l\in\mathcal{L}_0, \{k\in\mathcal{K}|k\neq l\}, p\in\mathcal{P}, t\in\mathcal{T}', \tag{6.41}$$

$$\mu^s_{ilbpt} \geq 0, \qquad i \in \mathcal{I}, l \in \mathcal{L}_0, b \in \mathcal{B}, p \in \mathcal{P}, t \in \mathcal{T}, \tag{6.42}$$

$$\nu^s_{ikbpt} \geq 0, \qquad i \in \mathcal{I}, k \in \mathcal{K}, b \in \mathcal{B}, p \in \mathcal{P}, t \in \mathcal{T}'. \tag{6.43}$$

In this problem, the variable y^s_{ilkpt} is relaxed and defined as continuous, shown in Equation (6.41). This relaxation is done in order to use the dual information from the solution of the sub-problem to generate the optimality cuts on the form given by equation (6.14).

6.2.3 Master Problem

The master problem consists of the objective function and constraints that corresponds to the first-stage problem of our mathematical model, where equations (5.1)-(5.4) correspond to equations (6.44)-(6.46) + (6.48). Additionally, the master problem contains the optimality cuts and the second stage cost estimator θ. Here, the master problem defines as a single-cut algorithm, as θ is an estimator for the sum of all the scenarios. Given the integration of penalty costs in the sub-problem equations (6.30) and (6.35), our model has relatively complete recourse, meaning that for all feasible solutions to the master problem, there is at least one feasible solution of the sub-problem. Under this condition, our master problem does not have a need for feasibility cuts and can be written as:

$$\min Z^{MP} = \sum_{i \in \mathcal{I}} \sum_{l \in \mathcal{L}_0} \sum_{p \in \mathcal{P}} C_{lp} \Big(\sum_{t \in \mathcal{T}'} R_t (x_{ilpt} - x_{ilp(t-1)}) + R_1 x_{ilp1} \Big) + \theta, \tag{6.44}$$

subject to:

$$\sum_{l \in \mathcal{L}_0} \sum_{p \in \mathcal{P}} x_{ilpt} \leq 1, \qquad i \in \mathcal{I}, t \in \mathcal{T}, \tag{6.45}$$

$$x_{ilpt} \geq x_{ilp(t-1)}, \qquad i \in \mathcal{I}, l \in \mathcal{L}_0, p \in \mathcal{P}, t \in \mathcal{T}', \tag{6.46}$$

$$\begin{aligned} \theta \geq \sum_{s \in \mathcal{S}} p^s \Big(& \sum_{i \in \mathcal{I}} \sum_{l \in \mathcal{L}_0} \sum_{p \in \mathcal{P}} \sum_{t \in \mathcal{T}'} \alpha^s_{ilpt} x_{ilp(t-1)} + \sum_{i \in \mathcal{I}} \sum_{l \in \mathcal{L}_0} \sum_{p \in \mathcal{P}} \sum_{t \in \mathcal{T}} \beta^s_{ilpt} x_{ilpt} \\ & + \sum_{i \in \mathcal{I}} \sum_{j \in \mathcal{J}} \sum_{t \in \mathcal{T}} \gamma^s_{ijt} L_{ij} D^s_{jt} + \sum_{j \in \mathcal{J}} \sum_{t \in \mathcal{T}} \tau^s_{jt} D^s_{jt} \Big) \end{aligned} \tag{6.47}$$

$$x_{ilpt} \in \{0, 1\}, \qquad i \in \mathcal{I}, l \in \mathcal{L}_0, p \in \mathcal{P}, t \in \mathcal{T}, \tag{6.48}$$

$$\theta \geq 0. \tag{6.49}$$

Our master problem is given by objective function (6.44) and constraints (6.45) -

(6.49), where inequality (6.47) represents the optimality cuts iteratively generated by solving the sub-problem in order to approximate the lower bound θ, for the second-stage expected value function. The solution of the master problem grants an investment solution, $\hat{x}$, which in turn is input for the sub-problem. Solving the sub-problem to optimality gives dual values in constraints (6.31), (6.33), (6.36) and (6.37), that in turn are the dual values utilised in restriction (6.47). As the rest of the sub-problem constraints only contain second-stage variables, they do not affect the optimality cut as the sum of their dual variables and parameters are equal to zero.

6.3 L-shaped Implementation

In a finite number of iterations of the L-shaped, the established optimality cuts ensure convergence (Van Slyke & Wets 1969). Equations (6.50) and (6.51) present calculations for lower and upper bound, respectively. The lower bound is the current best master problem objective value. The upper bound comes from replacing the estimator for total second-stage costs (θ) with the actual total second-stage costs from the sub-problems ($\Psi^s(\hat{x})$) given the fixed first stage investment decisions ($\hat{x}$) and binary adjustment variables (y^s_{ilkpt}). If the latest iteration's current upper or lower bound is respectively lower and higher than before, the bounds update. The algorithm terminates either when reaching maximum iterations or time or when the gap between the upper bound or θ has reached a predetermined value. The latter implies that the estimation of the second-stage costs is close to or equal to the actual costs, giving a feasible solution where no improvements are possible. Consequently, the algorithm reaches the global optimum.

$$LB = Z^{MP} \tag{6.50}$$

$$UB = Z^{MP} - \theta + \sum_{s \in \mathcal{S}} p^s \Psi^s(\hat{x}) \tag{6.51}$$

The L-shaped algorithmic implementation of our reformulated problem in Section 6.2 is presented in Algorithm 1. Firstly, we build master and sub-problems and initialise bounds. Next, in every iteration, the master problem is solved before the sub-problem with fixed investment variables. After solving the sub-problem, we add optimality cuts and then update bounds. Since for every feasible master problem solution, there exists at least one feasible sub-problem solution in our Benders reformulation, we have *relatively complete recourse* and can then ignore feasibility cuts. Reaching a predetermined gap between θ and the sub-problems objective value terminates the algorithm. After reaching this gap, we solve the problem again with binary adjustment variables (y^s_{ilkpt}) using fixed investment variables from the last solved master problem.

Algorithm 1 Proposed algorithm

```
procedure L-SHAPED METHOD FOR OUR PROBLEM
    Build master problem
    Build S sub-problems
    UB ← ∞,   LB ← −∞,   Continue ← True
    while Continue do
        Solve master problem to optimality
        for all s ∈ S do
            Fix investment variables in sub-problem s
            to solution from master problem
            Solve sub-problem s
            Update UB and LB
            if Termination criteria met then
                Continue ← False
            else
                Add optimality cut
            end if
        end for
    end while
    return Solved master problem
    Solve problem with binary adjustment variables, using fixed investment
    variables from the solved master problem
end procedure
```

6.4 Acceleration Methods

This section presents and explains the theory behind some well-known acceleration methods for the L-shaped method. First, in Section 6.4.1, we introduce ways to add more cuts in each iteration of the Benders Decomposition. After that, in Section 6.4.2, we present alternative strategies for solving the master problem. In Section 6.4.3 we introduce approaches that combine some of the well-known methods. Lastly, in Section 6.4.4, we discuss an alternative by warm-starting the algorithm.

6.4.1 Adding multiple cuts

The generalised Benders optimality cut for our mathematical model (Section 6.2) derived in constraint (6.47) is in a single-cut form. There is one cut covering all sub-problems per iteration. A single-cut implementation extension is augmenting contributions from every sub-problem, with a probability of an optimality cut for each sub-problem. This extension implies that separating information from each sub-problem can give more than one optimality cut in each iteration. A multi-cut extension of the Benders optimality cuts was introduced by Birge & Louveaux (1988), where they separate into one sub-problem per scenario and add a cut per sub-problem in every iteration instead of one aggregated in the single-cut implementation. Their key point is that the multi-cut provides more information with outer approximations from all the sub-problems and converges in fewer iterations. Nevertheless, neither the single- or multi-cut method is unconditionally better than the other, as the convergence rate is dependent on problem characteristics. On the other side, a general rule is that the multi-cut is better than the single-cut if the dimension space of the master problem variables is just smaller than the number of sub-problems (Birge & Louveaux 1988). The corresponding multi-cut for our mathematical model is presented in restrictions (6.52). Note that the θ^s-variables now are estimators for the second-stage costs in a single scenario s. Consequently, the master problems objective function has to accumulate θ^s, for all scenarios $\mathcal{S}$. The L-shaped for our mathematical model with a multi-cut implementation is similar to Algorithm 1. We only replace the optimality cut (6.47) with constraints (6.52), and replace θ with $\sum_{s\in\mathcal{S}} p^s\theta^s$ in the objective function (6.44).

$$\begin{aligned}
\theta^s \geq & \sum_{i\in\mathcal{I}}\sum_{l\in\mathcal{L}_0}\sum_{p\in\mathcal{P}}\sum_{t\in\mathcal{T}'} \alpha^s_{ilpt} x_{ilp(t-1)} + \sum_{i\in\mathcal{I}}\sum_{l\in\mathcal{L}_0}\sum_{p\in\mathcal{P}}\sum_{t\in\mathcal{T}} \beta^s_{ilpt} x_{ilpt} \\
& + \sum_{i\in\mathcal{I}}\sum_{j\in\mathcal{J}}\sum_{t\in\mathcal{T}} \gamma^s_{ijt} L_{ij} D^s_{jt} + \sum_{j\in\mathcal{J}}\sum_{t\in\mathcal{T}} \tau^s_{jt} D^s_{jt}, \qquad s\in\mathcal{S}
\end{aligned} \tag{6.52}$$

An alternative to the multi-cut technique for adding several cuts in every iteration is to utilise incumbent solutions to the master problem. For example, storing the five best solutions found in the master problem, including the optimal one, solving the sub-problem and adding single-cuts for each solution. We call this technique for the *several cut approach*. With this technique, we have an opportunity to cut away more sub-optimal solutions in every iteration. Our sub-problem is fast to solve, so this will not effectively affect our total computational time. On the other hand, our master problem increases in size at a speedier rate and possibly is harder to solve.

This technique adds a line between lines (6) and (7) in Algorithm 1. Saying that for all investments solution from the master problem, do line (7) to line (16). The technique results in more sub-problems calculations and adds more optimality cuts in every iteration.

6.4.2 Alternative Master Problem solution strategy

When having an integer first stage, it is common to solve the master problem in the standard L-shaped algorithm to optimality through branch-and-bound (BB) in each iteration. Solving the master problem to optimality could be a very time-consuming process because of the problem's integer nature. Magnanti & Wong (1981) and Zarandi (2010) state that the master problem represents over 90 % of the total computational time. Therefore, we can create adjustments to the general L-shaped algorithm by ending the master problem execution before it reaches optimality. After that, the algorithm sends the investment decisions earlier to the sub-problems to create optimality cuts. One alternative to reduce time spent on the master problem is to terminate the master problem and move to the sub-problem as the solver finds the first integer solution of the BB-tree, indifferent to optimality. This method is frequently mentioned as Branch-and-Benders-cut (B&BC) (Rahmaniani et al. 2013). B&BC is very applicable early in the computational process since significant changes in the solution from the Bender decomposition algorithm are happening here.

Another strategy for the master problem is an approach, first introduced by Geoffrion & Graves (1974), referred to as the ϵ-approach. In this approach, the execution of the master problem terminates as the optimality gap achieves a value less or equal to a preset limit, ϵ. As the computational process continues, the value of ϵ is commonly reduced or completely removed. This reduction gives better master problem solutions like the ϵ-process approaches optimality.

Changing line (6) of Algorithm 1 is the only change to utilise either B&BC or the ϵ-approach for the master problem. The B&BC approach jumps to the sub-problem when it finds the first integer solution to the master problem. The ϵ-approach moves to the sub-problem when it finds an integer solution to the master problem that reaches a gap less or equal to ϵ. Note that the techniques above utilise the single-cut approach if the use of multi-cut is not explicitly stated.

6.4.3 Combinations of methods

As some of the acceleration techniques discussed above focus on different areas to improve solution time, we want to improve solution time by adding additional steps simultaneously. Combining techniques may lead to an even more significant effect on solution time than implementing them separately. We combine the multi-cut approach with the two alternative strategies for solving the master problem resulting in two new approaches. We assume that exploiting the ability to solve the master problem faster, from the B&BC or the ϵ-approach, in combination with the additional cuts added in multi-cut, can faster find a better lower bound. This assumption is based on problems where the master problem takes significantly longer to solve than the sub-problems. Therefore, the additional time used for solving more sub-problems might be neglected due to the positive effect of new optimality cuts removing wrong solutions.

Lastly, we combine the ϵ-approach with the several cuts approach. The advantage of connecting the latter with the ϵ-approach is to spare time from solving the master problem to optimality. A downside of this combination is the extra time used to solve additional sub-problems, but it might be neglected under the assumption of fast solving sub-problems.

6.4.4 Warm-start

Rubiales et al. (2013) point out that an issue with the original L-shaped method is that it requires many iterations to converge, both at the beginning and when getting close to the optimal solution. A well-known possibility to avoid this issue is an algorithmic extension called warm-start. Here, we start with a reasonable solution acquired from a simplified variety of the problem. For our problem, this could save time from the L-shaped algorithm working around the 0-solution area, i.e., zero investments in facilities, which are bad solutions with a lot of penalty costs for not satisfying demand. Standard simplified versions of warm-start for stochastic problems commonly use the solutions from the deterministic expected value problem (Geoffrion & Graves 1974). A general assumption is that the gain from an initial solution is greater than the computational costs of solving the deterministic problem since the stochastic model is more complex than the deterministic one. Algorithm 2 presents the algorithmic alternative using warm-start. The main change is the swap in the initial iteration with the solution from solving the deterministic problem with the expected demand scenario.

Algorithm 2 warm-start

procedure L-SHAPED METHOD COMBINED WITH WARM-START
    Lines (2)-(4) of Algorithm 1
    Solve expected value problem
    for all $s \in \mathcal{S}$ **do**
        Fix investment variables in sub-problem s to solution from deterministic problem
        Solve sub-problems s
        Add optimality cut
    end for
    Lines (5)-(19) of Algorithm 1
end procedure

Chapter 7

Case Study

To be able to test and analyse our proposed algorithm, we solve a case study for possible future hydrogen demand levels. First, we present the input data for sets and cost parameters in Section 7.1. Next, in Section 7.2 we identify and discuss potential maritime industry segments for hydrogen fuel and future demand scenarios. Lastly, we present how we construct the hydrogen scenarios combining the different maritime industry segments in Section 7.3.

7.1 Infrastructure and Cost Data

This section presents data for customer and facility location candidates, investment, production and adjustment costs, and distribution costs. Overall, the data are based on calculations done in Aglen & Hofstad (2021).

7.1.1 Customer Locations

Our set of identified customer locations, which are the ones we will use in this, consists of 50 unique demand locations ranging from Hammerfest in the North to Stavanger in the south. These locations are presented in work by (Ocean Hyway Cluster 2020*a*) and (Aarskog & Danebergs 2020*a*), which both present projections for hydrogen demand towards 2030 for the Norwegian domestic maritime transportation and high-speed ferry sector, respectively. These customer locations are bunkering locations that are relevant for bunkering hydrogen based on current bunkering locations used by the Kystruten (Bergen-Kirkenes), high-speed passenger ferries and car ferries today. The projections assume that in future public transportation service contract negotiations, the contracts require zero-emission technology. Routes with less than 20,000 L/year of diesel are neglected, corresponding to 10 out of 95 high-speed ferry routes. Furthermore, the end stops are emphasised as bunkering locations to avoid additional travelling time due to bunkering time at intermediate stops. Lastly, ferries that run on electric batteries do not contribute to demand. The customer locations are displayed in Figure 7.1 below.

Figure 7.1: Customer Locations for hydrogen in Norway.

7.1.2 Facility location candidates

Figure 7.2 displays the set of candidates for facility locations of large-scale hydrogen production in Norway. The figure includes 16 out of 17 possible locations presented by Ocean Hyway Cluster in their interactive map (Ocean Hyway Cluster 2020*c*). The map was later extended to include additional locations and revised to assign each facility location with specific production technology. In this case study, we disregard the newest changes for electrolysis. The established locations we consider essential are evaluated as natural points for the distribution of hydrogen in terms of distance to the customers identified above. In addition, the facility locations are justified through ongoing or future publicly-known projects for producing hydrogen-based fuels. We use all 16 locations for electrolysis to define the set of potential facility locations. For SMR+, we restrict the set of locations to just 4 out of the 16. These four locations have some connection to the delivery or processing of natural gas in common, making them feasible for producing blue hydrogen through SMR+ (Ocean Hyway Cluster 2020*c*).

Figure 7.2: Facility Location candidates in Norway.

7.1.3 Investment Costs

We study the investment costs for feasible hydrogen production technologies, which in this case study correspond to electrolysis (EL) and steam methane reforming with carbon capture and storage (SMR+). We base our calculations on the model presented by Jakobsen & Åtland (2016) to estimate the investment costs. A facility can invest in different capacities, and the investment costs are represented by eight discrete capacity points for electrolysis and seven points for SMR+. We neglect investment in the smallest capacity for steam methane reforming, as it favours large-scale production and therefore lacks data for small-scale investment in this technology. Table 7.1 summarises the costs for the different capacities given in million Euros.

Table 7.1: Investment costs for electrolysis and SMR+ at the set of discrete capacity points (Aglen & Hofstad 2021).

Discrete Capacities	1	2	3	4	5	6	7	8
Capacity [tonnes/day]	0.6	3.1	6.2	12.2	30.3	61.0	151.5	304.9
Investment EL [mill. €]	1.4	6.0	11.2	20.5	46.5	87.2	197.7	371.5
Investment SMR+ [mill. €]	-	23.9	39.9	65.2	127.7	204.3	402.1	709.2

7.1.4 Adjustment Costs

In addition to the initial investment in capacity at a facility, these decisions can be revised through capacity adjustments later. The adjustments are made as a change between its invested capacity point and a new different capacity point, with the option to adjust to zero capacity (facility shutdown). With every decision of capacity adjustment, we assign an adjustment cost. The adjustment cost for adjusting a facility from capacity point k to l is related to the difference in investment costs of opening a facility with initial capacity k and a facility with initial capacity l, where $k \neq l$, in addition to a mark-up, α, which we assign to 10% in this case study. Equation 7.1 expresses the relation:

$$E_{klp} = |C_{lp} - C_{kp}| * (100 + \alpha)\% \tag{7.1}$$

7.1.5 Production Costs

We assign a piece-wise linear convex short-term production function to each discrete capacity point. We approximate the short-term production costs at specific breakpoints, 15%, 30%, 50%, 80%, and 100% of installed production capacity. Electrolyser units feasible for hydrogen production in Norway have a characteristic dynamic range varying between 15% to 100% capacity. For simplicity, we apply the same dynamic capacity range for SMR+ production, explaining the chosen short-term production cost breakpoints.

Table 7.2 summarises the production costs for both production technologies for the set of discrete capacities identified above. We base our data for production costs in euros per kilogram upon Aglen & Hofstad (2021). The table reflects properties such as large-scale production advantages for SMR+ compared to electrolysis, as production costs are significantly lower for SMR+ beyond discrete capacity point 3.

Table 7.2: Production costs for electrolysis and SMR+ at the discrete capacity points at maximum utilisation (Aglen & Hofstad 2021).

Discrete Capacities	1	2	3	4	5	6	7	8
Capacity [tonnes/day]	0.6	3.1	6.2	12.2	30.3	61.0	151.5	304.9
Production Costs EL [€/kg]	1.95	1.61	1.53	1.45	1.43	1.42	1.40	1.38
Production Costs SMR+ [€/kg]	-	1.91	1.61	1.42	1.28	1.18	1.04	1.00

7.1.6 Distribution Costs

In order to estimate the distribution costs between the identified feasible facility locations and customers, we establish a general distribution cost function with distance as the single variable. Aarskog & Danebergs (2020*b*) identifies a cost function based on the estimated levelised cost of hydrogen (LCOH) for a 2030-case where 1 tonne of hydrogen is transported in a 40-foot container at 300 bar, which Stadlerova & Schütz (2021) further extend to 1000 km by extrapolation. As a result, we have established a general cost function for the distribution of hydrogen at 300 bar, which in practice reflects the distribution costs of compressed hydrogen. The general cost function for distribution is shown in Table 7.3 for a set of distance intervals.

Table 7.3: Hydrogen distribution costs in [€/km/kgH_2] (Aglen & Hofstad 2021).

Distance (km)	1-50	51-100	101-200	201-400	401-800	801-1000
LCOH (€/km/kgH_2)	0.00498	0.00426	0.00390	0.00372	0.00363	0.00360

As identified in Section 2.2, compressed gaseous and liquid hydrogen are the two main technologically - and economically - viable options and our main focus for the distribution of hydrogen. Therefore, our distribution cost function should ideally reflect both distribution technologies. Our cost function could, for example, handle this by using distribution technology as an extra input variable or using different weights for each technologies' distribution costs within different distance intervals. However, we decided to base our hydrogen distribution cost function independent of distribution technology, where compressed hydrogen constitutes the basis for estimation. This decision is due to uncertainties in distribution costs for large-scale liquid hydrogen in Norway as well as liquefaction cost and a liquid hydrogen distribution cost estimate that does not capture economies of scale,

7.2 Demand

This section presents demand scenarios for different sectors relevant to future hydrogen consumption. In Section 7.2.1, we investigate the maritime passenger transportation sector, consisting of domestic car ferries, high-speed passenger ferries and the coastal route. Next, we look further into the domestic fishing sector in Section 7.2.2. Lastly, we investigate the Norwegian offshore fleet concerning activities on the Norwegian Continental Shelf in Section 7.2.3.

7.2.1 Maritime Passenger Transportation Sector

We define the maritime passenger transportation sector as domestic car ferries, high-speed passenger ferries and the coastal route. Furthermore, we present the expected hydrogen demand for each customer segment throughout the following subsection. The data and information presented are mainly based on different work packages from Ocean HyWay Cluster (Ocean Hyway Cluster 2020*a*).

In these work packages, the following assumptions hold:

- Efficiencies are based on 2020 engine and fuel-cell technology for calculations.
- Hydrogen is developed and mature by 2030 when considering on board storage, bunkering, conversion, integration and regulations.
- Future hull performance and energy consumption of different vessels are assumed to be the equivalent level to modern 2020 vessels.
- The same existing timetables and vessel capacities will apply for new contracts for known routes and contracts.
- All future public tenders for high-speed passenger ferries, domestic car ferries and the coastal route operation requires zero emissions, if technically feasible.

- Liquid hydrogen is only relevant for vessels with hydrogen consumption greater than 1000kg between bunkering. Compressed hydrogen is considered for consumption less than 1000kg.

7.2.1.1 Domestic Car Ferries

Domestic car ferries are one of the identified segments in the transportation sector to serve as a future hydrogen customer in Norway. This sector includes over 130 ferry connections consisting of the operation of over 250 vessels along the entire coast of Norway. The data used in this case study is not publicly available but is a part of extensive and ongoing work from the Ocean Hyway Cluster. The confidential report C.2 rev.01 "Mapping of 2030 hydrogen demand in the Norwegian domestic car ferry sector" as part of the HyInfra project work package C (Ocean Hyway Cluster 2020*d*), constitutes the basis for establishing the future hydrogen demand along with the publicly available report from Ocean Hyway Cluster (2020*a*). However, some shared assumptions exist in both reports:

- **Competing technology:** Plug-in-battery ferries are already operating in Norway, which is considered a viable solution for some cases of short fjord crossings. The future energy mix is most likely to be diverse.
- **Compressed H_2 vs. Liquid H_2:** Liquid hydrogen is the only viable option for routes that require more than 1000kg of hydrogen per day.

7.2.1.2 High-speed Passenger Ferries

The high-speed passenger ferry segment consists of approximately 100 operating routes throughout the coastline of Norway. It has a yearly diesel consumption of 56 million litres, equivalent to 0.7% of all petroleum products sold in Norway. Aarskog & Danebergs (2020*a*) look into how this diesel demand can be translated to hydrogen fuel demand in terms of quantity, routes and time of demand. The study evaluates both fuel cells powered by green hydrogen and batteries with fast charging from the grid, and these are competing for alternatives as a zero-emission solution. The results show that 51 routes are suitable for hydrogen operation and 30 for electric batteries out of 96 evaluated routes.

The methodology consists of fuel conversion rates and estimating diesel consumption for the routes using a conservative but realistic approach. Only routes with a diesel consumption greater than 20,000 L/year are evaluated. For the timing of demand, they use information from public tenders and contract periods and the assumption that each route will change to zero-emission solutions at the end of its current contract period. Figure 7.3 displays the demand scenario for hydrogen in Norway's high-speed passenger ferry sector.

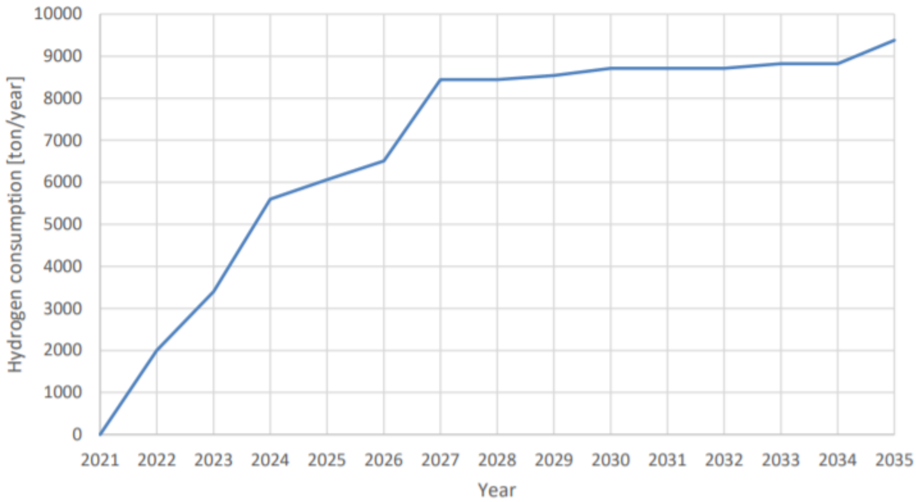

Figure 7.3: Hydrogen demand scenario for high-speed passenger ferries in Norway (Aarskog & Danebergs 2020*a*).

Overall the sector can potentially contribute to a stable hydrogen demand as the ferries return to the same ports daily along with high fuel consumption.

7.2.1.3 Coastal Route

The Norwegian coastal route sails from Bergen to Kirkenes and vice-versa. Ocean HyWay Cluster has launched its report C.3 rev. 01 "2030 hydrogen demand for the Coastal route Bergen-Kirkenes" as part of the HyInfra project work package C (Ocean Hyway Cluster 2020*a*). This study presents several scenarios for the expected hydrogen demand from 2032. Each realisation and its respective demand varies based on the number of vessels that run on hydrogen and the corresponding ports for bunkering. Demand timing is again based on public tenders and contract periods. The coastal route has already experienced many restrictions regarding CO_2-emissions in the current contract spanning from 2021 to 2031 and will experience additional restrictions in the contract that starts in 2032. The results are not publicly available to display in this report.

7.2.2 Domestic Fishing

7.2.2.1 Estimation of hydrogen fuel demand

To estimate the hydrogen demand of the Norwegian fishing vessels, we first establish an overall fuel consumption for the fishing sector based on the report from Ocean Hyway Cluster (2021). Here, we extract the quantity of Marine Diesel Oil (MDO) consumed by the fishing sector in Norway today. By utilising the fuel conversion factors for MDO presented in Table 7.4, we can estimate an upper limit for future hydrogen demand for a fishing fleet of today's scale, technological standard and operational level.

Table 7.4: Fuel conversion factors for MDO and H_2 (DNV 2015).

	Calorific values [MJ/kg]	**Fuel conversion factor [-]**
Marine Diesel Oil (MDO)	44	143/44
Hydrogen	143	44/143

7.2.2.2 Timing of transition to hydrogen fuel

The fishing sector has not been affected by CO_2-tax until 2020 due to complete refunds of the fishers' expenses regarding the CO_2-tax. Since 2020 the government has practised a compensation scheme that aims to slowly degrade to zero compensation by 2025 (Ocean Hyway Cluster 2021). Afterwards, the fishing sector will experience an increase in emission taxes like other industries that already are subject to emission taxes. By 2030, the CO_2-tax is to increase to 2000 NOK/kg according to Norway's "Klimaplan 2021-2030" (Det Kongelege Klima- og Miljødepartement 2020). In the same report, we find projections for the future emission taxes, which will constitute the basis for our stepwise increase in hydrogen demand towards 2030. Note that this development assumes that it is technologically feasible for all fishing vessels to utilise hydrogen by 2030, assuming the exact energy requirements and efficiencies today. Table 7.5 displays the projected tax price for CO_2-emissions based on the projection given in (Det Kongelege Klima- og Miljødepartement 2020), along with the change between years and the cumulative change.

Table 7.5: Conversion rate of diesel to fuel demand based on the relative change in projected CO_2-tax for 2021-2030 (Det Kongelege Klima- og Miljødepartement 2020).

Year	2021	2022	2023	2024	2025	2026	2027	2028	2029	2030
Projected tax price (Euros/tonnes CO2)	28	30	32	33	37	41	51	63	77	97
%change	-	3.39%	3.39%	1.69%	6.78%	6.78%	16.95%	20.34%	23.73%	16.95%
Cum.%change	-	3.39%	6.78%	8.47%	15.25%	22.03%	38.98%	59.32%	83.05%	100%

Based on the assumption that the increase in the projected CO_2-tax will result in a similar increase in hydrogen demand, the cumulative change in the CO_2-tax can be assumed to correspond to a certain amount of turnover from fossil fuel to zero-emission fuels like hydrogen. The cumulative change represents the highest scenario, as Table 7.5 displays. From this assumption, we derive the following scenarios using 50%, 70% and 100% as turnover, which results in a low, medium and high demand scenario. The resulting hydrogen demand for the different scenarios is showcased in Figure 7.4.

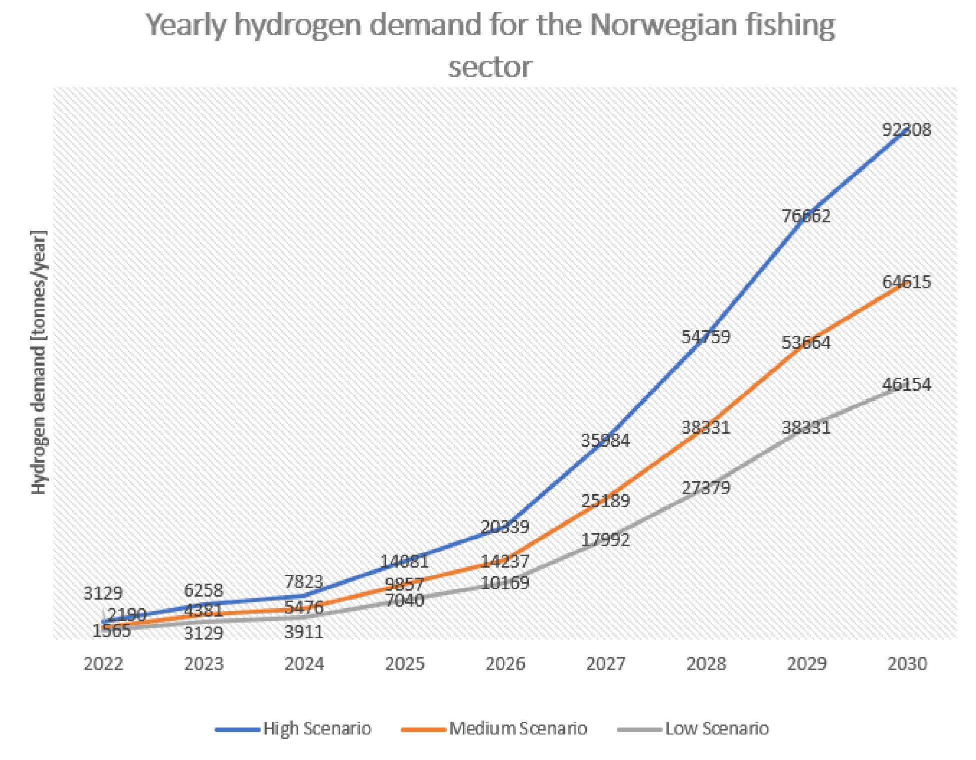

Figure 7.4: Estimated hydrogen demand for the Norwegian fishing sector 2022-2030.

7.2.2.3 Allocation of demand

To allocate demand to different regions throughout Norway, we turn to "Fiskeridirektoratet", responsible for keeping statistics for the Norwegian fishing fleet. The standard procedure for a fishing vessel is to travel to a fishing site and return to a fish reception to discharge. The most relevant data containing regional info which fits the description of standard use of fishing vessels are catch and fishing vessel data, precisely round weight in tonnes by vessel county and registered vessels by length and county (Fiskeridirektoratet 2022*b*, 2021). Round weight is the weight of the fish on catch, where no processing of the fish has found place. Using the regions where the fishing vessels are registered, we get input on where the fishing vessels typically operate. Combining this with regional catch data, we can also allocate demand to regions experiencing seasonal fishing or having large fishing vessels consuming more fuel. Furthermore, we use catch and vessel data from 2017, which has more extensive detail on the geography of the data since this was the last year before the start of the regional reform. Table 7.6 displays the choice of regions from the data. Catch quantities have been checked against the last catch and vessel data to validate the split in terms of a year.

The overall fuel demand will be distributed based on a weighted sum of regional catch and vessel data. Initially, we assume the weights used in the calculation to be equal, but numbers from various reports suggest that some registered vessels do not participate in fishing during a year. Therefore, we estimate the fraction of active vessels based on historic numbers from DNV and Fiskeridirektoratet. DNV estimate and utilise in their 2013-calculations that of 6128 registered vessels, 5169 of them are active in fishing (delivered fish the last year), resulting in just below 85% share of active vessels (DNV 2014). Today there are 5633 registered vessels with a steady trend of slight decrease (Fiskeridirektoratet 2022*a*). We assume the fraction from the 2013-calculations to be still valid for later registered vessel data and will serve as our measure for the share of active vessels.

In the catch data, some volumes are unspecified and not assigned to the county it has been caught in. Since emissions are associated with this volume, we evenly distribute this across all counties. The fraction of demand based on a total will then follow the proposed equation below:

$$x_{county} = 0.5 \cdot \alpha_V \cdot V_{county} + 0.5 \cdot (1 - \alpha_V) \cdot (C_{county} + \frac{C_{unspecified}}{no.of counties}) \tag{7.2}$$

Equation 7.2 shows calculation of hydrogen demand by county where x_{county} denotes hydrogen demand per county, α_V fraction of active vessels, V_{county} fraction of vessels by county, C_{county} fraction of catch per county and $C_{unspecified}$ number of unspecified catch.

Table 7.6: Registered vessels and delivered round weight per region for 2017 (Fiskeridirektoratet 2021, 2022*b*).

Year 2017	**Registered vessels** [%]	**Delivered round weight** [%]	**Demand share** [%]
Finnmark	16.66 %	6.59 %	11.21 %
Troms	13.11 %	6.94 %	9.92 %
Nordland	24.55 %	23.41 %	24.27 %
Nord-Trøndelag	2.49 %	1.30 %	2.18 %
Sør-Trøndelag	4.47 %	1.70 %	3.24 %
Møre og Romsdal	10.58 %	21.83 %	17.46 %
Sogn og Fjordane	4.19 %	4.42 %	4.70 %
Hordaland	8.98 %	22.23 %	17.02 %
Rogaland/Vest-/ Øst-Agder	11.35 %	4.90 %	7.99 %
Oslo/Buskerud/ Akershus/ Vestfold/Telemark	3.62 %	0.19 %	2.09 %
Unspecified	-	6.47 %	-

In order to assign the hydrogen demand identified in each region to specific customers, we look further into governmental fishing ports in each region. Each governmental fishing port could represent a potential customer with a respective fuel demand, as the ports often have infrastructure such as bunkering facilities. However, due to a large number of governmental fishing ports (close to 500 in 2020 (Avisa Nordlys 2020)), we choose to define hydrogen customers within domestic fishing as the already identified customer locations in the maritime transportation sector with an additional requirement of a nearby governmental fishing port (<10 km). This definition also recognises 36 out of the 50 customers in the maritime transportation sector as hydrogen customers in the domestic fishing sector. These 36 customers will cover all demand from fisheries. For Nord-Trøndelag and Sør-Trøndelag, we make an exception from the requirement as we only have one customer location in each region, Namsos and Trondheim, and neither of them satisfies the requirement. These two locations will then be assigned hydrogen demand according to catch and vessel data for Nord- and Sør-Trøndelag. Due to uncertainty of how the quantities of round weight and number of vessels distribute across each identified customer within each county, we will distribute the demand uniformly across the hydrogen customers in the fishing sector.

7.2.3 Offshore Fleet on the Norwegian Continental Shelf

From the report Ocean Hyway Cluster (2020*a*) we extract numbers for the CO2-reduction potential for high-speed crafts, car ferries, coastal route and the offshore sector. Combining this with the projections for the fishing sector established in this case study, Figure 7.5 clearly shows that the Norwegian offshore fleet on the Norwegian Continental Shelf (NCS) is the most significant contributor to CO_2-reduction potential. The fleet consists of a large number of vessels working on a regular basis, which results in significant CO_2-emissions during normal activity levels on the NCS.

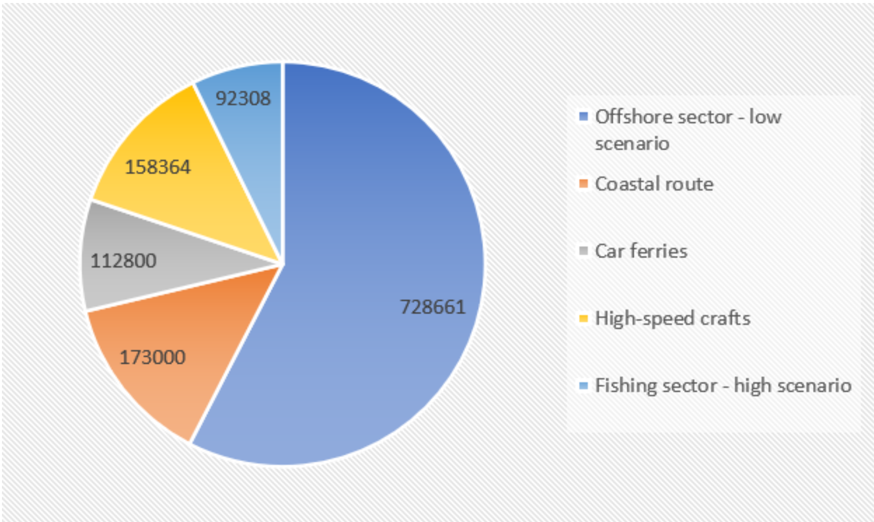

Figure 7.5: CO_2 Reduction Potential $[\frac{tonnes}{year}]$.

7.2.3.1 Ammonia demand projection for the NCS

From the report Ocean Hyway Cluster (2020*b*), we gather information about estimates for the future yearly ammonia demand of the Norwegian Offshore Fleet operating on the NCS towards 2030. Figure 7.6 shows this estimated development in ammonia demand towards 2030 with the lowest and highest scenario, which is based upon a market penetration rate for ammonia technology.

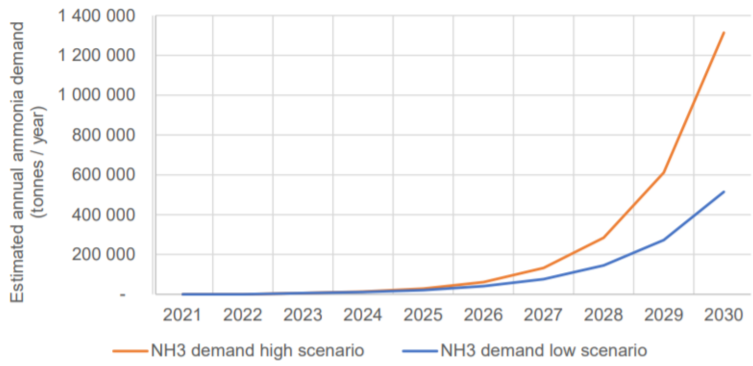

Figure 7.6: Estimated development in ammonia demand towards 2030 (Ocean Hyway Cluster 2020*a*).

7.2.3.2 Estimating the hydrogen demand through fuel conversion

To estimate the offshore demand for hydrogen, we will use fuel conversion factors for the estimated quantities of ammonia. Table 7.7 shows the fuel conversion factors we will use to forecast the hydrogen demand quantities. These fuel conversion factors will be used on diesel-equivalent fuel consumption which the report Ocean Hyway Cluster (2020*b*) establishes for the most relevant vessel segments in the offshore sector. The market penetration rate for hydrogen as zero-emission technology for the offshore sector will follow the same fractions throughout the low-, medium- and high-scenario as for the ammonia used in Ocean Hyway Cluster (2020*b*).

Table 7.7: Fuel conversion factors for ammonia and hydrogen.

	Calorific values [MJ/kg]	**Fuel conversion factor [-]**
Ammonia	18.9	(143/18.9)
Hydrogen	143	(18.9/143)

7.2.3.3 Timing of hydrogen demand

The fuel conversion factors allow us to convert any of the ammonia demand to hydrogen demand. However, there are a handful of assumptions that have to be addressed in order to time the demand. Ocean Hyway Cluster (2020*b*) look into the age distribution of the four different vessel segments to identify conversion and replacement candidates among the vessels. They present three different scenarios low-, medium- and high-scenario. In each scenario, a certain fraction of new buildings and upgrade candidates converted to run on ammonia is set, and these two shares are varied simultaneously to create each scenario. For simplicity, our prediction of hydrogen scenarios will follow the same distribution of new buildings and conversion of upgrade candidates as in Ocean Hyway Cluster (2020*b*). This results in a similar timing of hydrogen demand as the different ammonia scenarios. We further extend the forecast of fuel demand from Ocean Hyway Cluster (2020*b*) to 2035 by assuming that every new-built vessel from 2030 will have zero-emission solutions in the form of hydrogen and that the fleet size will be held constant throughout the years 2030-2035. Since the report from Ocean Hyway Cluster (2020*b*) map the age distribution for the vessel segments they consider most relevant for the offshore sector, we choose to rely on these numbers rather than the procedure done for the fishing sector as (Ocean Hyway Cluster 2020*b*) provide another level of detail for the offshore sector.

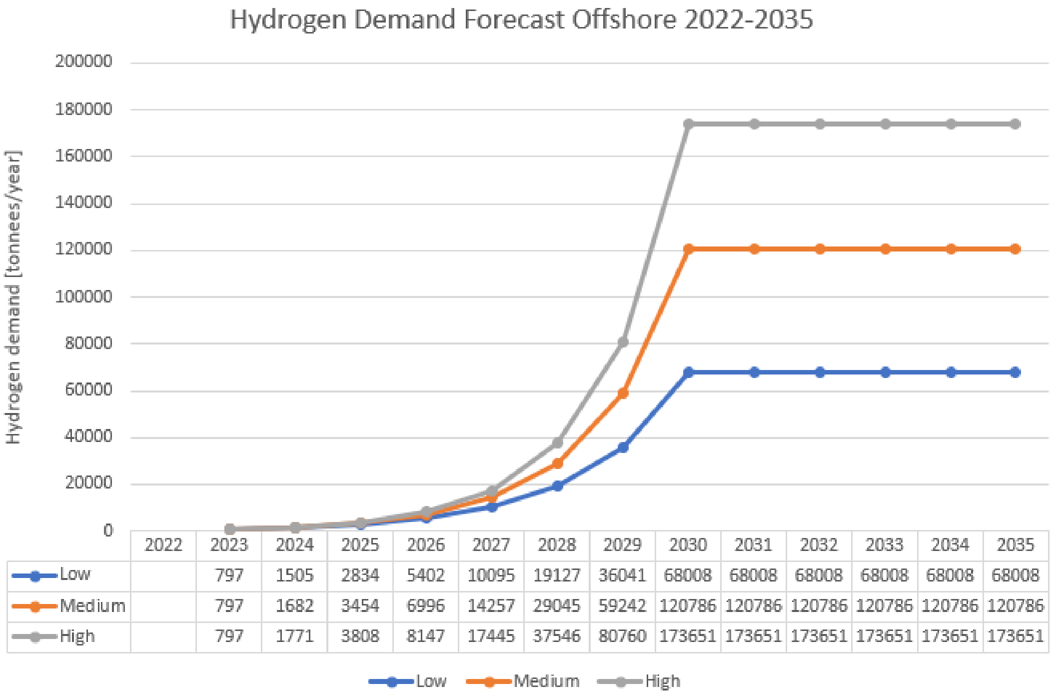

Figure 7.7: Hydrogen Demand Forecast for the Offshore sector 2022-2035.

With the timing of hydrogen demand and quantities, we are able to present our hydrogen demand estimation for the offshore sector. Figure 7.7 presents the set of scenarios we have established for hydrogen demand using the fuel conversion factors.

7.2.3.4 Allocation of hydrogen demand

Figure 7.8 shows the distributed ammonia demand for different 2030-scenarios clustered on different operational areas along the Norwegian coast.

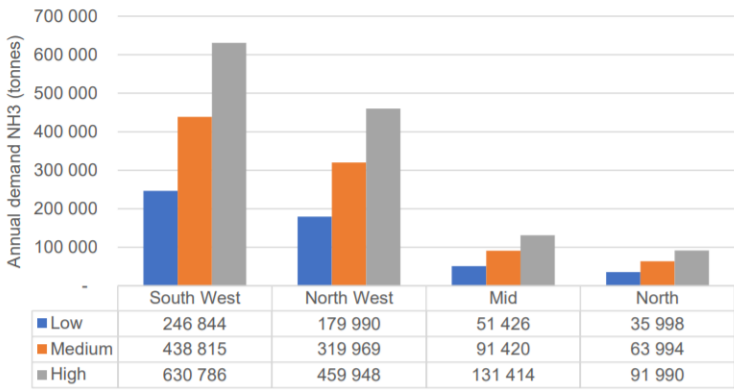

	South West	North West	Mid	North
Low	246 844	179 990	51 426	35 998
Medium	438 815	319 969	91 420	63 994
High	630 786	459 948	131 414	91 990

Figure 7.8: Estimated ammonia demand in different operational areas along the Norwegian coast in different 2030-scenarios (Ocean Hyway Cluster 2020*a*).

Ocean Hyway Cluster (2020*b*) already use appropriate operational areas along the Norwegian coast to allocate demand in their 2030-scenario, as shown earlier in Figure 7.8. These operational areas consist of South-West, North-West, Mid and North. We find a small set of offshore harbours in each region to allocate the regional demands to specific customer locations. Here, we assume a share for each port based on harbour size. In the North region, we locate Hammerfest as the only offshore harbour. In the Mid region, we find Sandnessjøen. In the North-West region, we find Kristiansund and Florø, and we define the South-West region to consist of Bergen and Stavanger. For Kristiansund and Florø, we define the demand to follow an 80%-20% relationship for each harbour. For Bergen and Stavanger, the regional demand relationship is 35%-65%.

To allocate shares of the estimated hydrogen demand each year to each region, we will look into the historical and expected overall activity level on the NCS and the remaining reserves.

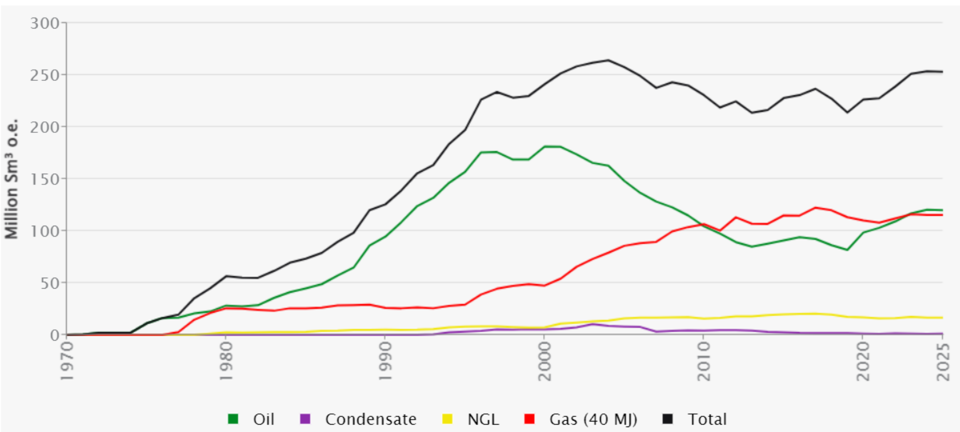

Figure 7.9: Historical and expected petroleum production 1970-2025 (NorskPetroleum 2021).

As Figure 7.9 illustrates, a stable production is expected towards 2025 with a more even ratio of oil and gas than historically. The size and number of discoveries will be of the most significant importance for the total production level in the long term. However, due to the technological development within tiebacks (connection between a new oil and gas discovery and an existing production facility (Wikipedia 2021)), it is more attractive to use already existing and producing fields for the production in both discoveries and the large remaining reserves. Tiebacks utilise the already existing infrastructure resulting in lower costs and an extended and more stable production for today's producing fields. Figure 7.10 displays that already existing fields constitute the bulk of production in the years to come.

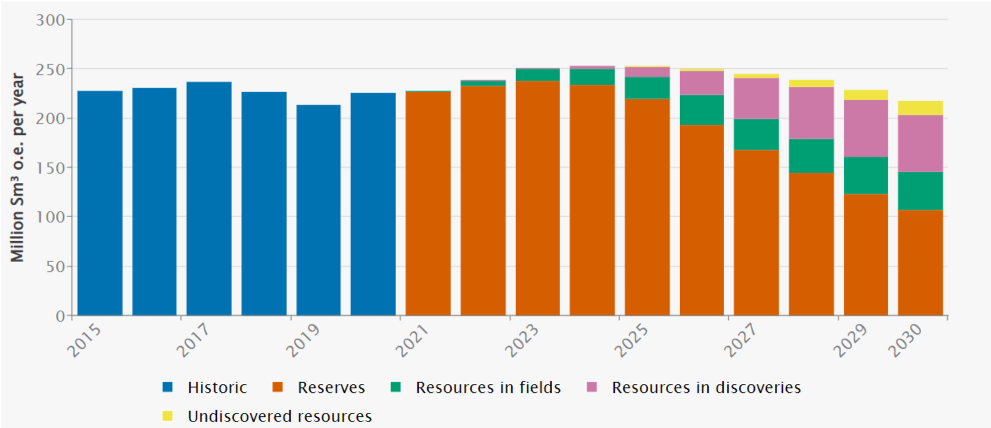

Figure 7.10: Historical petroleum production and forecast 2015-2030 (NorskPetroleum 2021).

Table 7.8: Remaining reserves at producing fields on the NCS (NorskPetroleum 2021).

	Barents Sea	**Norwegian Sea**	**North Sea**
Remaining Reserves at producing fields [mill. Sm^3]	187.49	400.36	1976.76
[% of total]	7	16	77

Now that we have established that currently producing fields will contribute to most of the future activity, we look into the remaining reserves at these fields on the NCS. We divide it into the regions Barents Sea, Norwegian Sea and the North Sea. Here, the Barents sea represents the North region, and the Norwegian Sea represents the Mid region and a split share of the North-West region. The North Sea corresponds to the South-West region with the remaining split share from the North-West region. Table 7.8 shows the distribution both in standard cubic meters and as fraction of total. The regional fuel demand from Figure 7.8 corresponds to 48%, 35%, 10% and 7% for the different regions. Based on the assumption that offshore activities related to remaining reserves and regional hydrogen demand follow a proportional relationship with a constant of approximately one, the regional demand is approximately equal at the beginning of the time horizon as in 2030.

Overall, we are able to split the overall demand into the regional demands showcased in Figure 7.11 for the low scenario.

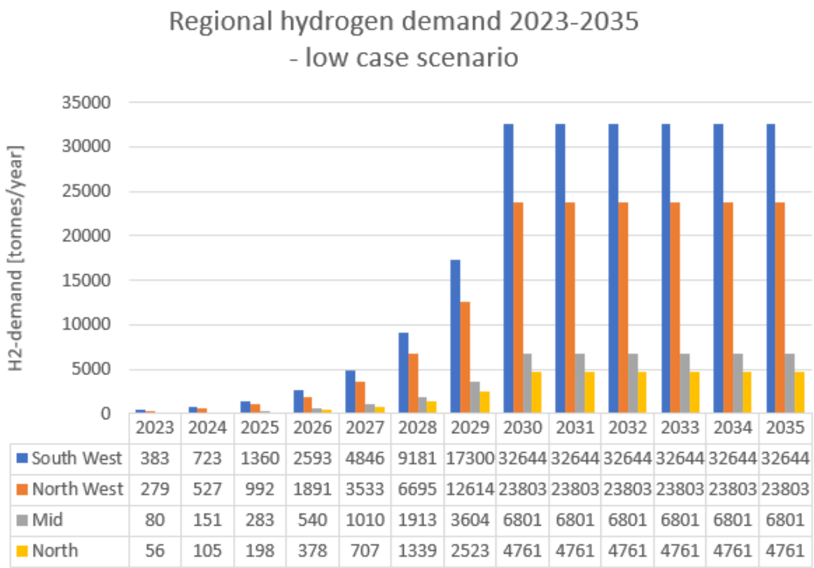

Figure 7.11: Regional hydrogen demand 2023-2035 low-scenario

7.3 Generation of hydrogen demand scenarios

Figure 7.12 presents the minimum and maximum scenario constructed from the earlier hydrogen demand identified in each sector. Here, the minimum scenario consists of the hydrogen demand from the maritime passenger transportation sector. The maximum scenario consists of the demand established in the minimum scenario in addition to the medium scenario from the fishing sector and the medium scenario from the offshore sector.

We use the medium scenarios from both the fishing and offshore sectors as we judge this as the most likely scenario based on our discussion throughout this chapter. From the scenarios illustrated in Figure 7.12, we generate a predetermined number of scenarios for our computational studies to be used in problem instances. These scenarios are equally likely to happen, randomly generated between the minimum and maximum scenario, and follow a uniform distribution. Random scenarios 1 and 2 in Figure 7.12 illustrates an example of how two randomly generated scenarios look.

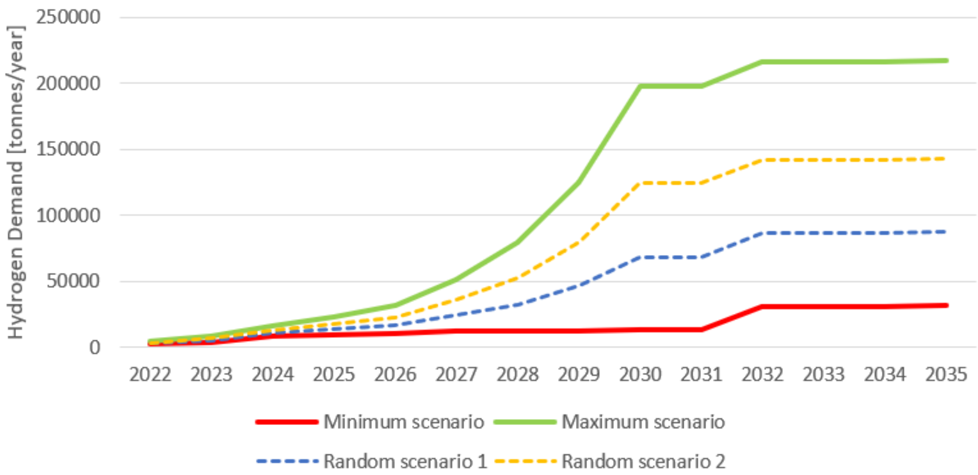

Figure 7.12: Aggregated Hydrogen Demand Forecast 2022-2035.

7.4 Problem instances

We solve our model for different numbers of possible facility locations, customers, time periods, technology, demand scenarios, and decomposition technique. Possible facility locations are either a subset of 7 located south of Trondheim or all 16 for electrolysis. For SMR+, we always use all 4 facility locations. The number of customers consists of a subset of 20 customers located south of Namsos, or the 50 total customers. The number of time periods we use is the full 14 or the last 10. The demand scenarios correspond to 2, 5, 10, 25 and 50 scenarios. We apply the proposed implementations presented in Chapter 6 to the problem instances for electrolysis and the standard non-decomposed Gurobi Solver. For the SMR+ instance, we use the standard non-decomposed Gurobi Solver and the single-cut algorithm. We use notation to differentiate the instances further. For example, an instance with 16 possible facility locations (F), 50 customers (C), 14 time periods (T) and 2 scenarios (S) is F16C50T14S2. Note that an instance with F4CxTxSx illustrates that SMR+ is the chosen production technology.

To make investing earlier in hydrogen production facilities more attractive to reach the CO_2-emission targets faster, we use a discount factor equal to one for each period in each problem instance. The penalty costs are set to a value equal to 110% of the highest production price.

Chapter 8

Computational Results

This chapter presents computational results for the two-stage stochastic facility location model with capacity adjustments. Section 8.1 studies the performance behaviour of different decomposition techniques and compares them with the standard Gurobi solver. The aim of Section 8.1 is to establish how well each decomposition technique works and the reason behind this distinct behaviour. In Section 8.2, we provide decision support and economic analysis for the optimal solutions obtained from solving our model for SMR+ and electrolysis. The aim is to provide managerial insight into different supply chain configurations.

8.1 Model performance analysis

This section presents and discusses performance results for the instances presented in Section 7.4. We focus on how the optimality gap and bounds evolve over time and iteration for different modelling techniques. All instances are run with 172 800 seconds, a maximum number of iterations of 6 000, and a 0.1% optimality gap as termination criteria. The master problem is run to optimality for all L-shaped implementations, except for acceleration techniques where the opposite is stated. Section 8.1.1 compares results between running instances on our single-cut L-shaped algorithm and the commercial solver Gurobi. Afterwards, the comparison of our single-cut L-shaped algorithm, and the acceleration techniques mentioned in Section 6.4, follows in Section 8.1.2.

We have used PyCharm as the integrated development environment (IDE) combined with Gurobi Python Interface to implement the model. All problem instances are run on a computational cluster provided by the Department of Industrial Economics and Technology Management at NTNU. We have utilised the same computational node for each run with the specifications displayed in Table 8.1.

Table 8.1: Hardware description.

Computer	*HP bl685c G7*
Processor	*4 x 2.2GHz AMD Opteron 6274 – 16 core*
RAM	*128Gb*
Python Version	*3.9.6*
Gurobi Version	*9.5*

8.1.1 Single-cut vs commercial solver

This subsection compares our L-shaped single-cut implementation and the commercial solver, Gurobi. In Section 8.1.1.1, the results are from runs on our smallest instance, F4C20T10Sx. The aim is to establish how the L-shaped works compared to the commercial solver on a small case. After that, we scale up to instances F7C20T10Sx to illustrate the behaviour of the single-cut implementation when increasing problem size in Section 8.1.1.2. Further on, in Section 8.1.1.3, we present results from instances F16C50T14Sx, which is our entire case from Chapter 7, to compare performances on a full-scale case. Lastly, in Section 8.1.1.4, we present some alternative approaches to our single-cut implementation.

8.1.1.1 Results from instances F4C20T10Sx

Figure 8.1 displays the upper and lower bound development for the single-cut algorithm and Gurobi on the instances F4C20T10Sx. We observe that both Gurobi and the single-cut find their optimal solution long before the time limit of 172 800. In both instances, Gurobi outperforms the single-cut implementation by finding the optimal value the fastest. As F4C20T10S2 and F4C20T10S5 are relatively small instances, the built-in functions in the commercial solver have an advantage over the L-shaped algorithm. The advantages of L-shaped relaxation by solving easier problems early and gradually adding cuts are outperformed on these small problems, where Gurobi is good enough to handle the problem size.

Figure 8.1 illustrates the fact that there is a gap between the upper and lower bound for single-cut. This gap comes from the lower bound originating from the relaxed problem. The upper bound is the objective value after the reinstatement of the binary requirements on the second-stage adjustment variables. Therefore, the lower bound for the single-cut is often lower as it illustrates the gap between the relaxed and original problem, but the lower one is always valid as Laporte & Louveaux (1993) states. However, even though there is a gap, the results in Figure 8.1 show that there are small differences in the upper bounds, which are the objective value of the original problem and are feasible solutions. Therefore, it illustrates that our single-cut algorithm is an appropriate technique for finding a good solution.

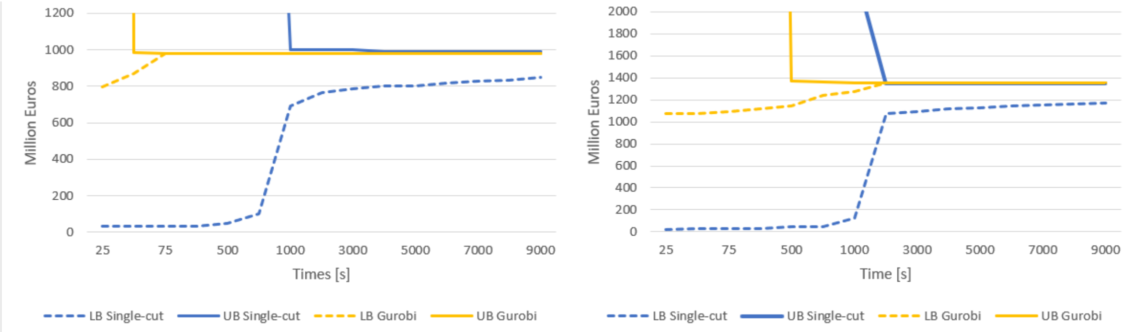

(a) F4C20T10S2. (b) F4C20T10S5.

Figure 8.1: Upper and lower bound development for the single-cut algorithm and Gurobi on the instances F4C20T10Sx.

8.1.1.2 Results from instances F7C20T10Sx

To further compare the performance of our single-cut implementation with Gurobi, we scale up problem size to instances F7C20T10Sx. Figure 8.2 compares upper and lower bound development for the single-cut algorithm and Gurobi on the instances F7C20T10Sx. Note that the y-axis scales differently to show the difference between the single-cut and Gurobi on each instance. Additionally, remark that F7C20T10S50 does not solve to optimality within the time limit.

We observe in the Figure 8.2 that Gurobi finds the optimal solution faster than L-shaped in four instances. In the last one (F7C20T10S50), the L-shaped achieves almost a nine times better objective value than Gurobi, which is a positive result for the L-shaped implementation. In the instances F7C20T10S5, F7C20T10S10 and F7C20T10S25, single-cut finds better solutions than Gurobi early in the process but uses a long time to iterate towards the optimal solution as Gurobi then surpasses single-cut. As the single-cut is decomposed into two smaller problems, it is easier to solve than Gurobi early on, where there are not added many cuts. Further in the process, the strength of the cuts affects how good or fast the L-shaped implantation approaches optimality.

The results in Figure 8.2 illustrate that, when scaling up the problem size, the single-cut has the advantage from the decomposition early on, but as the cuts are not sufficiently strong enough, it uses a long time to reach optimality. Additionally, the results in Figure 8.2e illustrate that the early advantage becomes more vital for larger instances where Gurobi is far off the objective value from single-cut within the time limit. This result indicates a potential for using L-shaped when problem size increases.

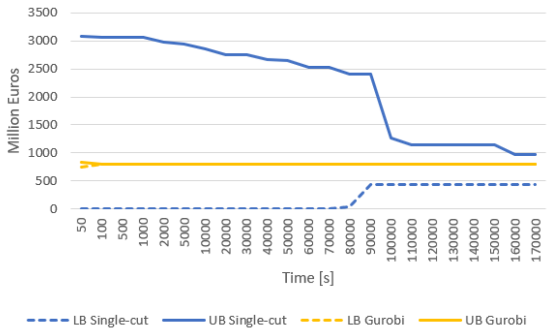

(a) F7C20T10S2.

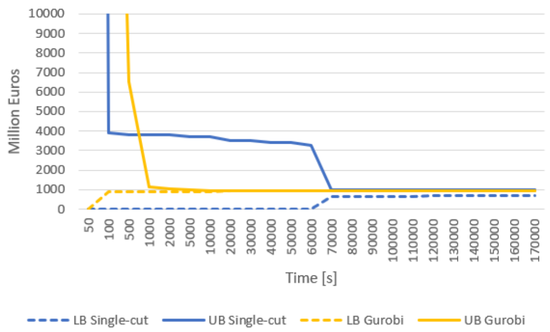

(b) F7C20T10S5.

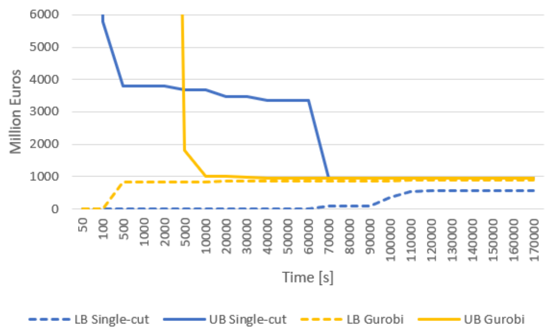

(c) F7C20T10S10.

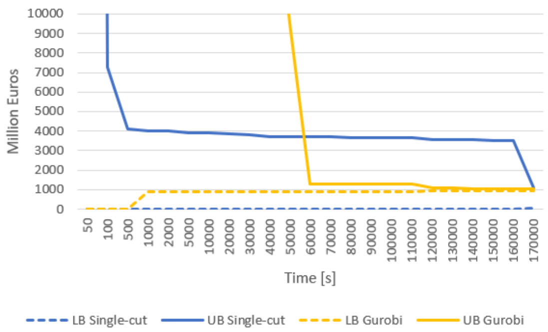

(d) F7C20T10S25.

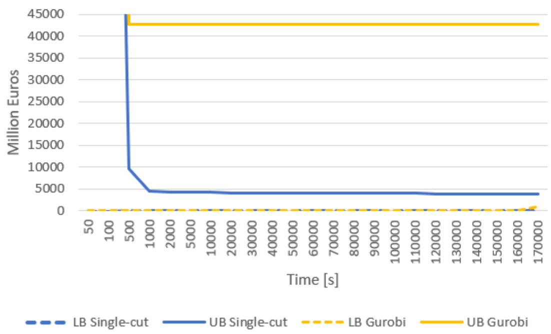

(e) F7C20T10S50.

Figure 8.2: Upper and lower bound development for the single-cut algorithm and Gurobi on the instances F7C20T10Sx.

8.1.1.3 Results from instances F16C50T14Sx

To analyse the full extent of the performances of our implementations, we scale the problem size even further. Figure 8.3 illustrates a comparison of performance results using the single-cut L-shaped algorithm and the commercial solver on the

F16C50T14Sx instances with 2, 5, 10, 25 and 50 scenarios. These are our largest instances and represent the entire case from Chapter 7. The blue line represents the single-cut, while the yellow indicates the Gurobi results. On the x-axis, we have the solution time in seconds, and the y-axis represents upper and lower values in millions of euros. Note that the y-axis scales differently to compare results between the single-cut algorithm and Gurobi in each instance.

In Figure 8.3, we notice that the single-cut implementation finds better upper bounds than Gurobi in both instances F16C50T14S25 and F16C50T14S50. Additionally, in the remaining three instances, we see that the single-cut finds a better solution early in the computational process than Gurobi, until Gurobi eventually outperforms the single-cut. These results correspond well with the results for the F7C20T10Sx, where single-cut uses much time to iterate towards the optimal solution. A general trend is that the solution quality from Gurobi gets worse when increasing the number of scenarios, i.e. increasing problem size, which Aglen & Hofstad (2021) also observed. The fact that the L-shaped implementation outperforms Gurobi for the two largest instances is promising results.

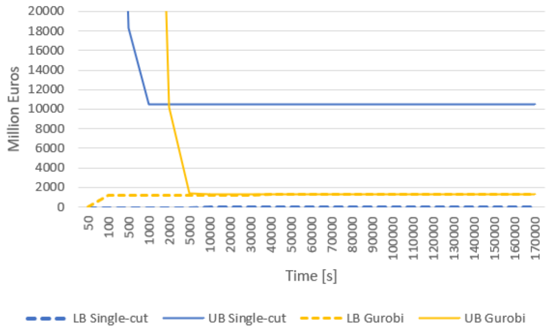

(a) F16C50T14S2.

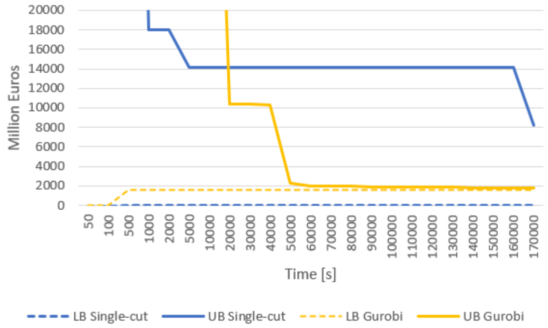

(b) F16C50T14S5.

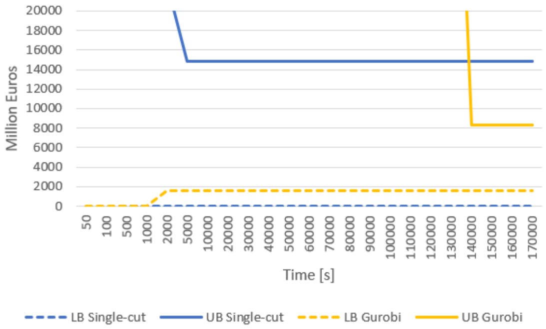

(c) F16C50T14S10.

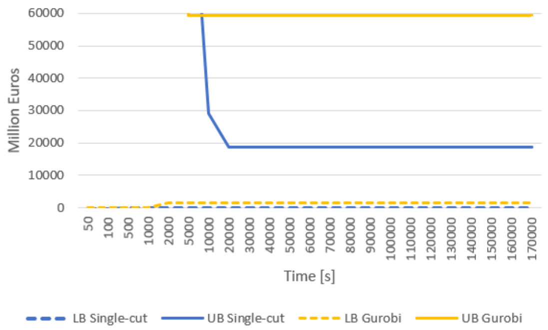

(d) F16C50T14S25.

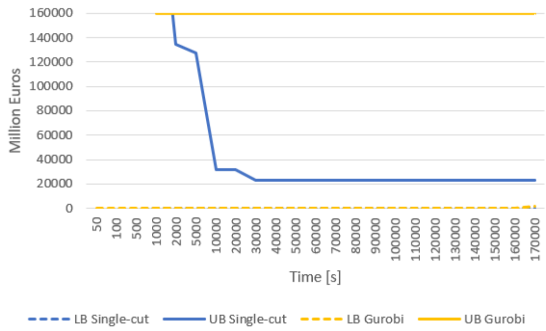

(e) F16C50T14S50.

Figure 8.3: Upper and lower bound development for the single-cut algorithm and Gurobi on the instances F16C50T14Sx.

Table 8.2 presents additional results from single-cut and Gurobi for the F16C50T14Sx instances. Here, we notice that for the F16C50T14S25 instance, the single-cut algorithm finds a solution with a 68% lower objective value than Gurobi. The results for F16C50T14S50 illustrate the same trend, as the single-cut obtains an objective value of 23 235 million Euros, while Gurobi is reaching a value of 159 889 million Euros. In addition, the single-cut finds the F16C50T14S25 solution in only 10 327 seconds compared to 172 800 seconds when Gurobi finds its best solution. For F16C50T14S50, the single-cut also finds a lower objective value than Gurobi, in which the single-cut uses 29 724 seconds compared to Gurobis 172 800 seconds. These results illustrate that our L-shaped implementation finds feasible solutions for all instances. On top of that, the L-shaped illustrates a potential to outperform Gurobi for large instances.

On the other side, we notice a higher gap for the single-cut (99.9%) than for Gurobi (97.2%) for F16C50T14S25. However, Table 8.2 illustrates that the reason behind this is that the lower bound for single-cut is very low. The definition of optimality gap in our results is $(UB-LB)/UB*100\%$. Therefore, the optimality gap is smaller for Gurobi, even though the objective value is, in fact, worse. A low value on the lower bound for the L-shaped indicates that the cuts generated are not exceptionally strong. Strong optimality cuts will limit the master problem solution space and thus push the objective value (lower bound) closer to the optimal solution.

From Table 8.2 we see that the highest number of iterations in the F16C50T14Sx instances are 1 734. Correspondingly, the lower bound for the F7C20T10Sx instances increased in value at iterations greater than 2 449. These results illustrate that the larger instances do not iterate enough to create cuts that increase the lower bound to approach the optimal solution. Correspondingly, it does not find reasonable upper bounds within the time limit. The increasing problem size makes the problem harder to solve, and each iteration will need more computational time as we see a decreasing number of iterations when increasing scenarios. Overall, these results illustrate that L-shaped has a more significant potential for solving large problems than Gurobi. Stronger cuts will reduce the number of iterations needed as the solution space in the master problem gets smaller. Accordingly, a reduced solution space will create an easier master problem to solve. Therefore, further research into applications of cut strengthening reduces the computational time to achieve better solution values in a reasonable time.

Table 8.2: The results from L-shaped and Gurobi for the F16C50T14Sx instances.

	Iter.	**Time**	**LB**	**Obj. Val.**	**Gap**
Single-cut F16C50T14S2	1 734	172 800	4.26	10 480	99.9
Gurobi F16C50T14S2	-	172 800	1 261	1312	3.8
Single-cut F16C50T14S5	1 583	172 800	4.26	8 182	99.9
Gurobi F16C50T14S5	-	172 800	1 610	1 834	12.2
Single-cut F16C50T14S10	1 338	172 800	4.26	14 802	99.9
Gurobi F16C50T14S10	-	172 800	1 550	8 335	81.4
Single-cut F16C50T14S25	862	172 800	4.26	18 827	99.9
Gurobi F16C50T14S25	-	172 800	1 651	59 213	97.2
Single-cut F16C50T14S50	496	172 800	2.83	23 235	99.9
Gurobi F16C50T14S50	-	172 800	1 821	159 889	98.9

8.1.1.4 Alternative approaches

In the results (Figure 8.3), we observe that the solution with the best objective value is found long before reaching the single-cut termination criteria. As we state in Section 6.3, our L-shaped single-cut algorithm calculates the objective value (upper bound) with binary second-stage variables first after reaching the termination criteria to save computational time during iterations. Therefore, we see that there is a possibility that a good solution may be found earlier in the computational process. An alternative approach is calculating the objective value with binary second-stage variables when a better lower bound is found in the master problem. The downside is the extra computational time needed when using binary second-stage variables, which may be justified by finding reasonable solutions earlier and terminating the process.

It is an alternative approach for strengthening cuts to use integer cuts similar to Chen et al. (2012), Qi & Sen (2016) and Angulo et al. (2016). This approach is more complicated and extensive to implement but has an advantage in stronger cuts that avoid the options for continuous solutions. In that case, the cuts are more binding in earlier iterations, and the possible extra computational time in the mixed integer sub-problems is neglectable.

Another way to avoid variable relaxations is to include the investment and adjustment variables in the master problem as binary variables. This approach implies that the original second-stage adjustment variables must be put in the first stage and made independent of scenarios. The change affects both problem and model and makes the model less flexible. The upside is that this approach will get a tighter lower bound for the recourse function. We will not have to deal with extra computation to obtain a final feasible solution where the adjusted variables are binary.

8.1.2 Acceleration technique results

This subsection compares the single-cut algorithm results with the accelerating techniques described in Section 6.4. We run all implementations with accelerating techniques on F4C20T10Sx instances for 2, 5, 10, 25 and 50 scenarios. We use these instances as single-cut manages to solve them within the time limit of 172 800. The comparison focus is when the technique's upper bound approaches the optimal solution. This selection of comparison is chosen because the objective value is the critical value in decision support. Note that techniques that do not explicitly state that their using multi-cuts use the single-cut approach. In Section 8.1.2.1, we present a comparison between the single-cut and acceleration techniques. The goal is to identify if some techniques are better than single-cut and an object for further research. After that, we present and discuss results from instances with or without using warm-start in Section 8.1.2.2.

8.1.2.1 Comparing single-cut with acceleration techniques

Figure 8.4 presents the objective value results over time for single-cut and acceleration techniques for instances F4C20T10Sx. Note that the y-axis scale is different to better compare methods with different problem sizes. Additionally, some techniques approach optimality at an almost similar time and close to each other. Figure 8.4a shows this with single-cut, epsilon and M&B&BC reaching optimality in approximately 1 000 seconds.

First, the results show that multi-cut (M) outperforms single-cut in all five instances. Birge & Louveaux (1988) states that a rule of thumb is that single-cut is better than multi-cut if there are more sub-problems than master problem variables. In the instances run, there are fewer sub-problems, explaining why the multi-cut technique performs better than single-cut. These results correspond well with the theory as long as the number of sub-problems is low. Therefore, we can say that it is preferred that the multi-cut approach is utilised over single-cut for these problem sizes.

Further on, we observe the results for the acceleration techniques using alternative master problem strategies, Benders Branch & Cut (B&BC) and the epsilon approach (ϵ-approach). We initially set ϵ(the optimality gap termination criteria of the master problem) to 30% after some quick investigation on early iterations for different ϵ values. The value decreases by 1% for every hundred iterations. The results show that B&BC only outperforms single-cut in the largest instance, F4C20T10S50, while the ϵ-approach only outperforms single-cut in the F4C20T10S25. Comparing B&BC with the ϵ-approach results in the ϵ-approach performing better in all instances except F4C20T10S50. There is no clear indication from these results that none of these approaches is preferred over single-cut. However, as the ϵ-approach is dependent on choosing an appropriate initial ϵ and decreasing rate, there may be more potential in tuning this parameter to our problem.

In Figure 8.4 we observe that combining B&BC and the ϵ-approach with multi-cut produces the best results. The combination of multi-cut and ϵ-approach give the best result in the three instances F4C20T10S2, F4C20T10S5 and F4C20T10S10, and only beaten by the combination of multi-cut and B&BC in the two last instances. Improved results for the acceleration techniques using alternative master problem strategies when using multi-cut instead of single-cut corresponds well with our results comparing multi-cut with single-cut. That these combinations perform best is a result of the fact that the master problem solves faster with B&BC and the ϵ-approach. At the same time, the fast solving LP sub-problems do not negatively affect solving them separately with multi-cut. Therefore, are these combination objects for future research on our L-shaped implementation.

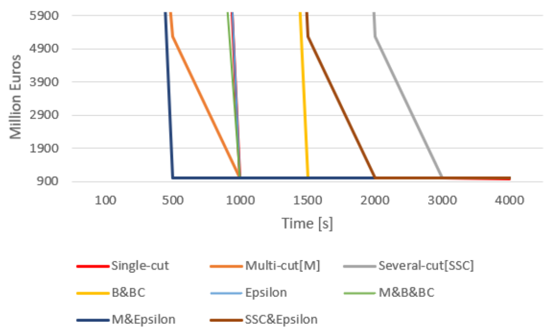

(a) F4C20T10S2.

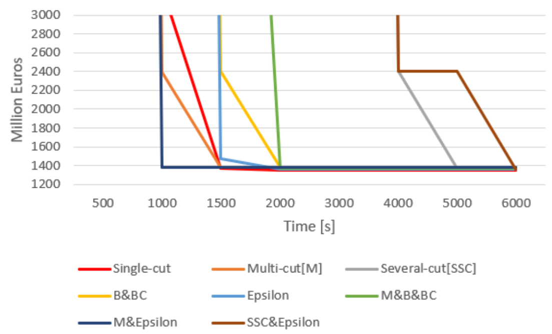

(b) F4C20T10S5.

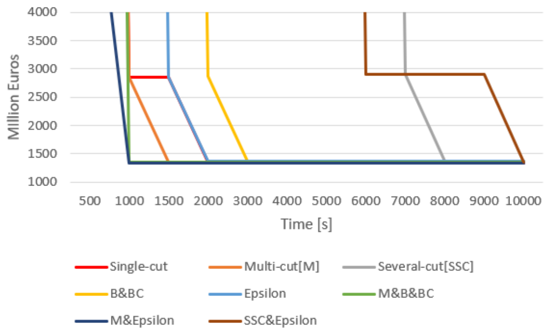

(c) F4C20T10S10.

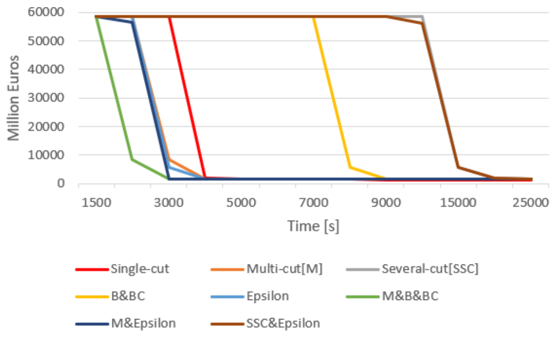

(d) F4C20T10S25.

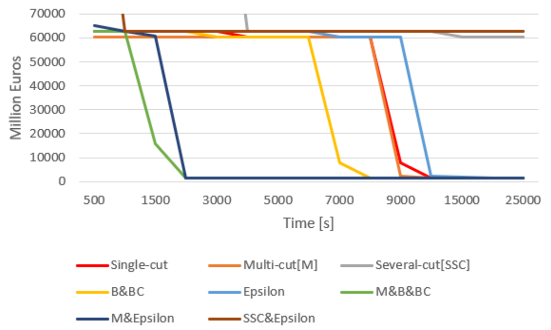

(e) F4C20T10S50.

Figure 8.4: Development in objective value for single-cut vs. acceleration techniques for instances F4C20T10Sx.

Lastly, we observe that the implementations using several-cuts (SSC and SSC&B&BC) perform worst in all instances. SSC uses the five best solutions from the master problem to produce optimality cuts with a single-cut approach in every iteration. In Figure 8.4e we see that these two implementations do not reach optimality within

25 000 seconds, as the other techniques do. We can then say that using incumbent solutions to create cuts when the master problem solves to optimality harms the total solution time, as these extra cuts do not give any advantage.

8.1.2.2 Comparing results with or without warm-start

Figure 8.5 reports the results from running single-cut with and without the warm-start technique. The goal is to see if there is a gain in warm-starting our algorithms. The warm-start begins by solving the expected demand scenario problem and creating a cut using this solution before continuing with a single-cut algorithm. We observe that in all instances except F4C20T10S50 (Figure 8.5e), the single-cut without the warm-start outperforms the other with warm-start in the matter of reaching its final objective value. Another thing we see is that single-cut without warm-start are always faster in finding a better solution in the early iterations. However, for the F4C20T10S50 instance, the implementation with warm-start surpasses the one without and finds the optimal solution first. Using warm-start is slower early because it uses the additional time to calculate the expected demand scenario.

The gain from solving the expected demand scenario should result in a better result in the long run (Geoffrion & Graves 1974). As the F4C20T10Sx instances are relatively small, the additional gain from the first cut with warm-start does not overweight the extra computational time it needs. The scale up to F4C20T10S50 illustrates that the effect is favourable when using a warm-start increase the problem size. This scale-up shows potential for using a warm-start when the problem reaches a certain level. This potential may apply in combination with other techniques and is an object for further research.

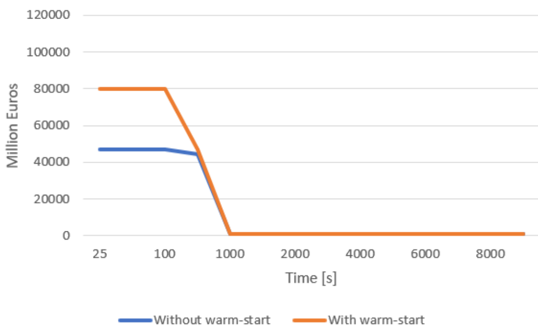

(a) F4C20T10S2.

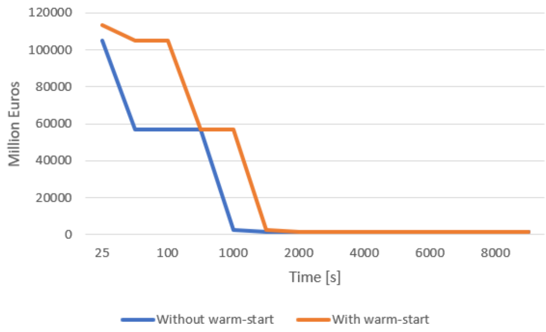

(b) F4C20T10S5.

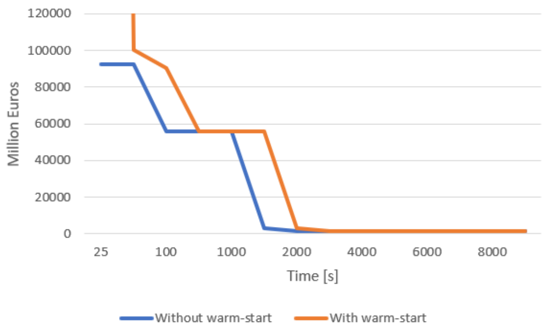

(c) F4C20T10S10.

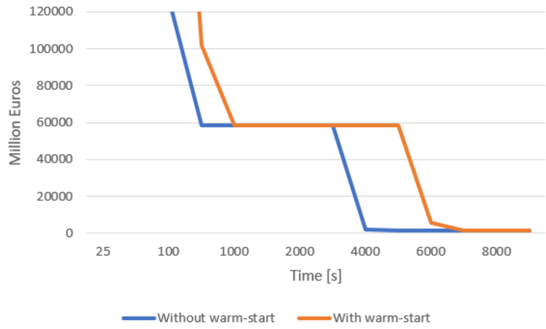

(d) F4C20T10S25.

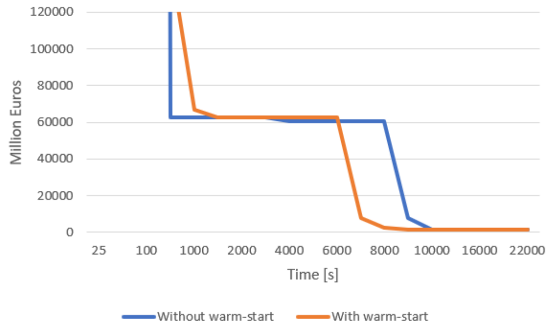

(e) F4C20T10S50.

Figure 8.5: Comparing single-cut with or without using warm-start for instances F4C20T10Sx.

8.2 Economic analysis and decision support

This section presents and discusses the value of stochastic programming and the results for solving the model for electrolysis and SMR+. We discuss the optimal supply chain configuration for the set of different technologies using the 5-scenario problem instance. We use the standard Gurobi solver, as our decomposition techniques have proven unsatisfactory enough on our F16C50T14S5 and F4C50T14S5 instances compared to Gurobi. Furthermore, we evaluate the value of the stochastic solution for electrolysis for 2-, 5-, and 10-scenarios. Our goal is to provide managerial insight into creating the most cost-efficient supply chain for covering the future uncertain hydrogen demand solved with five scenarios for the two production technologies.

8.2.1 Value of stochastic programming

In this subsection, we evaluate the performance of our two-stage stochastic facility location problem with capacity adjustments compared to a simpler deterministic model, the expected value problem (EV), in terms of capturing the uncertainty in future hydrogen demand. We use the Value of Stochastic Solution (VSS) to evaluate the performance. VSS measures the value of knowing and utilising the probability distributions for future outcomes. The equation for calculating the VSS is stated below for a *minimisation* problem (Birge & Louveaux 2011).

$$VSS = EEV - RP \tag{8.1}$$

EEV is the expected result by using expected value solutions. RP represents the value of the solution to the stochastic program (the recourse problem).

To obtain the results by using expected value solutions, EEV, we first solve our model with a singular expected demand scenario, providing an expected value solution, EV. Afterwards, we solve our model for the same set of scenarios as for the RP. However, we use the fixed first stage solutions from the EV, resulting in the EEV. Since our model uses scenarios from a discrete uniform distribution, the average demand is equal to the expected demand scenario.

Table 8.3 shows the VSS for the 2-, 5- and 10-scenario problem instances. We observe that the problem instance with 2 scenarios has a positive VSS of 13 million Euros, while the 5- and 10-scenario instances show negative and decreasing VSS. The magnitude of the VSS for the 5- and 10-scenario instance is heavily affected by the fact that these solutions have a 12.2% and 81.4% optimality gap, respectively. Even if there is a value in using stochastic programming, there is a significant difference in solution time to obtain solutions for the RP and EEV with the same optimality gap using Gurobi to solve the stochastic program. Solving the EV and EEV requires less time to obtain solutions of a similar optimality gap as the RP. For problem instances containing 5 or more scenarios, EV provides better first-stage decisions in less time than Gurobi, which in turn solves faster than any of the implemented solution methods. In other words, EV and EEV can provide a better stochastic solution for managerial insight for the problem sizes we study in this section.

The VSS of 13 million Euros for two scenarios constitutes less than 1% of the stochastic solution. Even though the VSS has the potential to grow larger by decreasing the gap, the VSS will be marginal compared to the solution value of the RP and EEV problem. This marginal fraction may suggest that our second stage variables grant considerable flexibility to our model, allowing it to respond well to the realisation of different demand scenarios even with fixed first-stage variables.

Our model's uncertainty is represented through the number of scenarios and the difference in demand within the scenarios. Hence, when we include only two scenarios, the uncertainty is limited relative to five and ten scenarios. In other words, we expect the VSS to increase for the five and ten scenario instances compared to two scenarios with a similar optimality gap.

Table 8.3: Value of stochastic programming for 2-, 5- and 10-scenario instances.

Number of scenarios	**VSS [mil. Euros]**	**RP [mil. Euros]**	**EEV [mil. Euros]**	**Gap RP [%]**	**Gap EEV [%]**
2	13	1 312	1 325	3.8	0
5	- 29	1 834	1 805	12.2	0
10	- 6585	8 335	1 750	81.4	0

Figure 8.6a and Figure 8.6b display the first stage decisions for the stochastic and expected value problem solution for the 5-scenario instance, respectively. Furthermore, Table 8.4 shows the initial investment in capacity and time of investment for the 5-scenario RP and EV.

Figure 8.6 and Table 8.4 show some general properties that are valid for the 2-, 5- and 10-scenario problem instances. One property is the EV having larger first stage investments, and these investments are more spread throughout the entire planning horizon. These decisions result from the EV being a deterministic problem in combination with the nature of our problem, which is to build facilities to minimise the expected costs for a set of scenarios. When the problem knows the future for certain through a single expected scenario, it makes more aggressive first stage decisions compared to the stochastic model that does not know what scenario will be realised. The aggression is best illustrated through Figure 8.7, which shows that the EV has a higher maximum installed capacity throughout the planning horizon except for time period 2.

Another implication of the EV being deterministic is that the optimality gap for the stochastic program solution is always more significant than the EEV for our problem instances when applying our solution methods. Neither Gurobi nor our proposed solution methods can obtain a solution with a lower optimality gap than 3.8, 12.2 and 81.4% within 48-hours solution time for the 2-, 5- and 10-scenario problem instances. The optimality gap affects the magnitude of the VSS, as larger gaps for the RP result in poorer objective values.

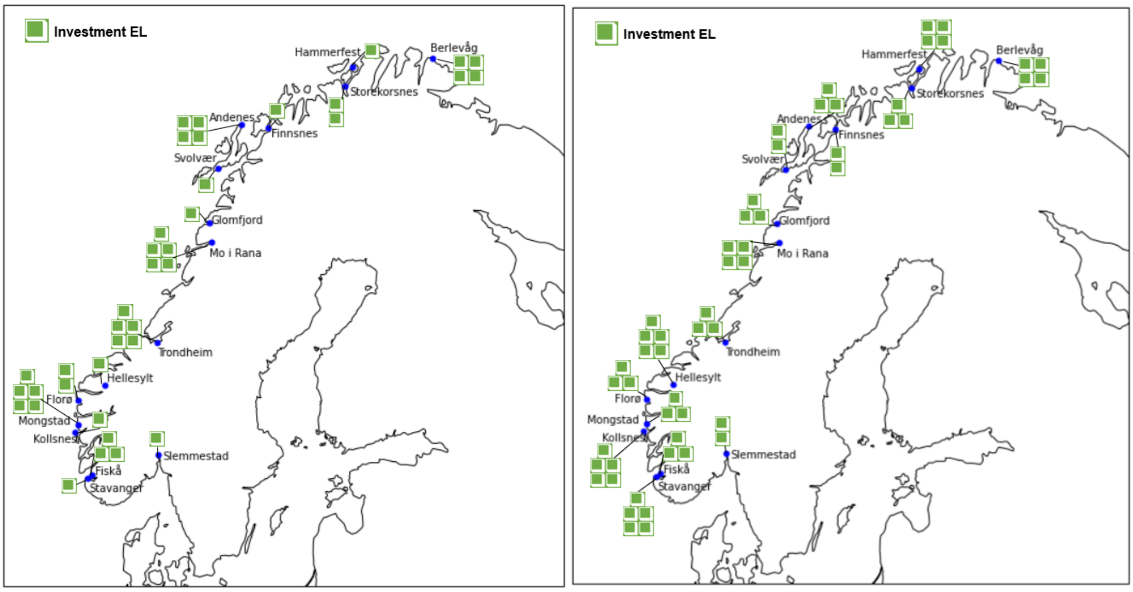

(a) First stage decisions RP.

(b) First stage decisions EV.

Figure 8.6: First stage decisions 5-scenarios.

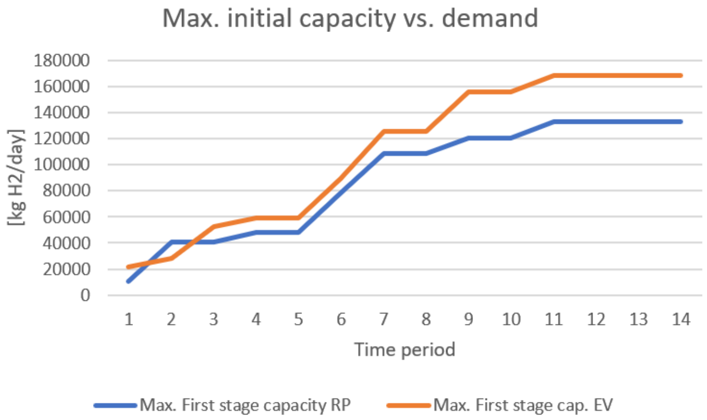

Figure 8.7: Max. installed initial capacity for RP and EV.

Table 8.4: Initial capacity and time of investment for the RP and EV.

	RP		EV	
Location	**Capacity**	**Time Period**	**Capacity**	**Time Period**
Andenes	4	9	3	7
Berlevåg	4	11	4	11
Finnsnes	1	1	2	1
Fiskå	3	4	3	3
Florø	2	1	3	3
Glomfjord	1	1	3	3
Hammerfest	1	4	4	7
Hellesylt	1	1	5	6
Kollsnes	1	1	5	9
Mo I Rana	5	2	4	1
Mongstad	5	7	3	1
Slemmestad	1	1	2	3
Stavanger	1	1	5	7
Storekorsnes	2	1	3	4
Svolvær	1	1	2	3
Trondheim	5	6	3	2

8.2.2 Electrolysis vs. SMR+

As discussed earlier in Section 7.1.2, the set of facility location candidates for SMR+ restricts to four locations. These locations are: Hammerfest, Trondheim, Mongstad and Kollsnes, as seen in Figure 8.8b. All 16 candidate locations are used for electrolysis, and the first-stage decisions can be seen in Figure 8.8a. The results presented in this subsection are all solutions to the problem instance containing 5 scenarios, meaning that we study the $F16C50T14S5$ and $F4C50T14S5$ for the electrolysis and SMR+ instance, respectively. This subsection aims to provide decision support for configuring a hydrogen supply chain for electrolysis and SMR+. In addition, we will discuss the economic effects of each supply chain configuration.

8.2.2.1 Supply chain configuration - EL & SMR+

The best solution for electrolysis corresponds to an objective value of 1 834 million Euros at a 12.2% optimality gap. The first-stage decisions of this solution are shown in Figure 8.8a. For SMR+, the optimal solution corresponds to an objective value of 2 624 million Euros and with the supply chain configuration shown in Figure 8.8b and Table 8.5.

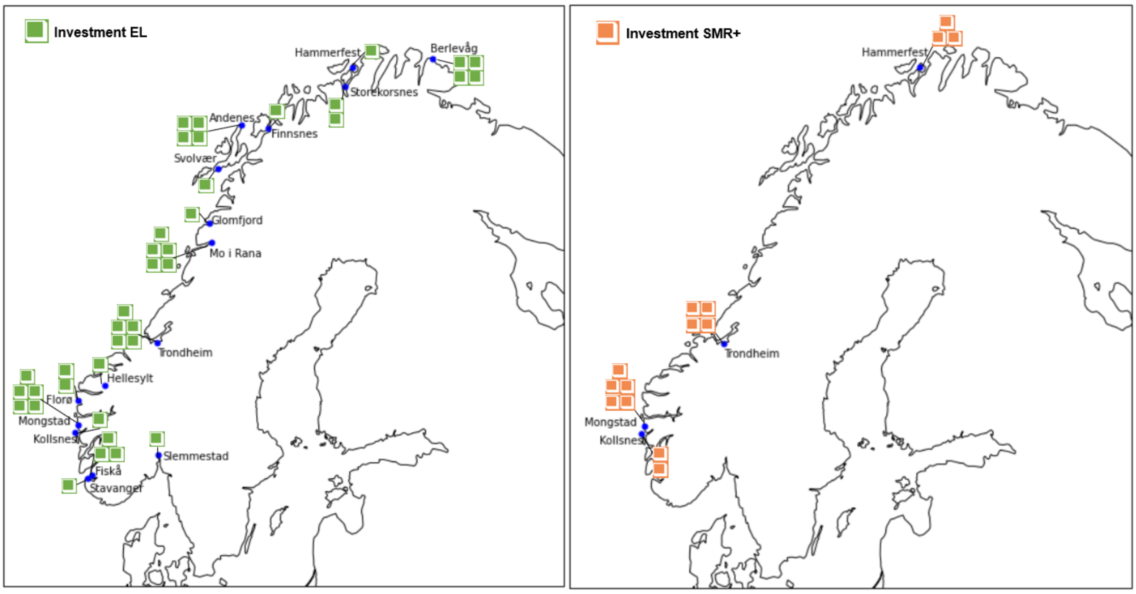

(a) Electrolysis - F16C50T14S5.

(b) SMR+ - F4C50T14S5.

Figure 8.8: First stage decisions 5-scenarios.

Table 8.5: First stage decisions for EL & SMR+.

	EL		SMR+	
Location	**Capacity**	**Time Period**	**Capacity**	**Time Period**
Andenes	4	9	-	-
Berlevåg	4	11	-	-
Finnsnes	1	1	-	-
Fiskå	3	4	-	-
Florø	2	1	-	-
Glomfjord	1	1	-	-
Hammerfest	1	4	3	1
Hellesylt	1	1	-	-
Kollsnes	1	1	2	1
Mo i Rana	5	2	-	-
Mongstad	5	7	5	3
Slemmestad	1	1	-	-
Stavanger	1	1	-	-
Storekorsnes	2	1	-	-
Svolvær	1	1	-	-
Trondheim	5	6	4	1

Figure 8.8a and Table 8.5 show that facilities are built in all 16 locations for electrolysis. Nine locations are opened straight away in time period 1, and 7 out of these 9 are opened with initial capacity 1. The facilities built in the first period handled the low but spread hydrogen demand. Each facility built in later time periods invests in a much larger capacity once the demand increases, as shown in Table 8.5.

Figure 8.8b and Table 8.5 show that facilities are built in all 4 locations for SMR+. Investments are made for three out of the four locations in time period 1. Each location opening in time period 1 is geographically spread throughout Norway, as these will serve the spread initial hydrogen demand while satisfying the maximum distribution limit. The latest investment in facility location is made in time period 3, with an initial capacity of 5, which is larger than any other facility at the time. It invests in a larger initial capacity as demand is strictly increasing. Investing in initial capacity is always cheaper than investing and then adjusting capacity with the relation between investment, adjustment and production costs for SMR+.

SMR+ has to initially open three facilities in each region to satisfy the initial spread customer demand. When demand picks up, it chooses to open the last facility with the highest initial capacity in the South-west region with the most demand to minimise distribution costs. The investment decisions contain more significant investments in capacity on average for SMR+, as SMR+ only has four potential facility locations. On the other hand, electrolysis has more potential facility locations to choose from. The model can decide whether to invest at a new location or adjust capacity at an existing facility to minimise the combined costs of distribution, production, and investment/adjustment to handle the increased customer demand. In other words, electrolysis can consider the trade-off between investing or adjusting capacity, while SMR+ has to adjust as each facility location has already been built. We notice this flexibility for electrolysis in the adjustment decisions, as some facilities increase capacities before every facility is built. In contrast, the facilities in the solution for SMR+ adjust capacities after every facility is built.

8.2.2.2 Economic analysis

Overall, the supply chain configuration with electrolysis appears to be the cheaper configuration with a total cost including investment, adjustment, production and distribution of 1 834 million Euros compared to 2 624 million Euros for SMR+. The solution for electrolysis and SMR+ present two different supply chain structures. Electrolysis has the opportunity to invest in a much larger set of facility locations and chooses to do so, creating a decentralised supply chain. On the other hand, the solution for SMR+ only has a set of facility locations of four, resulting in a much more centralised hydrogen production. For each supply chain configuration, we examine its cost distribution. Table 8.6 shows the cost contribution for investment, adjustment, production and distribution of the solution for SMR+ and electrolysis, respectively.

Table 8.6: SMR+ compared to 5-scenario solution with EL at 12.2% gap.

Cost contribution [mill. Euro]	**SMR+ [0% Gap]**	**Share**	**Electrolysis [12.2% Gap]**	**Share**
Investment	257	9.8 %	215	11.7 %
Adjustment	698	26.6 %	252	13.7 %
Production	877	33.4 %	1038	56.6 %
Distribution	792	30.2 %	329	18.0%
Total	2 624		1 834	

8.2.2.2.1 Investment Costs

The investment costs are slightly higher for SMR+ with 257 compared to 215 million Euros for electrolysis, where SMR+ establishes a few extensive facilities while electrolysis invests in many smaller facilities. Figure 8.9 shows that with the current investment decisions, electrolysis can establish twice as much initial capacity as SMR+ for the exact cost. The costs for electrolysis are distributed over sixteen different locations, each with capacities ranging from capacity point 1-5 and time period 1-11, allowing electrolysis to follow the expected demand level closely through investment decisions. Investments cap out in time period 3 for SMR+, which is also the time period where over half of the capacity is installed. SMR+ ability to respond to additional hydrogen demand relies on the adjustment decisions.

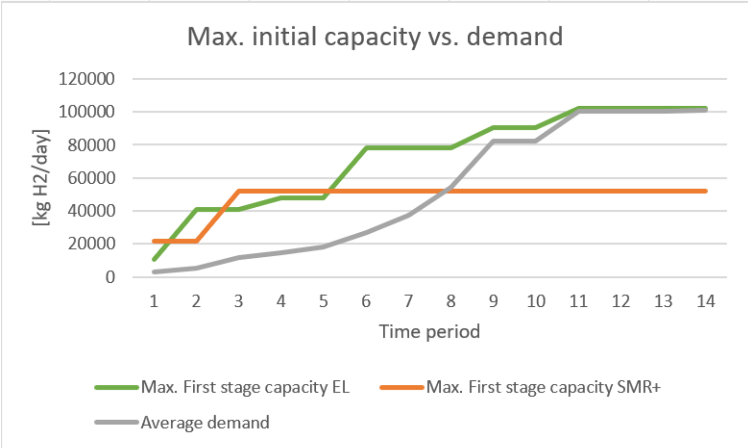

Figure 8.9: Initial facility capacity vs. expected demand.

8.2.2.2.2 Adjustment Costs

The adjustment costs are also greater for SMR+ than for electrolysis. Table 8.6 shows that SMR+ has adjustment costs corresponding to 698 million Euros, compared to electrolysis, which has adjustment costs corresponding to 252 million Euros. First of all, the investment costs and thereby adjustments costs for SMR+ relative to electrolysis are more expensive on a general level. Furthermore, SMR+ has to use adjustment decisions to satisfy the pick up in hydrogen demand, implying high adjustment costs as each facility location has already been built early in the time horizon. Electrolysis has a choice to avoid these higher adjustment costs by investing in capacity by building facilities in new locations later on in the time horizon. This choice does not mean that electrolysis does not engage in adjustment decisions but only does so when the trade-off between adjusting, producing and distributing from an existing facility is sufficiently large compared to investing, producing and distributing from a facility at a new location.

8.2.2.2.3 Production Costs

In order to justify the high additional adjustment costs for SMR+, the costs have to be offset by production savings. From Table 8.6, we observe that SMR+ has lower production costs than electrolysis with 877 million Euros compared to 1 038 million Euros. Having larger facilities makes it easier to realise economies of scale in production.

Figure 8.10 shows the average unit production costs per kg of hydrogen produced with each production technology throughout the time horizon. We observe that SMR+ becomes strictly cheaper halfway through the time horizon, starting in time period 7. SMR+ shows early potential to produce cheaper hydrogen on average but experiences several spikes in production cost early on. These cost jumps can directly relate to investment and "the average" adjustment decisions for SMR+. As pointed out earlier, the investment and adjustment decisions for SMR+ are pretty vast. They may result in facilities running on lower utilisation grades shortly after the decisions until the demand increases.

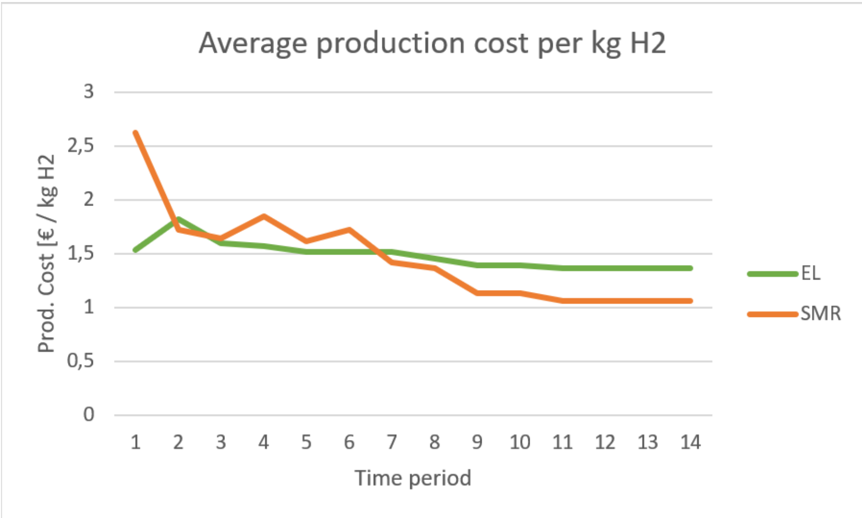

Figure 8.10: Average production cost per kg H_2 based on expected demand.

As we reach maximum demand, SMR+ produces hydrogen at the cost of 1,06 $\frac{Euro}{kg}$ compared to 1,37 $\frac{Euro}{kg}$, representing a 0,31 cost save per kg. This production cost margin may cover the additional investment and adjustment costs in the long term for SMR+. Still, as we now turn to distribution costs, we can observe that the centralised production has consequences for distributional costs.

8.2.2.2.4 Distribution Costs

The number of facilities in each solution affects the distribution costs, given the widespread customer demand. Studying Table 8.6, we see that SMR+ has over twice the distribution costs compared to electrolysis in total costs, 792 million Euros compared to 329 million Euros. The facilities built for SMR+ have to cover great distances to its customers and larger quantities per facility than electrolysis. Recall that the distribution costs solely depend on distance and amount, resulting in this significant difference in distribution cost. The large centralised facilities offer savings of 161 million Euros in production costs through economies of scale compared to electrolysis. The savings in production is easily offset by increased distribution cost due to the diseconomy of demand density.

8.2.2.3 Decision support

In many ways, electrolysis seems to be the optimal choice when designing a hydrogen supply chain for maritime transportation in Norway. We can identify some properties of technology for electrolysis. One of these properties is the smaller investment costs relative to SMR+ and a more extensive set of potential facility locations, making it possible for electrolysis to establish a decentralised supply chain, which in turn implies cost savings for distribution through shorter distribution distances. Electrolysis has more options to respond to changes in customer demand, given the many more potential facility locations. More facilities to spread the production over also make it more likely to have a higher average utilisation rate per produced hydrogen than SMR+. The increased costs of investment and adjustments do not have time to be counterbalanced by the savings in large-scale production during the time horizon. In our case study, the current demand density, combined with the limited facility locations for SMR+, introduces an element of diseconomy for distribution.

Finally, we observe that the solutions presented in Table 8.6 have an optimality gap of 0% and 12.2% for SMR+ and electrolysis, respectively. This gap would imply that there possibly exists further cost savings for the electrolysis instance if they can solve the computational requirements. In contrast, the SMR+ problem instance has already been solved to optimality.

Chapter 9

Future Research

From the computational study, we notice that even though our decomposition technique finds feasible solutions in every problem instance, it struggles to iterate toward optimality within our defined termination criteria for instances other than those reduced to a limited number of customers and scenarios. As our solution's quality in capturing the real world can be directly linked to the number of scenarios we can solve, it becomes apparent that our decomposition technique needs further work to solve the problem faster.

As stated in Chapter 8, the generated cuts through our decomposition technique are weak and generally not binding for many scenarios. Hence it would be beneficial to look further into strengthening these cuts. One suggestion is to follow up on the discussion of integer L-shaped cuts in Section 6.1.3, as the generated cuts are based on linear relaxed sub-problems and therefore serve as a lower bound approximation for the recourse function.

Chapter 10

Concluding Remarks

In this thesis, we formulate a two-stage stochastic facility location problem with capacity adjustments and an L-shaped solution method for designing the hydrogen supply chain for maritime transportation in Norway. Solving the model provides decision support for the problem of deciding when and where to invest in production facilities, capacity adjustments, production technology and the distribution pattern for hydrogen, given uncertain future demand while minimising the overall expected cost. The solution methods are based on applying an L-shaped algorithm with different acceleration techniques on a Benders reformulated version of our model.

We construct large instances of our problem containing up to 16 facility locations, 50 customers, 50 demand scenarios and a time horizon over 14 years from our case study. The different problem instances were constructed by extracting data from Ocean Hyway Cluster and SSB and are used to establish demand projections for the maritime passenger transportation sector, offshore sector and the domestic fishing industry.

The results show that the decomposition technique can always find feasible solutions within our termination criteria and optimal solutions for the smallest instances. Additionally, the technique accomplishes better objective values than Gurobi for large instances. However, we see that the problem is hard to solve for the largest instances with our decomposition technique. The results show that the technique needs many iterations before approaching optimality, resulting in slow convergence, poor lower bounds, and a high gap. Spending more time studying generating strengthened cuts may realise the potential we have established for our proposed decomposition technique and acceleration methods. The most promising acceleration techniques were the combinations of the multi-cut approach, the B&BC-technique, the multi-cut approach, and the ϵ-approach. Additionally, the results show potential for using warm-start for large instances.

For our 5-scenario instance with 16 facility locations and 50 customers, we have established that electrolysis will constitute the production technology for the future hydrogen supply chain. With significant savings in investment, adjustment and distribution costs compared to SMR+, electrolysis chooses to build facilities in every location. The solution has the potential for further cost savings in the overall supply chain configuration as the current optimality gap for the solution corresponds to 12.2%.

Bibliography

Aarskog, F. G. & Danebergs, J. (2020*a*), 'Estimation of energy demand in the norwegian high-speed passenger ferry sector towards 2030', *IFE/E-2020/003* .

Aarskog, F. G. & Danebergs, J. (2020*b*), 'Future compressed hydrogen infrastructure for the domestic maritime sector', *IFE/E-2020/006* .

Aglen, T. M. & Hofstad, A. (2021), 'Designing the hydrogen supply chain for maritime transportation'. Project work for TIØ4500, NTNU.

Ahmed, S., King, A. & Parija, G. (2003), 'A multi-stage stochastic integer programming approach for capacity expansion under uncertainty', *Journal of Global Optimization* **26**, 3–24.

Alonso-Ayuso, A., Escudero, L., Garín, A., Ortuño, M. & Pérez, G. (2003), 'An approach for strategic supply chain planning under uncertainty based on stochastic 0-1 programming', *Journal of Global Optimization* **26**, 97–124.

Angulo, G., Ahmed, S. & Dey, S. S. (2016), 'Improving the integer l-shaped method', *INFORMS Journal on Computing* **28**, 483–499.

arbeidslivet.no (2019), 'Fakta: Hviler og pauser for yrkessjåfører', https://www.arbeidslivet.no/Arbeid1/Arbeidsmiljo-og-HMS/Fakta-Hviler-og-pauser-for-yrkessjaforer/. Visited on 2022-03-11.

Arya, V., Garg, N., Khandekar, R., Munagala, K. & Pandit, V. (2004), 'Local search heuristic for k-median and facility location problems', *SIAM Journal on computing* **33**, 544–562.

Avisa Nordlys (2020), 'Skal kvitte seg med flere havner i fylket vart stor interesse', https://www.nordlys.no/skal-kvitte-seg-med-flere-havner-i-fylket-vart-stor-interesse/s/5-34-1406147. Visited on 2022-03-11.

Birge, J. & Louveaux, F. (1988), ‘A multicut algorithm for two-stage stochastic linear programs’, *European Journal of Operational Research* **33**, 384–392.

Birge, J. R. & Louveaux, F. (2011), *Introduction to Stochastic Programming*, Springer series in operations research and financial engineering, New York, NY.

Broadleaf (2021), ‘The colour of hydrogen’, https://broadleaf.com.au/resource-material/the-colour-of-hydrogen/. Visited on 2022-02-15.

Chen, B., Küçükyavuz, S. & Sen, S. (2012), ‘A computational study of the cutting plane tree algorithm for general mixed-integer linear programs’, *Oper. Res. Lett.* **40**, 15–19.

Correia, I. & Captivo, M. (2003), ‘A lagrangean heuristic for a modular capacitated location problem’, *Annals OR* **122**, 141–161.

Correia, I. & Melo, T. (2019), ‘Dynamic facility location problem with modular capacity adjustments under uncertainty’, *Technical Reports on Logistics of the Saarland Business School* **17**.

Correia, I. & Melo, T. (2021), ‘Integrated facility location and capacity planning under uncertainty’, *Computational and Applied Mathematics* **40**.

Det Kongelege Klima- og Miljødepartement (2020), ‘Klimaplan for 2021–2030’, *regjeringen.no* .

DNV (2014), ‘Sammenstilling av grunnlagsdata om dagen skipstrafikk og drivstofforbruk’, *Klima- og miljødepartementet* . Visited on 2022-03-05.

DNV (2015), ‘Fuels & fuel converters’, *Maritime Academy* .

DNV (2019), ‘Synteserapport om produksjon og bruk av hydrogen i norge’, *PRODUKSJON OG BRUK AV HYDROGEN I NORGE* .

European Comission (2022), ‘Eu emissions trading system’, https://ec.europa.eu/clima/eu-action/eu-emissions-trading-system-eu-ets_en. Visited on 2022-04-26.

Fiskeridirektoratet (2021), ‘Economic and biological figures from norwegian fisheries 2021’.

Fiskeridirektoratet (2022*a*), ‘Fiskeflåten - offisiell statistikk’, https://www.fiskeridir.no/Yrkesfiske/Tall-og-analyse/Fiskere-fartoey-og-tillatelser/Fartoey-i-merkeregisteret/fiskeflaaten. Visited on 2022-03-11.

Fiskeridirektoratet (2022*b*), 'Rundvekt fordelt på fartøysfylke - norske fartøy', https://www.fiskeridir.no/Yrkesfiske/Tall-og-analyse/Fangst-og-kvoter/Fangst/Fangst-fordelt-paa-fartoeyfylke. Visited on 2022-03-11.

Geoffrion, A. M. & Graves, G. W. (1974), *Multicommodity Distribution System Design by Benders Decomposition*, Vol. 20, Management Science.

GlobalCCSInstitute (2020), 'Replacing 10% of nsw natural gas supply with clean hydrogen: Comparison of hydrogen production options', *GlobalCCSInstitute* .

Govindan, K., Fattahi, M. & Keyvanshokooh, E. (2017), 'Supply chain network design under uncertainty: A comprehensive review and future research directions', *European Journal of Operational Research* **263**, 108–141.

H2Bulletin (2021), 'Hydrogen production through electrolysis', https://www.h2bulletin.com/knowledge/hydrogen-production-through-electrolysis/. Visited on 2022-03-07.

Ioan, C. & Ioan, A. (2014), 'About short-term costs and long-term costs', *Journal of Accounting and Management* **4**, 61–68.

IRENA (2020), 'Green hydrogen - a guide to policy making', *International Renewable Energy Agency* .

Jakobsen, D. & Åtland, V. (2016), 'Concepts for large scale hydrogen production', *Master thesis at NTNU* pp. 1–145.

Jena, S. D., Cordeau, J.-F. & Gendron, B. (2015), 'Dynamic facility location with generalized modular capacities', *Transportation Science* **49**, 484–499.

Konkraft (2020), 'The energy industry of tomorrow on the norwegian continental shelf'.

Laporte, G. & Louveaux, F. V. (1993), 'The integer l-shaped method for stochastic integer programs with complete recourse', *Operations Research Letters* **13**, 133–142.

Lee, C. Y. (1991), 'An optimal algorithm for the multiproduct capacitated facility location problem with a choice of facility type', *Computers & Operations Research* **18**, 167–182.

Louveaux, F. & Birge, J. R. (2009), *L-shaped method for two-stage stochastic programs with recourse*, Springer US, Boston, MA, pp. 1943–1945.

Lucas, C., Mirhassani, S. A., G, M., C.A, P. & Correspondence (2001), 'An application of lagrangian relaxation to a capacity planning problem under uncertainty', *Journal of the Operational Research Society* **52**, 1256–1266.

Luedtke, J. (2016), 'Benders decomposition for solving two-stage stochastic optimization models', https://www.ima.umn.edu/materials/2015-2016/ND8.1-12.16/25378/Luedtke-spalgs.pdf. Visited on 2022-03-16.

Magnanti, T. L. & Wong, R. T. (1981), *Accelerating Benders Decomposition: Algorithmic Enhancement and Model Selection Criteria*, Vol. 29, Operations Research.

Mathis, S. & Koscianski, J. (2002), *Microeconomic Theory: An Integrated Approach*, Prentice Hall.

Matos Dias, J., Captivo, M. & Clímaco, J. (2007), 'Dynamic location problems with discrete expansion and reduction sizes of available capacities', *Investigação Operacional* **27**.

Mazzola, J. & Neebe, A. (1999), 'Lagrangian - relaxation - based solution procedures for a multiproduct capacitated facility location problem with choice of facility type', *European Journal of Operational Research* **115**, 285–299.

Moseman, A. (2021), 'How efficient is carbon capture and storage?', https://climate.mit.edu/ask-mit/how-efficient-carbon-capture-and-storage. Visited on 2022-02-25.

Mäkitie, T., Danebergs, J., Hanson, J. & Medbø, E. G. (2021), 'Solving the chicken and egg problem in maritime hydrogen value chains in western norway', *FME NTRANS report* .

NCE (2020), 'Norwegian future value chains for liquid hydrogen', *NCE Maritime Cleantech* .

NDC-Registry (2020), 'Update of norway's nationally determined contribution', https://www4.unfccc.int/sites/ndcstaging/PublishedDocuments/Norway%20First/Norway_updatedNDC_2020%20(Updated%20submission).pdf. Visited on 2022-02-28.

NEL (2019), 'The world's most efficient and reliable electrolysers', https://nelhydrogen.com/wp-content/uploads/2020/03/Electrolysers-Brochure-Rev-C.pdf. Visited on 2022-03-10.

NorskPetroleum (2021), 'Historisk produksjon', https://www.norskpetroleum.no/fakta/historisk-produksjon/. Visited on 2022-03-07.

Nunes, P., Oliveira, F., Hamacher, S. & Almansoori, A. (2015), 'Design of a hydrogen supply chain with uncertainty', *International Journal of Hydrogen Energy* **40**, 16408–16418.

Ocean Hyway Cluster (2020*a*), '2030 hydrogen demand in the norwegian domestic maritime sector', *OHC HyInfra project* . Workpackage C: Mapping future hydrogen demand.

Ocean Hyway Cluster (2020*b*), '2030 offshore market nh_3 fuel demand', *OHC HyInfra project* . Workpackage C: Mapping future hydrogen demand, report C.4 rev. 05.

Ocean Hyway Cluster (2020*c*), 'Interactive map - potential maritime hydrogen in norway'. OHC HyInfra project, Workpackage C: Mapping future hydrogen demand.

Ocean Hyway Cluster (2020*d*), 'Mapping of 2030 hydrogen demand in the norwegian domestic car ferry sector', *OHC HyInfra project* . Workpackage C: Mapping future hydrogen demand, report C.2 rev. 01.

Ocean Hyway Cluster (2021), 'Nullutslipps havgående fiskefartøy - utredning av fartøystyper og relevant teknologi', *OHC HyAqua project* .

Oliveira, F., Grossmann, I. & Hamacher, S. (2014), 'Accelerating benders stochastic decomposition for the optimization under uncertainty of the petroleum product supply chain', *Computers & Operations Research* **49**, 47–58.

Oljedirektoratet (2022), 'Eus kvotesystem', https://www.npd.no/fakta/publikasjoner/rapporter/rapportarkiv/kraft-fra-land-til-norsk-sokkel/2---utslipp-til-luft-fra-petroleumssektoren/eus-kvotesystem/. Visited on 2022-04-26.

Pindyck, R. S. & Rubinfeld, D. L. (2018), 'Microeconomics'.

Qi, Y. & Sen, S. (2016), 'The ancestral benders' cutting plane algorithm with multi-term disjunctions for mixed-integer recourse decisions in stochastic programming', *Mathematical Programming* **161**.

Rahmaniani, R., Crainic, T. G., Gendreau, M. & Rei, W. (2013), *The Benders decomposition algorithm: A literature review*, Vol. 259, European Journal of Operational Research.

Ravi, R. & Sinha, A. (2004), Hedging uncertainty: Approximation algorithms for stochastic optimization problems, *in* D. Bienstock & G. Nemhauser, eds, 'Integer Programming and Combinatorial Optimization', Vol. 3064, Springer Berlin Heidelberg, Berlin, Heidelberg, pp. 101–115.

Regjeringen (2019), 'Handlingsplan for gronn skipsfart', https://www.regjeringen.no/contentassets/2ccd2f4e14d44bc88c93ac4effe78b2f/handlingsplan-for-gronn-skipsfart.pdf. Visited on 2022-03-04.

Rubiales, A. J., Lotito, P. A. & Parente, L. A. (2013), *Stabilization of the Generalized Benders Decomposition applied to Short-Term Hydrothermal Coordination Problem*, Vol. 11, IEEE Latin America Transactions.

Samferdselsdepartementet (2021), 'Nasjonal transportplan 2022-2033', *regjeringen.no* .

Santoso, T., Ahmed, S., Goetschalckx, M. & Shapiro, A. (2005), 'A stochastic programming approach for supply chain network design under uncertainty', *European Journal of Operational Research* **167**, 96–115.

Schütz, P. (2009), 'Managing uncertainty and flexibility in supply chain optimization', *Doctoral thesis at NTNU 2009:89* . Department of Industrial Economics and Technology Management, Trondheim, Norway.

Shapiro, A. & Philpott, A. (2007), 'A tutorial on stochastic programming', pp. 1–35.

Shulman, A. (1991), 'An algorithm for solving dynamic capacitated plant location problems with discrete expansion sizes', *Operations Research* **39**, 423–436.

Silva, A., Aloise, D., Coelho, L. C. & Rocha, C. (2021), 'Heuristics for the dynamic facility location problem with modular capacities', *European Journal of Operational Research* **290**, 435–452.

SINTEF (2020), 'Largescale hydrogen production in norway - possible transition pathways towards 2050', https://ife.brage.unit.no/ife-xmlui/bitstream/handle/11250/2650236/Final%2breport%2b2020-00179.pdf?sequence=2&isAllowed=y. Visited on 2022-03-11.

SINTEF (2021), 'Ammoniakk på skipstanken kan gi stor gevinst – også for miljøet', https://www.sintef.no/siste-nytt/2021/ammoniakk-pa-skipstanken-kan-gi-stor-gevinst-ogsa-for-miljoet/. Visited on 2022-04-28.

SSB (2021*a*), 'Norwegian registered vessels. all ships. classification of type of vessel by statistics norway 2007 - 2020', https://www.ssb.no/en/statbank/table/08203/. Visited on 2022-03-11.

SSB (2021*b*), 'Utslipp til luft', https://www.ssb.no/statbank/table/08940/tableViewLayout1/. Visited on 2022-02-20.

Stadlerova, S. & Schütz, P. (2021), 'Designing the hydrogen supply chain for maritime transportation in norway', *Department of Industrial Economics and Technology Management* . Trondheim, Norway.

Standards Norway (2021), 'Norsok standards', https://www.standard.no/en/sectors/energi-og-klima/petroleum/norsok-standards/#.YmerxuhBxPY. Visited on 2022-04-26.

U.S Department of Energy (2021), 'Hydrogen storage', https://www.energy.gov/eere/fuelcells/hydrogen-storage. Visited on 2022-03-10.

Van Slyke, R. M. & Wets, R. (1969), 'L-shaped linear programs with applications to optimal control and stochastic programming', *SIAM Journal on Applied Mathematics* **17**, 638–663.

Wesolowsky, G. O. & Truscott, W. G. (1975), 'The multiperiod location-allocation problem with relocation of facilities', *Management Science* **22**, 57–65.

Wikipedia (2021), 'Tieback', https://en.wikipedia.org/wiki/Tieback. Visited on 2022-03-16.

Zarandi, M. M. F. (2010), *Using decomposition to solve facility location/fleet management problems*, University of Toronto.

Øvrebø, O. A. (2022), 'Kvotemarked: Eu og verden', https://energiogklima.no/klimavakten/kvotemarked-eu-og-verden/. Visited on 2022-04-20.

Trygve Magnus Aglen & Andreas Hofstad

L-shaped decomposition for the two-stage stochastic facility location problem with capacity adjustments

NTNU
Norwegian University of
Science and Technology